SOME INVESTIGATIONS ON CONTROL OF DISTRIBUTION STATIC COMPENSATOR

DISSERTATION

SUBMITTED IN PARTIAL FULFILLMENT OF THE REQUIREMENTS
FOR THE AWARD OF THE DEGREE
OF

MASTER OF TECHNOLOGY
IN
POWER SYSTEM

Submitted by:

KULDEEP SINGH
Roll No. 2K14/PSY/11

Under the supervision of

Dr. ALKA SINGH

DEPARTMENT OF ELECTRICAL ENGINEERING
DELHI TECHNOLOGICAL UNIVERSITY
(Formerly Delhi College of Engineering)
Bawana Road, Delhi-110042
2016

SOME INVESTIGATIONS ON CONTROL OF DISTRIBUTION STATIC COMPENSATOR

DISSERTATION

SUBMITTED IN PARTIAL FULFILLMENT OF THE REQUIREMENTS
FOR THE AWARD OF THE DEGREE
OF

MASTER OF TECHNOLOGY
IN
POWER SYSTEM

Submitted by:

KULDEEP SINGH
Roll No. 2K14/PSY/11

Under the supervision of

Dr. ALKA SINGH

DEPARTMENT OF ELECTRICAL ENGINEERING
DELHI TECHNOLOGICAL UNIVERSITY
(Formerly Delhi College of Engineering)
Bawana Road, Delhi-110042

2016

CERTIFICATE

I hereby certify that the work which is being presented in the M.Tech. Dissertation entitled **"SOME INVESTIGATIONS ON CONTROL OF DISTRIBUTION STATIC COMPENSATOR",** in partial fulfillment of the requirements for the award of the **Degree of Master of Technology in Power Systems** and submitted to the Department of Electrical Engineering of Delhi Technological University is an authentic record of my own work carried out under the supervision of **Dr. Alka Singh (Associate Professor), EE Department**.

The matter presented in this report has not been submitted by me for the award of any other **Degree/Diploma** elsewhere.

Signature of Candidate

Kuldeep Singh

2K14/PSY/11

Supervisor

Date: 15th July, 2016

Dr. Alka Singh

Associate Professor

EE Dept., DTU

ABSTRACT

This thesis presents work on power quality problems faced in power distribution system and ways to mitigate these problems. A three phase three wire distribution system is considered which incorporates Distribution Static Compensator (DSTATCOM) at the Point of Common Coupling (PCC). Different controls algorithms are developed verified for power factor correction and voltage regulation mode. The operation of DSTATCOM is verified in power factor correction and voltage regulation modes. The control is modeled such that DSTATCOM provides the total reactive power requirement of the load as well as mitigation of power quality problems where as the source meets only the active power requirement of the load.

This thesis is presented in five chapters which include power quality issues and custom power devices used in distribution system. The second chapter presents literature review and two conventional control algorithms namely Power Balance Theory (PBT) and Instantaneous Reactive Power Theory (IRPT). Some new control techniques have been developed and presented in chapter 3 which include Linear Quadratic Regulator (LQR), Composite Observer and Proportional Resonant Controller (PR). Chapter 4 deals with the control of DSTATCOM under distorted supply mains. The last chapter discusses some modeling and design aspects of Wind connected Permanent Magnet Synchronous Generator.

ACKNOWLEDGEMENT

I would like to thank Prof. Madhusudan Singh (HOD) Electrical Department for supporting this work.

I also give my high, respectful gratitude to my supervisor Dr. Alka Singh, for her guidance, supervision and help throughout this project. I have learned a lot throughout this project work with many challenging yet valuable experiences.

Finally I would like to thank all those people who have directly or indirectly helped me in successfully completing this project.

List of Tables

List of figures

List of Symbols and Abbreviations

1. $v(t)$ = single phase voltage
2. $i(t)$ = single phase current
3. V = Root mean square (rms) value of voltage $v(t)$
4. I = Root mean square value of current $i(t)$
5. $\emptyset$ = phase difference between voltage and current
6. $p(t)$ = single phase power
7. P = single phase active power
8. Q = single phase reactive power
9. S= single phase apparent power
10. $v_a(t)$ = 'a' phase line to neutral voltage of three phase system
11. $v_b(t)$ = 'b' phase line to neutral voltage of three phase system
12. $v_c(t)$ = 'c' phase line to neutral voltage of three phase system
13. $i_a(t)$ = 'a' phase current of three phase system
14. $i_b(t)$ = 'b' phase current of three phase system
15. $i_c(t)$ = 'c' phase current of three phase system
16. $P_{3\emptyset}(t)$ = three phase instantaneous active power
17. $S_{3\emptyset}$ = three phase apparent power
18. $Q_{3\emptyset}$ = three phase reactive power
19. THD = total harmonic distortion
20. IEEE = institute for electrical and electronics engineers
21. FACTS = flexible ac transmission system
22. TCSC = Thyristor Controlled Series Capacitor or compensator
23. SSSC = Static Synchronous Series Compensator
24. SVC = Static Var Compensator
25. STATCOM = Static synchronous Compensator
26. DVR = Dynamic voltage regulator
27. UPFC = Unified Power Flow Controller
28. IPFC = Interline Power Flow Controller
29. UPQC = Unified Power Quality Conditioner
30. TCR = Thyristor Controlled Reactor
31. FC = fixed capacitor

32. SCR = silicon controlled rectifier
33. VSC = voltage source converter
34. TSR = thyristor switched reactor
35. PWM = pulse width modulation
36. DSTATCOM = distribution static compensator
37. IGBT = insulated gate bipolar transistor
38. PCC = point of common coupling
39. IRPT = instantaneous reactive power theory
40. ISC = instantaneous symmetrical component
41. SRF = synchronous rotating frame
42. PI = proportional integral
43. LQR = linear quadratic regulator
44. SAF = shunt active filter
45. PR = proportional resonant
46. PMSG = permanent magnet synchronous enerator
47. DFIG = doubly fed induction generator
48. HVDC = high voltage direct current
49. C_{dc} = dc link capacitor
50. L_s = source inductance
51. L_f = interfacing inductance
52. PBT = power balance theory
53. V_t = amplitude of terminal voltage
54. v_{sa} = phase voltage of phase 'a'
55. L = Interfacing Inductor
56. R = Leakage Resistance of Interfacing Inductor
57. R_{load} = Load Resistance
58. L_{load} = Load Inductance
59. i_{La} = load current of phase 'a'
60. i_{La}, i_{Lb} and i_{Lc} = three-phase load currents
61. i_α , i_β = αβ components of load currents
62. $G_c(s)$ = controller transfer function in 's' domain kp, kr the proportional gain, integral gain
63. w = angular frequency in rad/sec
64. w_c = cutoff angular frequency in rad/sec

65. k_{rh} = the resonant gains and h indicates the order of the harmonic
66. $i_{\alpha 1}$ $i_{\beta 1}$ = The fundamental αβ components
67. i_{Lp} = fundamental weight component of the load current
68. h_{th} = order of harmonic
69. V_t = amplitude of three phase voltage at PCC
70. V_a ,V_b , V_c = voltage of phase 'a', 'b'and'c'
71. u_{sa} = Unitemplate of phase 'a'
72. u_{sb} = Unitemplate of phase 'b'
73. u_{sc} = Unitemplate of phase 'c'
74. $V^*_{dc(n)}$ = Reference DC link voltage
75. $V_{dc(n)}$ = sensed DC link voltage
76. $I_{loss(n)}$ = loss component of current
77. K_p and K_i = proportional and integral gain constant of the PI controller
78. I^*_{active} = total active power component of the grid current
79. i_{sa}*, i_{sb}* and i_{sc}* = in-phase components or active power components of the reference instantaneous grid currents
80. i_{sa}, i_{sb} and i_{sc} = actual supply currents
81. T_s = sampling time
82. $F_{1(z)}$ = the transfer function of the PR filter tuned for the fundamental frequency
83. I_s = supply currents
84. I_{La}, I_{Lb}, I_{Lc} = load currents
85. I_{ca}, I_{cb}, I_{cc} = compensating currents
86. P_L = instantaneous active power of load
87. $I_{L\ active}$ = amplitude of fundamental active power component of load current
88. $V_{dec(n)}$ = error in DC link voltage and sensed voltage at n_{th} sample
89. I^*_{sad} = active power source current reference for phase 'a'
90. I^*_{sbd} = active power source current reference for phase 'b'
91. I^*_{scd} = active power source current reference for phase 'c'
92. w_{sa} = Unitemplate in quadrature of phase 'a'
93. w_{sb} = Unitemplate in quadrature of phase 'b'
94. w_{sc} = Unitemplate in quadrature of phase 'c'
95. $I_{qloss(n)}$ = PI controller output for terminal voltage V_t
96. Q_L = instantaneous reactive power of load
97. $I_{L\ reactive}$ = amplitude of fundamental reactive power component of load current

98. $I^{*}_{reactive}$ = total reactive power component of the grid current
99. i^{*}_{saq} = reactive power source current reference for phase 'a'
100. i^{*}_{sbq} = reactive power source current reference for phase 'b'
101. i^{*}_{scq} = reactive power source current reference for phase 'c'
102. PFC = power factor correction mode
103. p_{loss} = power loss to maintain V_{dc} to desired value
104. X and U = state vector and input vector for LQR system
105. A and B = system matrix for LQR
106. J = LQR cost function for the system
107. u = control variable for LQR
108. K = LQR gains for the system
109. Q and R = weight and penality matrix for LQR
110. VSI = voltage source inverter
111. D = composite constant gain vector
112. V_d and V_q = d and q component of voltages
113. i_d and i_q = d and q component of currents
114. L_d and L_q = d and q component of stator inductance of PMSG
115. w_e = angular frequency in electrical radian per second
116. w_m = angular frequency in mechanical radian per second
117. $\emptyset_r$ = peak value flux in PMSG
118. R_s = stator resistance of PMSG
119. MPPT = maximum power point tracking
120. $P_{turbine}$ = wind turbine power
121. ρ = air density
122. $C_p(\lambda, \beta)$ = power coefficient
123. V_W = wind speed
124. λ = tip speed ratio
125. r = turbine blade radius
126. T_e = electrical torque in Nm
127. SVPWM = space vector pulse width modulation
128. T_{ref} = reference torque
129. i_{qs}^{*} = reference current of q component for PMSG
130. i_{ds}^{*} = reference current of d component for PMSG

CONTENTS

CHAPTER 1

INTRODUCTION

1.1 General

In present times power systems are designed to operate more efficiently to supply the power at various load centers with high reliability. The generation of power is either located at remote places as in case of hydro or can be located near load centers in the case of thermal power plants. In the former case, power transmission is required through transmission lines. The transmission lines accounts for the losses in transmitting power and also they do not have any provision for the control of power flow; the power flow in AC transmission lines is enhanced for higher power transfer capacity and to ensure system stability and reliability under dynamic conditions i.e. under disturbances subjected to the system.

On the other hand, there has been an increased concern for the quality of power delivered to factories, commercial localities, and residences. This is because use of harmonic-generating systems in use has increased. Some common examples of such loads are adjustable-speed drives, switching power supplies, arc furnaces, electronic fluorescent lamp ballasts, and other harmonic-generating equipment all of which contribute to generation of harmonic in the system.

1.2 Basic Definitions

In AC single phase system, for a resistive inductive load the voltage and current can be represented as following,

$$v(t) = \sqrt{2}\, V \sin(wt) \tag{1.1}$$

$$i(t) = \sqrt{2}\, I \sin(wt - \emptyset) \tag{1.2}$$

where V and I are the root mean square (rms) values of the voltage and current respectively and w is the angular frequency of the system, $\emptyset$ denotes the phase difference between voltage and current. The instantaneous active power is then given by the product of instantaneous values of voltage and current,

$$p(t) = 2\,VI\sin(wt)\sin(wt - \emptyset)$$

$$= VI\,Cos(\emptyset) - VI\sin(2wt - \emptyset)$$

$$= VI\,Cos(\emptyset)\,[1 - \cos(2wt)] - VI\sin(\emptyset)\sin(2wt) \quad (1.3)$$

Thus the instantaneous power comprises two parts, part I has an average value equal to $VI\,Cos(\emptyset)$ and as oscillating component of double the system frequency. Part II has pure oscillating component of double frequency and has a peak value of $VI\sin(\emptyset)$ and having zero average value.

The average value of the I part is known as active power which has SI units of Watt (W)

$$P = V\,I\,Cos\,(\emptyset) \quad (1.4)$$

Reactive power is defined as the peak value of the part II, its unit is VAR (volt ampere reactive)

$$Q = V\,I\,Sin\,(\emptyset) \quad (1.5)$$

Apparent power is generally used to define the power rating of electrical equipment, it is given by

$$S = V\,I \quad (1.6)$$

The SI unit for apparent power is VA (volt ampere)

Power factor is defined as the ratio between the active power P and apparent power S and is represented as $\cos(\emptyset) = P/S$.

In case of a balanced three phase system only positive sequence fundamental voltages and currents are present and can be written as following

$$v_a(t) = \sqrt{2}\,V\sin(wt) \quad (1.7)$$

$$v_b(t) = \sqrt{2}\,V\sin(wt - \tfrac{2\pi}{3}) \quad (1.8)$$

$$v_c(t) = \sqrt{2}\,V\sin(wt + \tfrac{2\pi}{3}) \quad (1.9)$$

$$i_a(t) = \sqrt{2}\,I\sin(wt + \emptyset) \quad (1.10)$$

$$i_b(t) = \sqrt{2}\, I \sin(wt + \emptyset - \frac{2\pi}{3}) \quad (1.11)$$

$$i_c(t) = \sqrt{2}\, I \sin(wt + \emptyset + \frac{2\pi}{3}) \quad (1.12)$$

where V and I are the root mean square (rms) values of the voltage and current respectively and w is the angular frequency of the system, ∅ denotes the phase difference between voltage and current. For three phase system instantaneous active power $p_{3\emptyset}(t)$ is given by

$$P_{3\emptyset}(t) = v_a(t)\, i_a(t) + v_b(t)\, i_b(t) + v_c(t)\, i_c(t) \quad (1.13)$$

On putting the above values in eq.1.13 and simplifying we get,

$$P_{3\emptyset}(t) = 3\, V\, I \cos\emptyset = 3\, P \quad (1.14)$$

where P is single phase power. This three phase instantaneous active power is a constant and not time dependent as in case of single phase system.

Similar to the definition of single phase apparent power, three phase apparent power can be defined and is written as

$$S_{3\emptyset} = 3\, V\, I = 3\, S \quad (1.15)$$

Further three phase complex power is defined as three times single phase complex power and definition of three phase reactive power can be derived from imaginary part of the three phase complex power

$$S_{3\emptyset}{}^{*} = 3\, V\, I^{*} = 3\, V\, I \cos\emptyset + j\, 3\, V\, I \sin\emptyset \quad (1.16)$$

Thus from the imaginary part of complex three phase power we have three phase reactive power as three times the single phase reactive power.

$$Q_{3\emptyset} = 3\, V\, I \sin\emptyset \quad (1.17)$$

1.3 Power Quality

The power equation given above in Eq (1.14) is valid for the case when the supply is sinusoidal and harmonic free. In case of harmonic pollution which can be estimated by a measure known as total harmonic distortion(THD),it has been observed that high harmonic distortion can have negative impact on electric distribution system,

and can generate excessive heat in power system equipment such as motors, causing early failures. These harmonics can also heat up wire insulation causing breakdown and failure. Increased operating temperatures can affect other equipment as well.

Poor power quality can affect the accuracy of utility metering, cause protective relays to malfunction, and it can also result in equipment downtime and even damage, resulting in loss of productivity and related economic losses. Harmonic voltages and currents can also cause false tripping of ground fault circuit interrupters. These devices are used extensively in residences for local protection of near appliances. Instrument and relay transformer accuracy can be affected by harmonics, which can also cause tripping of circuit breakers. Harmonics have adverse effect over frequency switching circuits such as switching power supplies, power factor correction circuits, and adjustable-speed drives.

Power quality is defined in IEEE Standard Terms as [75]:

The concept of powering and grounding electronic equipment in a manner that is suitable to the operation of that equipment and compatible with the premise wiring system and other connected equipment.

1.3.1 Typical Power Quality Problems

Apart from the harmonic problem discussed above, voltage related problems in the form of sag and swell are common. Generally voltage sag, also called a 'dip' is a small decrease in the rms line voltage of the system and affects the power quality. Common causes of sags in the system are the starting of large induction motors and utility faults. Another ill effect in voltage is called voltage swell which is the converse to the sag. A voltage swell is defined as the increase in the rms line-voltage of the system. Sources of voltage swells could be faults and incorrect tap settings in tap changers in substations.

Impulsive transients in the power system caused by lightning strikes, switching of inductive loads, or switching in the power distribution system produces unidirectional variation in voltage and current thus causes poor power quality. These transients can result in equipment shutdown or even complete damage to the power equipment. Similarly oscillatory transients which are bidirectional variation in voltage,

current and power has negative impact on power quality as well. Major cause for its occurrence is due to the switching of power factor correction capacitors, or transformer ferro resonance.

Voltage fluctuations are relatively small variations in the rms line-voltage. These variations can be caused by power electronic based cyclo-converters, arc furnaces, and other systems that draw current not in synchronization with the line frequency. Such fluctuations can result in variations in the lighting intensity due to an effect known as “flicker” which is visible to the end user. Voltage “imbalance” is a variation in the amplitudes of three-phase voltages, relative to one another.

Another common power-quality event is “notching,” which can be created by rectifiers that have finite line inductance. The notches show up due to an effect known as current commutation.

The discussion of different power quality problems highlights that power-quality events need to be detected and corrected to get the uninterrupted good quality electrical service. The possible mitigating strategies for poor power quality and required devices are detailed in the subsequent section. These are Custom power Devices

Some of these devices are used in the transmission system and commonly referred to as Flexible AC Transmission System (FACTS) devices.

1.4 FACTS and Custom Power Devices

Devices used for increasing power transfer capabilities and to have high stability in the system are called as FATCS devices. They are generally used in transmission systems at higher voltage level while the custom power devices are used in distribution systems for mitigation of power quality problems.

Some FACTS and custom power devices are:

i. Thyristor Controlled Series Capacitor or compensator (TCSC)
ii. Static Synchronous Series Compensator (SSSC)
iii. Static Var Compensator (SVC)
iv. Static synchronous Compensator (STATCOM)

v. Dynamic voltage regulator (DVR)

vi. Unified Power Flow Controller (UPFC)

vii. Interline Power Flow Controller (IPFC)

viii. Unified Power Quality Conditioner (UPQC)

A brief introduction of these devices is explained below.

1.4.1 Thyristor Controlled Series Capacitor or Compensator (TCSC)

TCSC comprises of a series capacitor bank, shunted by a Thyristor Controlled Reactor (TCR), to provide a smoothly variable series capacitive reactance. It is connected in series with transmission line; it uses natural commutation; its switching frequency is low; it contains insignificant energy storage and has no DC port. Insertion of a capacitive reactance in series with the line's inherent inductive reactance lowers the total, effective impedance of the line and thus virtually reduces its length. As a result, both angular and voltage stability gets improved. Fig.1.1 shows the circuit diagram of TCSC device.

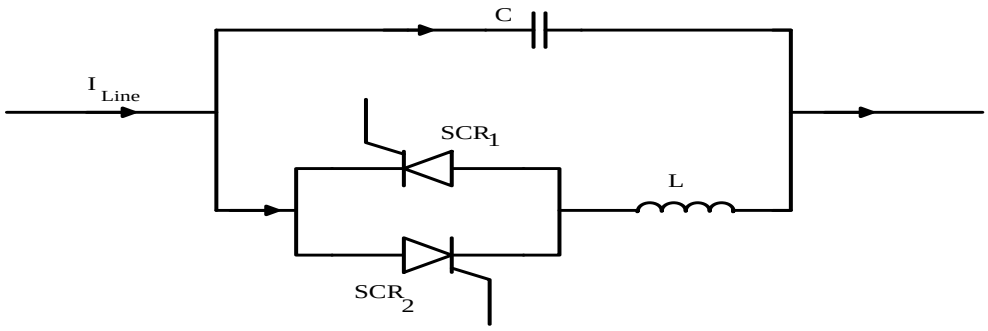

Fig.1.1 Schematic of TCSC device

1.4.2 Static Synchronous Series Compensator (SSSC)

SSSC is a FACTS device that employs a voltage source converter connected in series to a transmission line through a transformer. The SSSC operates like a controllable series capacitor and series inductor. The primary difference is that its injected voltage is not related to the line intensity and can be managed independently. This feature allows the SSSC to work satisfactorily with high loads as well as with lower loads.

The Static Synchronous Series Compensator has three basic components:

a. Voltage Source Converter (VSC) – main component

b. Transformer – couples the SSSC to the transmission line

c. Energy Source – provides voltage across the DC capacitor and compensate for device losses

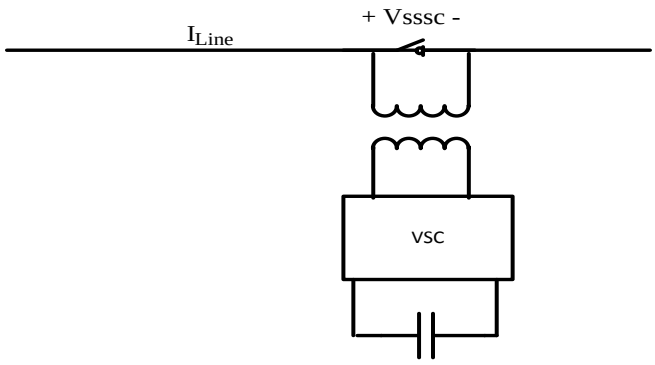

Fig.1.2 Schematic of SSSC device

1.4.3 Static Var Compensator (SVC)

Static Var Compensator is a shunt-connected static Var generator or absorber whose output is adjusted to exchange capacitive or inductive current so as to maintain or control specific parameters of the electrical power system such as bus voltage. SVC is constructed using thyristors without gate turn-off capability. The operating principlel and characteristics of thyristors realize SVC as a variable reactive impedance. SVC includes two main components and their combination: Thyristor-controlled and Thyristor-switched Reactor (TCR and TSR), and Thyristor-switched capacitor (TSC).

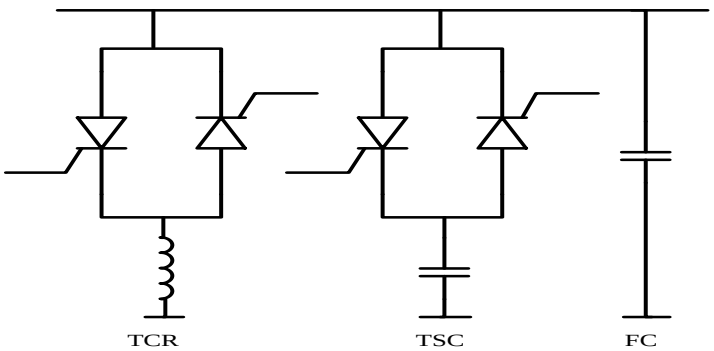

Fig.1.3 Schematic of SVC device

1.4.4 Static Synchronous Compensator (STATCOM)

The first power electronics based static shunt compensator is SVC which uses thyristor-controlled reactor in parallel with fixed or thyristor-switched capacitors. The problem associated with SVC was that the compensation provided by SVC depends upon the bus voltage on which it was connected; thus to overcome this problem STATCOM has been introduced. The emerging technology of high power voltage source converters using pulse width modulation (PWM) also replaced thyristor-based controllers and the application of VSC also permitted multi-function compensation that includes active filtering to prevent the flow of harmonic currents on the source side.

STATCOM is also known as static synchronous condenser (STATCON). This is used a regulating device in AC power transmission network. STATCOM is a device made of voltage-source converter and either a source or sink of reactive AC power of power system network. This device when connected to a source of power can also provide active AC power to the loads.

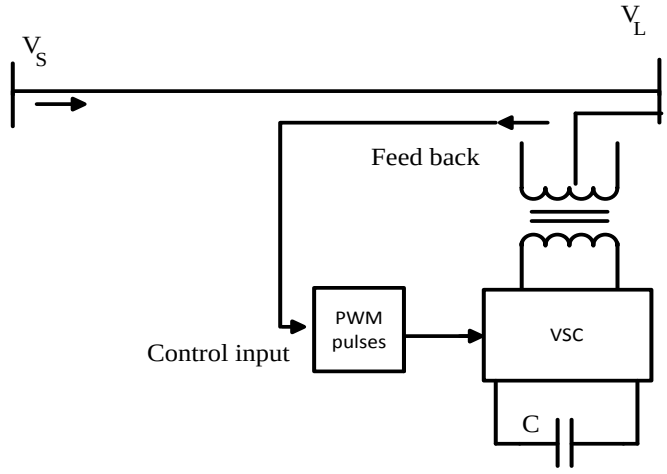

Fig. 1.4 Schematic of STATCOM

Generally a STATCOM device is installed in the electricity networks where poor power factor and poor voltage regulation are observed. STATCOM has other uses as well but most common use is for voltage stability. A STATCOM is a voltage source converter (VSC) based device having a voltage source. This voltage source is created from a DC capacitor and therefore a STATCOM has less active power capability than other devices but its active power capability can be increased if a suitable energy storage device is connected across the DC capacitor. The reactive power supplied by the STATCOM is dependent on the amplitude of the voltage source

connected. The response time of a STATCOM is less as compared to static VAR compensator (SVC), this is because of faster switching provided by the IGBTs of the voltage source converter. The STATCOM also provides better reactive power support at low AC voltages than an SVC, since the reactive power from a STATCOM decreases linearly with the AC voltage as voltage is reduced at low current as inferred from Fig.1.5.

An application of STATCOM is for reactive power compensation and voltage regulation in distribution system it is therefore termed as DSTATCOM (distribution static compensator). A DSTATCOM has obvious advantages over a SVC. A major advantage relates to the improved speed of response, capacity for transient overload (up to one second) in addition to the improved performance at reduced voltages as can be seen in the V-I characteristic of SVC and STATCOM.

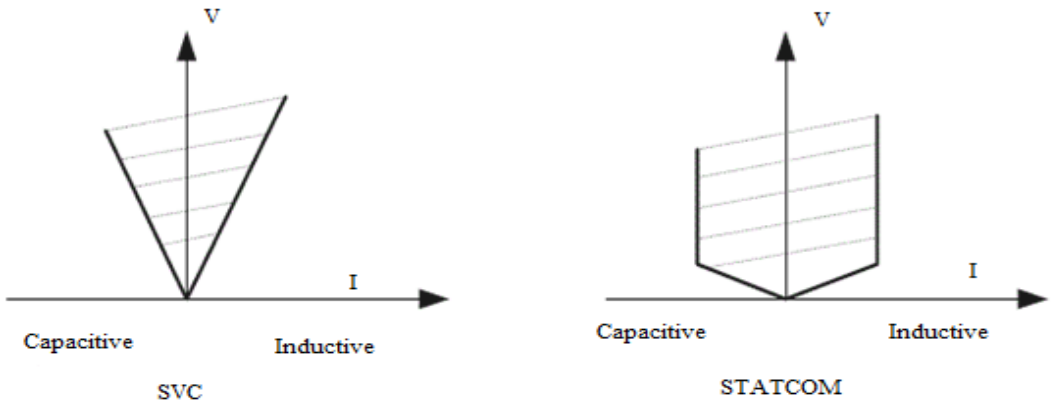

Fig.1.5 V-I characteristics of SVC and STATCOM

It can be inferred from the V-I characteristic of SVC that at reduced voltage the compensation provided by it is reduced as reactive power injected has reduced because at reduced voltage current is reduced whereas in case of STATCOM even at reduced voltage of the system, the current is same and thus provides same amount of reactive power irrespective of the reduction in voltage.

1.4.5 Dynamic Voltage Regulator (DVR)

The most common disturbances in the source voltages are the voltage sags or swell that can be due to either disturbances arising in the transmission system, adjacent feeder faults and fuse or breaker operation. Voltage sags of even 10% lasting

for 5-10 cycles can result in extensive damage to critical loads. A Dynamic Voltage Restorer or regulator has to is an solution to the voltage sag problem, it supply energy to the load during the voltage sags. If a DVR has to supply active power over longer periods, it is convenient to provide a shunt converter that is connected to the DVR on the DC side. The application of DVR for fundamental frequency voltage magnitude restoration is most common. The configuration of a DVR is shown in Fig1.6.

The voltage source converter is typically one or more converters connected in series to provide the required voltage rating. The DVR can inject a (fundamental frequency) voltage in each phase of required magnitude and phase. A DVR has mainly three components namely voltage source converter, injection transformer and the energy storage to provide active power to the load during voltage sag.

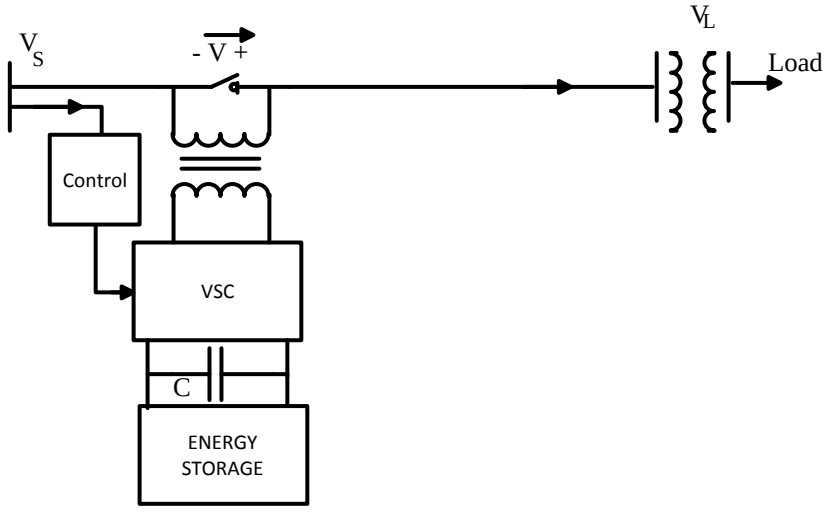

Fig. 1.6 Single line diagram of DVR

1.4.6 Unified Power Flow Controller (UPFC)

Unified Power Flow Controller is a device used for faster reactive power compensation in power transmission networks. UPFC uses two three-phase VSC bridges to produce current that is injected into a transmission line using a series transformer. The controller can control active and reactive power flows in a transmission line. The UPFC provides operational flexibility which is generally not available with conventional thyristor controlled systems. The UPFC is a combination of two FACTS devices which are static synchronous compensator (STATCOM) and a

static synchronous series compensator (SSSC) that is coupled through common DC voltage link. The main advantage of the UPFC is to control the active and reactive power flows in the transmission line. UPFC operates only under balanced sine wave source.

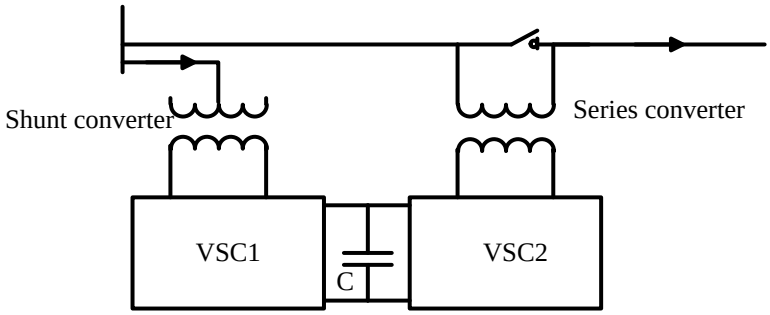

Fig.1.7 Single line diagram of UPFC

1.4.7 Interline Power Flow Controller (IPFC)

The interline power flow controller (IPFC) is one of the latest generation and advanced flexible AC transmission systems controller which can be used for dynamic compensation and effective power flow management among transmission lines. It is VSC-based FACTS controller for Series compensation with the unique capability of power management among multiline of a substation. It simultaneously controls the power flow in multiline systems or sub network. Since IPFC contains converters with common direct current link, any inverter within the IPFC is able to transfer real power to another and there by facilitate real power transfer among the lines of the transmission system. IPFC may be used to solve the complex transmission network overcrowding management problems that transmission companies are now a day facing to transmit a large power. Simplicity and fast system response are two main characteristics of Interline power flow controller. Out of the many FACTS devices today, IPFC is more advanced and has the capability to solve the overcrowding of the power management of the transmission system

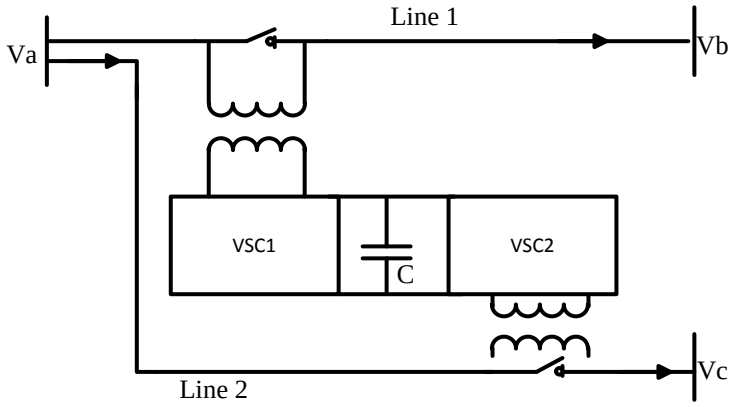

Fig.1.8 Single line diagram of IPFC

1.4.8 Unified Power Quality Conditioner (UPQC)

Both DSTATCOM and DVR are combined to have Unified Power Quality Conditioner that controls the power quality of the source current and the load bus voltage. In UPQC, if the DVR and STATCOM are connected to the common DC link, the DC bus voltage can be regulated by the shunt connected DSTATCOM while the DVR can supply the required energy to the load in case of the transient disturbances in source voltage. This UPQC is similar in structure to UPFC but difference lies in the control objective of both. The shunt converter in UPQC regulates DC bus voltage, balance supply current, compensates the harmonic content of load and also controls the power factor. On the other hand work done by series converter is to balance and regulate the load bus voltage.

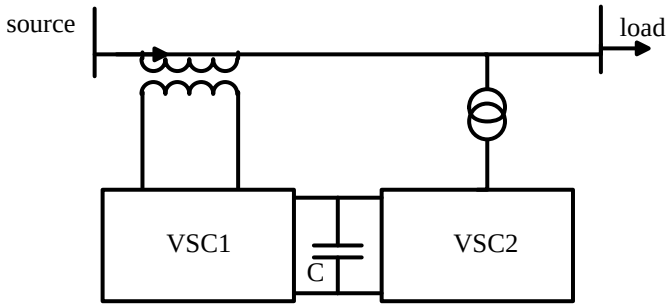

Fig.1.9 Single line diagram of UPQC

1.5 Conclusion

FACTS devices improve the power flow through the transmission lines and the custom power devices improve the power quality. Though there are plenty of FACTS/Custom power devices available; the choice of a particular device depends on

the need and application. Both types of these devices can be connected in shunt, series and unified manner. However their principle of operation and control algorithms are different. In this thesis work, studies are confined to DSTATCOM modeling, design and control for three phase three wire systems. Studies are performed to investigate the effect of DSTATCOM and how best it is suited for solving power quality issues in distribution system. The power quality problems considered for solving include power factor correction (PFC), harmonic reduction, load unbalancing and voltage regulation problems.

CHAPTER 2

LITERATURE SURVEY AND CONVENTIONAL ALGORITHMS

2.1 General

Reliability as well as quality of power are of great concern in distribution systems such as power delivered to factories, commercial localities and residences. Today widespread use of harmonic-generating equipment such as adjustable-speed drives, switching power supplies, arc furnaces, electronic fluorescent lamp ballasts, has deteriorated the power supply and caused a great concern to power engineers.

Common power quality issues include voltage regulation problems and voltage sags are commonly perceived. For an industry, voltage sags occur more often and cause severe problems and economical losses. Utilities often focus on disturbances from end-user equipment as the main causes of power quality problems. A high percentage of Total Harmonic Distortion or THD of the load current means the current demanded by the application is highly non-linear and this has adverse effect on the supply of the power system and also to the other connected loads.

2.2 Literature Survey

Three phase distribution systems have faced the poor power quality problems such as unbalanced loading, excessive neutral current and voltage distortion due to current harmonics. The reason for this is the majority of loads in the distribution systems are linear lagging power factor. Such power quality problems can be mitigated by the DSTATCOM (Distribution Static Synchronous Compensator) at the point of common coupling (PCC) [1-5]. A number of topologies of DSTATCOM are reported in the literature for the load compensation along with the neutral current compensation such as a 4-leg VSC (Voltage Source Converter) [4], 3-leg VSC with split capacitor [3], H-bridge VSC with star-hexagon transformer [6], H-bridge VSC with star-delta transformer [7] and three-leg DTATCOM with zigzag transformer [8-12] etc. The control of DSTATCOM is simple and many other control techniques are reported in the literature for extracting the reference source currents such as Synchronous Reference

Frame commonly known as SRF theory, Instantaneous Reactive Power theory(IRPT), Instantaneous Symmetrical Components theory (ISCT), PI controller based controller and Neural Network (adaline) control scheme [2- 5]. A conventional technique based on Power Balance Theory is proposed for the active filter for power factor correction [13-15].

Several other control schemes to track the reference currents have been proposed till date like two control schemes to enhance dynamic performance of DSTATCOM [16–18]. In LQR technique the optimization of a cost function or performance index of system, which includes weight for the state parameters provided by the design engineer according to their influence in the control action to obtain desired performance. The linear quadratic regulator (LQR) based on the optimal control of three-phase ac–dc converters with unity power factor was applied for sinusoidal current pulse width modulation (PWM) rectifiers and the neutral point clamped PWM rectifier in [17] and [18]. An optimal servo-controller was also applied in [19] to the current inner loop of the SAF in the cascade strategy where an outer loop used a simple PI regulator for the dc bus voltage. In Grid connected wind energy system for power quality improvement [19], in hysteresis current control (HCC) current control mode of the DSTATCOM was achieved. The HCC technique works on switching frequency that depends on the hysteresis band used this proves to be always stable for first-order systems [20]. In higher-order systems, to make actual currents closer to reference currents, hysteresis band must be narrow or nearing to zero that result in perfect tracking, but very high switching frequency is required, which is undesirable. Literature survey indicated that the linear quadratic regulator (LQR) is superior in its response and requires less control effort [21].

Advanced soft computing based controllers such as artificial neural network [22-24], fuzzy based, adaline [25], adaptive neuro fuzzy inference system (anfis) [26] based are interesting but slightly complex. Recently a number of new controllers [27-29] based on repetitive computation and updating of weights such as Anti Hebbian [27], adaptive notch based control [28] and recursive techniques[29] are also immensely popular, Lyapunov candidate-based algorithm which is developed using the Lyapunov stability theory [30], predictive current control [31], mixed-frame and stationary-frame repetitive control algorithm [32], modified SRF [33], sliding mode observer-based control [34], control based on state observers [35] and composite

observer [36, 37] for harmonic extraction and various PWM technique for PWM switching [38, 39]. The composite observer-based control algorithm [36] is very often used in single-phase system for extraction of harmonic current components and its implementation for three-phase shunt compensator.

Conventional PI controller is commonly used but has limitation that they cannot track non dc or sinusoidal references without error. Hence to overcome the drawbacks of conventional PI controller, proportional resonant (PR) controllers have been proposed in many recent works [40-48]. The PR controller essentially introduces an infinite gain at a selected resonant frequency for eliminating steady state error at that frequency. Hence, multiple PR controllers can be used for selectively compensating low order harmonics various applications are discussed in [40-45]. The performance of multi frequency PR regulator has been studied in [46-47]. Digital implementation can be performed using discretization methods such as zero order hold, first order hold, Euler method, Tustin approach etc. summarized in [48].

Most rapidly growing form of renewable energy source today is wind power. A wind turbine usually operates at a fixed or variable speed [49]. Most of the major wind turbine manufacturers are developing new megawatt scale wind turbines based on variable-speed operation with pitch control using either a permanent magnet synchronous generator (PMSG) or a doubly fed induction generator (DFIG) [50]. The variable speed wind turbine with a multiple pole PMSG integrated with fully controllable voltage source converters (VSCs) is considered to be a promising wind turbine concept [51]. The PMSG configuration offers advantages such as gearless construction [52] and the elimination of a dc excitation system [53] with full controllability of the system for maximum wind power extraction and grid interface. Therefore, the efficiency and reliability of a VSC-based PMSG wind turbine is assessed to be higher than that of a DFIG wind turbine [55]. Due to the intensified grid codes, a PMSG wind turbine with full VSC-based insulated gate bipolar transistor (IGBT) converters is becoming popular [51]–[55].At the present time, however, commercial PMSG technology mainly uses a passive rectifier followed by an IGBT inverter [56]–[59]. The highly efficient vector-controlled technology for a PMSG wind turbine that uses a full voltage-source IGBT converter configuration is still under investigation [60]–[62] and not widely adopted by the wind power industry. The direct-current vector control technology is a vector control technology that has been developed recently for

control of the synchronous generator only in a variable-speed PMSG wind turbine [63], [64] and for control of a VSC-based HVDC system [65]. Compared to the conventional vector control strategies, direct-current vector control has demonstrated many advantages in those applications, such as enhanced system stability, reliability, and efficiency.

2.3 System Considered

A general diagram of the three-phase, three wire system connected DSTATCOM is presented in Fig.2.1. Non-linear load is supplied by the three phase utility grid and the DSTATCOM is connected at the point of common coupling (PCC). DSTATCOM is realized as a three-phase, three-leg voltage source converter (VSC) with two insulated gate bipolar transistor (IGBTs) in each leg. A capacitor (C_{dc}) is connected at the DC link of the VSC. The shunt compensator is controlled to provide the necessary current injection so that utility grid currents are perfectly balanced, sinusoidal and phase displaced irrespective of the load changes. The DSTATCOM is incorporated into the system through practical inductors (L, R) that has some leakage resistance. The nonlinear load is modeled as a three phase diode rectifier with a load R-L connected at the DC link.

DSTATCOM compensators can be current controlled pulse-width modulated (PWM) converters which use a control structure comprising an internal current feedback loop for generation of pulses. The basic block diagram of current controlled PWM converter is shown in Fig.2.2. Pulse Width Modulation (PWM) technique is used to provide pulses to the VSC, in PWM technique reference currents generated through control algorithms are compared with sensed supply currents and fed to Hysteresis Current Control (HCC) to get the desired pulses. In HCC a band is generated around 2% on reference currents and through proper switching of the VSC, the supply currents are tend to follow this band and achieve sinusoidal variation.

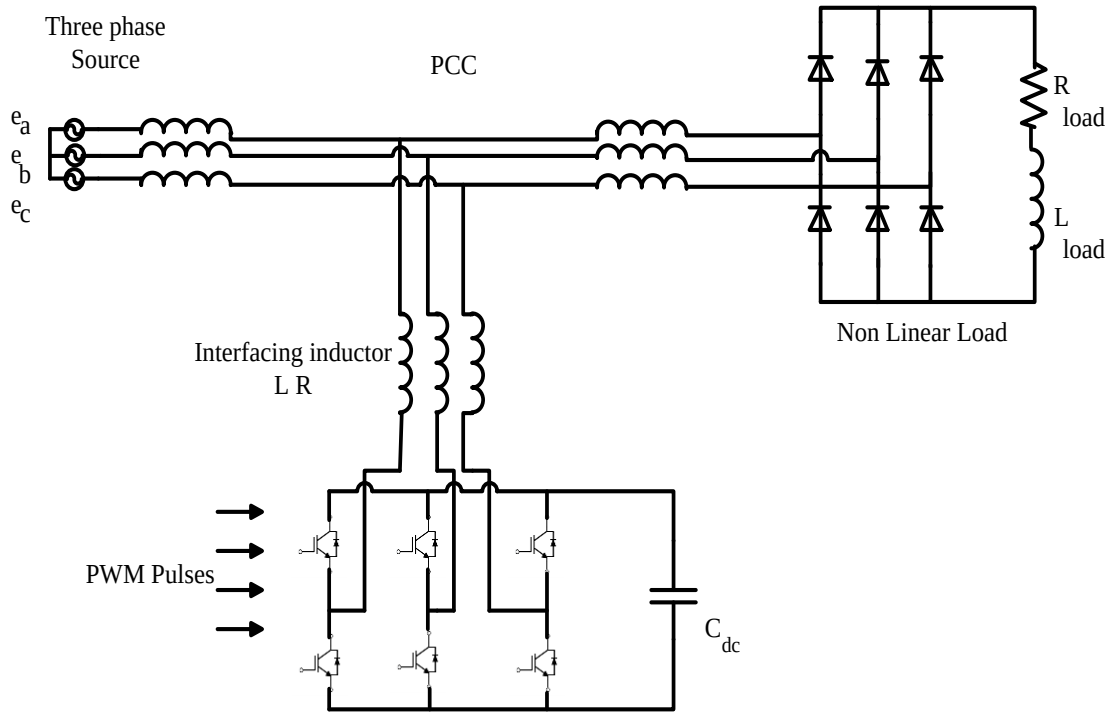

Fig.2.1 Integration of DSTATCOM into system

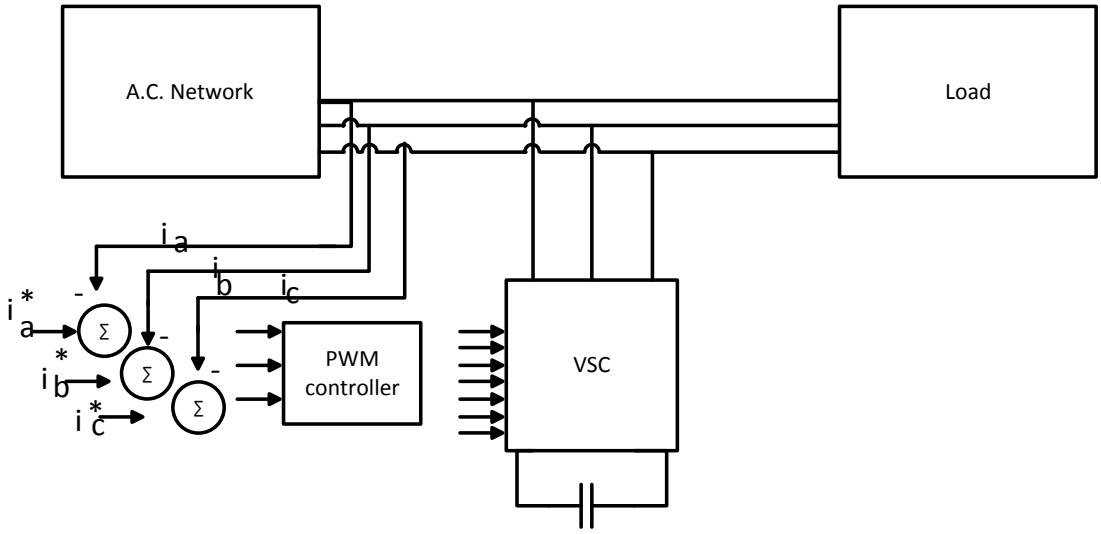

Fig 2.2 PWM current controller

2.4 System Parameters

Supply mains AC: 3phase-110 V, 50 Hz. Source inductance: L_s=0.01 mH for power factor correction mode and L_s=0.04mH for voltage regulation mode. DC-

link voltage: V_{dc}=200V and dc link capacitor=1500μF. Interfacing inductor: L_f =3mH. Nonlinear load: three-phase uncontrolled diode rectifier with 15Ω, 100 mH

2.5 Conventional Control Algorithms

In this section two conventional control algorithms have been discussed and results are obtained by simulating in Matlab/ Simulink environment. The two algorithms studied are Power Balance Theory and Instantaneous Reactive Power Theory. In former active power is calculated to get active current component and generate reference currents by multiplying with unit templates. The later involves 3 phase to 2 phase transformation using Clarke's transformation and calculate power so as to get reference current by inverse transformation.

2.5.1 Power Balance Theory

Power Balance Theory (PBT) [14] based control algorithm is a popular conventional algorithm used to derive the reference grid currents. This control can be applied to STATCOM to achieve the power quality improvement at AC mains. The three-phase VSC compensates the harmonic currents and reactive power, and balances the nonlinear loads. The PBT is tested for power factor correction and voltage regulation along with harmonics current elimination, and load balancing of nonlinear loads.

For generation of reference source currents, estimation of active power component of grid currents and its two components (active power of connected loads and output of DC link voltage controller) is needed.

Following are the fundamental equations involved in PBT for calculation of grid currents.

V_t is the peak value of the three phase voltages at the point of common coupling and it is calculated using following equation,

$$V_t = [(2/3)(v_{sa}^2 + v_{sb}^2 + v_{sc}^2)]^{1/2} \quad (2.1)$$

The unit vectors which are in phase to the voltages of the system are calculated as,

$$u_{sa}= \frac{v_{sa}}{v_t}, u_{sb}=\frac{v_{sb}}{v_t}, u_{sc} = \frac{v_{sc}}{v_t} \quad (2.2)$$

The instantaneous value of active power consumed by the load is calculated as

$$P_L = (v_{sa}i_{La} + v_{sb}i_{Lb} + v_{sc}i_{Lc}) \quad (2.3)$$

The instantaneous active and reactive powers of the connected load consists of two components which are AC and DC, so a LPF (low pass filter is used in order to filter out the DC component which is the fundamental active power component of the connected load represented as P_L. The amplitude of this active power component of the load current is derived as

$$I_{L\ active} = (2/3)\ (P_L/V_t) \quad (2.4)$$

The second component of active power is used to regulate DC link voltage of VSC. This second component of the active power is calculated by the following equations. For the calculation of this second component, the error in the reference value of DC link voltage and sensed DC link voltage at the nth instant of sampling is taken such that,

$$V_{dec(n)} = V^*_{dc(n)} - V_{dc(n)} \quad (2.5)$$

where $V^*_{dc(n)}$ is the reference value of DC voltage and $V_{dc(n)}$ is the sensed value of the DC link voltage of the inverter at nth instant.

This error in voltage is fed through the PI controller to maintain the DC link voltage of inverter, the output of PI controller at the nth instant is expressed as,

$$I_{loss(n)} = I_{loss(n-1)} + K_p\ [\ V_{decr(n)} - V_{decr(n-1)}\ ] + K_i V_{decr(n)} \quad (2.6)$$

where $I_{loss(n-1)}$ is output of PI controller and is considered to be second component of active power of connected load. In the equation of $I_{loss(n-1)}$ K_p and K_i are the proportional and integral gains PI controller respectively.

This second component of the active power let us to calculate the total active power component of the grid current i.e. I^*_{active} which is then calculated by taking sum of the DC component $I_{Lactive}$ and the PI controller output $I_{loss(n)}$ as

$$I^*_{active} = I_{L\ active} + I_{loss(n)} \quad (2.7)$$

Thus required total in phase component of active power called as reference instantaneous grid currents in phase to the PCC voltages are calculated as following,

$I^*_{sad} = I^*_{active} * u_{sa}$, $I^*_{sbd} = I^*_{active} * u_{sb}$, $I^*_{scd} = I^*_{active} * u_{sc}$ (2.8)

Now the quadrature current component of the connected load also known as reactive power component is taken to be zero for power factor correction (PFC) at PCC and if not zero then it is considered to take care of voltage drop in the grid (source) impedance through small leading reactive power currents flowing in to the grid. However, it may also be lagging in nature also if the loads are of leading power factor. Therefore, VSC must feed partially or completely reactive power of the consumer loads.

For voltage regulation purpose, a second voltage PI controller is used to regulate PCC voltage over the PCC voltage. The output PI voltage controller is considered as a fundamental reactive power component of currents provided by VSC. Therefore, the reactive power components of grid currents are estimated by the difference of an output of PI voltage controller and the fundamental reactive power components of the consumer load currents calculated by using eq. (2.13). These quadrature or reactive power components of grid currents are estimated through following basic equations which involves unit templates in quadrature calculation and subsequent reactive power calculation.

The unit vectors in quadrature with in phase templates u_{sa},u_{sb} and u_{sc} are derived using a quadrature transformation of the in-phase unit vectors as,

$$w_{sa} = \frac{u_{sc} - u_{sc}}{\sqrt{3}},$$

$$w_{sb} = \frac{u_{sb} - u_{sc}}{2\sqrt{3}} + \frac{\sqrt{3}u_{sa}}{2}, \quad (2.9)$$

$$w_{sc} = \frac{u_{sb} - u_{sc}}{2\sqrt{3}} - \frac{\sqrt{3}u_{sa}}{2},$$

A second PI controller is used for maintaining terminal voltage at the PCC. The amplitude of terminal voltage (V_t) is sensed and its error with the desired value (V_{ref}) is fed to the PI controller. The voltage error fed to PI controller is estimated as,

$$V_{er(n)} = V^*_{tref(n)} - V_{t(n)} \quad (2.10)$$

The output of PI controller is represented as $I^*_{qr(n)}$ is the current required to maintain the amplitude of the PCC voltage to the desired value at nth instant which is given by,

$$I_{qloss(n)} = I_{qr(n-1)} + K_p [V_{er(n)} - V_{er(n-1)}] + K_i V_{er(n)} \quad (2.11)$$

where K_p and K_i are the gains of the proportional and integral value for the controller. The instantaneous reactive power of the connected load is estimated as

$$Q_L = \frac{1}{\sqrt{3}} [(v_{sa} - v_{sb})i_{Lc} + (v_{sb} - v_{sc})i_{La} + (v_{sc} - v_{sa})i_{Lb}] \quad (2.12)$$

This instantaneous value of load reactive power also has two components which are DC and AC. So to extract fundamental component of reactive power of the load a LPF (Low Pass Filter) is used.

The amplitude of the fundamental component of reactive power of the connected load is found by using the following equation,

$$I_{L\ reactive} = (2/3)\ (Q_L/V_t) \quad (2.13)$$

Hence the total amplitude of reactive power component of grid current is given as,

$$I^*_{reactive} = I_{qloss(n)} - I_{L\ reactive} \quad (2.14)$$

This leads to the calculation of instantaneous quadrature component of the reference grid currents as,

$$i^*_{saq} = I^*_{reactive} * w_{sa},\ i^*_{sbq} = I^*_{reactive} * w_{sb},\ i^*_{scq} = I^*_{reactive} * w_{sc} \quad (2.15)$$

The total reference grid currents are sum of their active power and reactive power components of their currents. These are estimated as

$$i^*_{sa} = i^*_{sad} + i^*_{saq},\ i^*_{sb} = i^*_{sbd} + i^*_{sbq},\ i^*_{sc} = i^*_{scd} + i^*_{scq} \quad (2.16)$$

These reference grid currents along with sensed grid currents are fed to hysteresis current controller (HCC) to generate gating pulses for inverter.

2.5.2 Performance of the System with PBT

PBT based simulation model used for analysis of DSTATCOM is designed in Matlab/Simulink. The control algorithm is tested for two different modes of operation which are power factor correction (PFC) mode and Voltage regulation mode. The load used in the simulation is a non-linear load modeled with diode bridge. The Gains used in PI controller are $k_p = 0.2$ and $k_i = 0.5$ for power factor correction mode and $k_p = 0.3$ and $k_i = 0.5$ in voltage regulation mode.

2.5.2.1 Performance of DSTATCOM under PFC mode

In Fig.2.3 the PFC mode operation of DSTATCOM is shown under nonlinear load conditions. Results for different signals are obtained that includes, supply mains current (i_s), voltages at PCC (v_{pcc}), load currents (i_{la},i_{lb} , i_{lc}), DSTATCOM currents as i_{ca}, i_{cb} , i_{cc} and the Dc bus voltage (V_{dc}) are shown. The results show that the voltage of Dc bus is maintained at the reference value of 200 V. In the same figure steady state of the system is seen to be existed upto 0.4s and when unbalancing in phase 'a' from 0.4s to 0.5s is introduced, the DSTATCOM still maintains sinusoidal variation in supply currents.

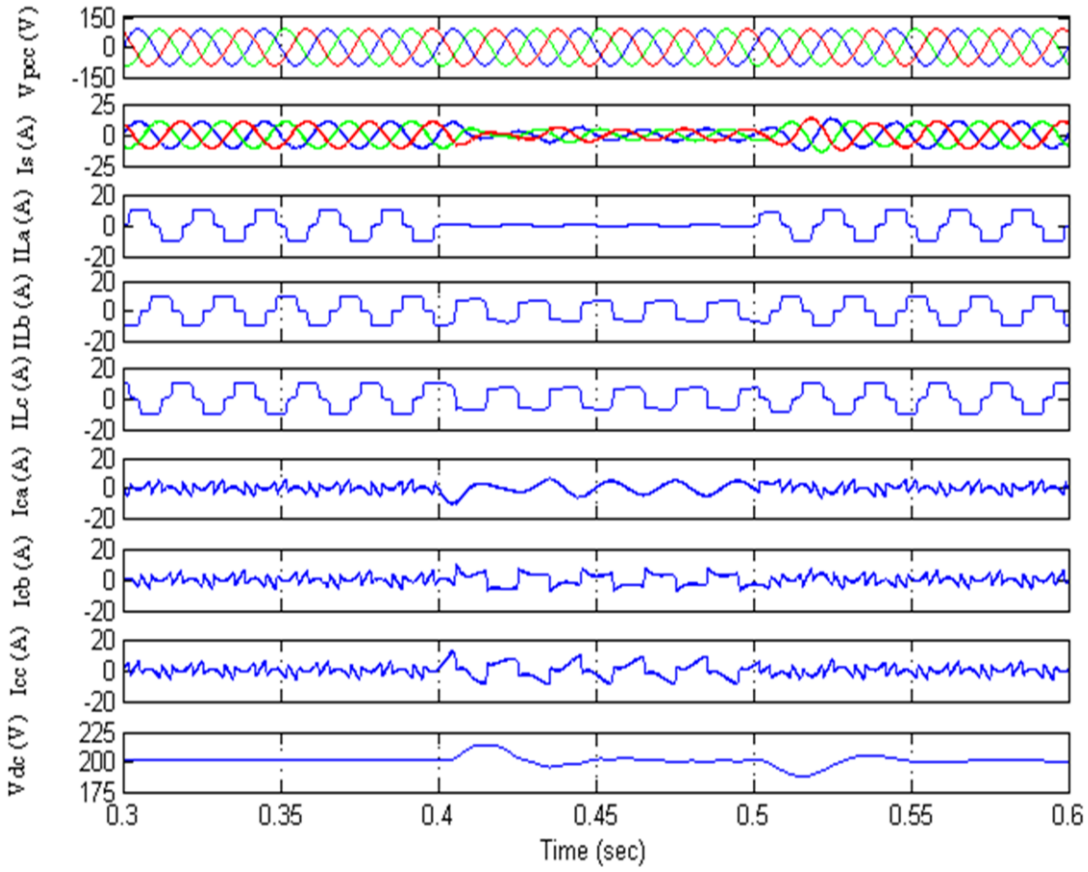

Fig. 2.3 Performance of DSTATCOM under PFC mode for PBT

In the following Fig.2.4, the harmonic analysis is shown, phase 'a' is taken of different signal for the harmonic spectrum. The result comprises of three signals namely supply current (i_{sa}), load current (i_{la}) and PCC voltage (v_{pcca}) in the power factor correction mode for nonlinear load. The results obtained provide the total

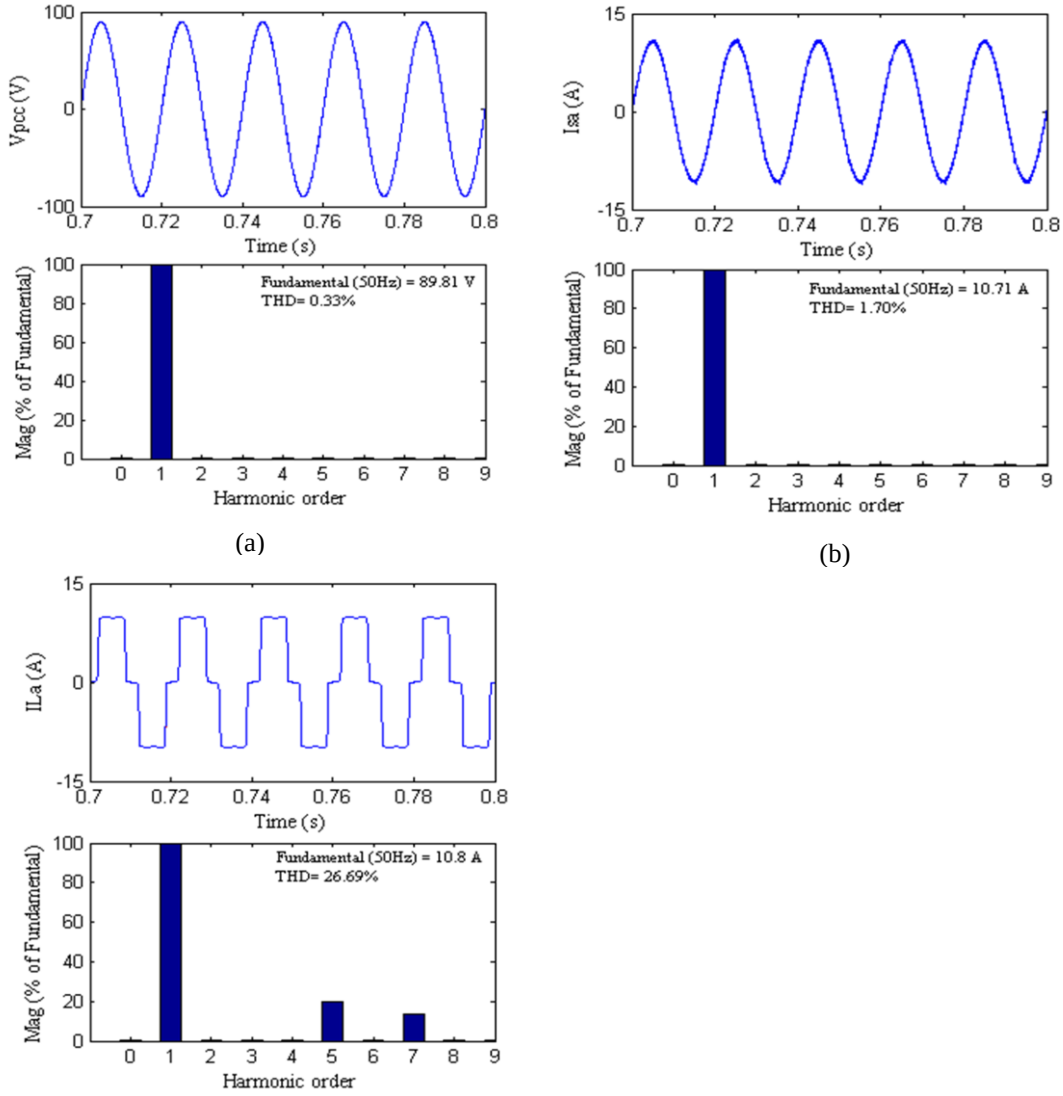

Fig. 2.4 Harmonic spectra of (a) Pcc voltage v_{pcc} , (b) supply current i_{sa} and (c) load current i_{la} in PFC mode for PBT

harmonic distortion (THD) value of supply current i_{sa}, PCC voltage v_{pcca}, and load current i_{la}. Summarizing results for THD analysis suggest that THD in supply current is reduced to 1.70% when the load current still has THD of 26.69%. The THD values of the supply current for PBT in PFC mode lies in the limits specified by IEEE-519 standards.

2.5.2.2 Performance of DSTATCOM under Voltage Regulation mode

In Fig.2.5 the operation of DSTATCOM is shown for voltage regulation mode under nonlinear load condition. The results are obtained for different parameters like supply currents (i_s), load currents (i_{la} , i_{lb} , i_{lc}), PCC voltages (v_{pcc}), DSTATCOM currents (i_{ca} , i_{cb} , i_{cc}) and the Dc bus voltage (V_{dc}). The results show that in addition to maintaining reference value of 200 V at Dc link, another PI controller is used to

maintain the PCC voltage to the reference value of 89V. In the same figure up to 0.4 s the steady state of system is shown and when unbalancing is injected in phase 'a' for time interval 0.4 s to 0.5 s, the supply currents are well maintained to be sinusoidal but have a reduction in magnitude.

In the Fig.2.6 the harmonic analysis is shown, phase 'a' is taken of different signal for the harmonic spectrum. The result comprises of three signals namely supply current (i_{sa}), load current (i_{la}) and PCC voltage (v_{pcca}) in the power factor correction mode for nonlinear load. The results obtained provide the total harmonic distortion (THD) value of supply current i_{sa}, PCC voltage v_{pcca}, and load current i_{la}. Summarizing results for THD analysis suggest that THD in supply current is reduced to 0.94% when the load current still has THD of 26.68%. The THD values of the supply current for PBT in PFC mode lies in the limits specified by IEEE-519 standards.

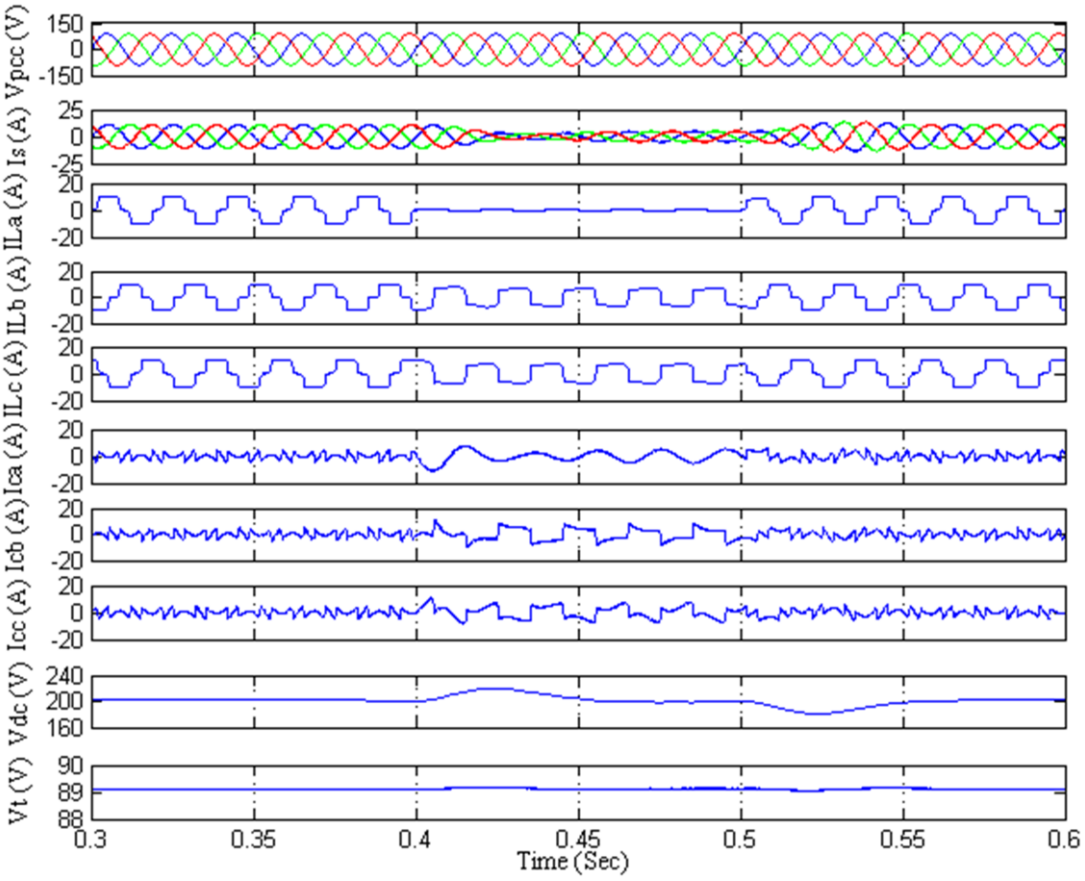

Fig. 2.5 Performance of DSTATCOM under voltage regulation mode for PBT

2.5.2.3 Intermediate Results for PBT

Intermediate results for Power Balance Theory are given in Fig.2.7 for PFC mode. The results are taken for fundamental component of active load current

$I_{Lactive}$, PI output for V_{dc} $I_{loss(n)}$, fundamental component of reactive load current $I_{Lreactive}$, PI output for terminal voltage V_t $I_{qloss(n)}$ and reference currents generated i_s^*. It is observed that the system is under steady state till 0.4s and unbalancing is introduced in phase 'a' from 0.4s to 0.5s.

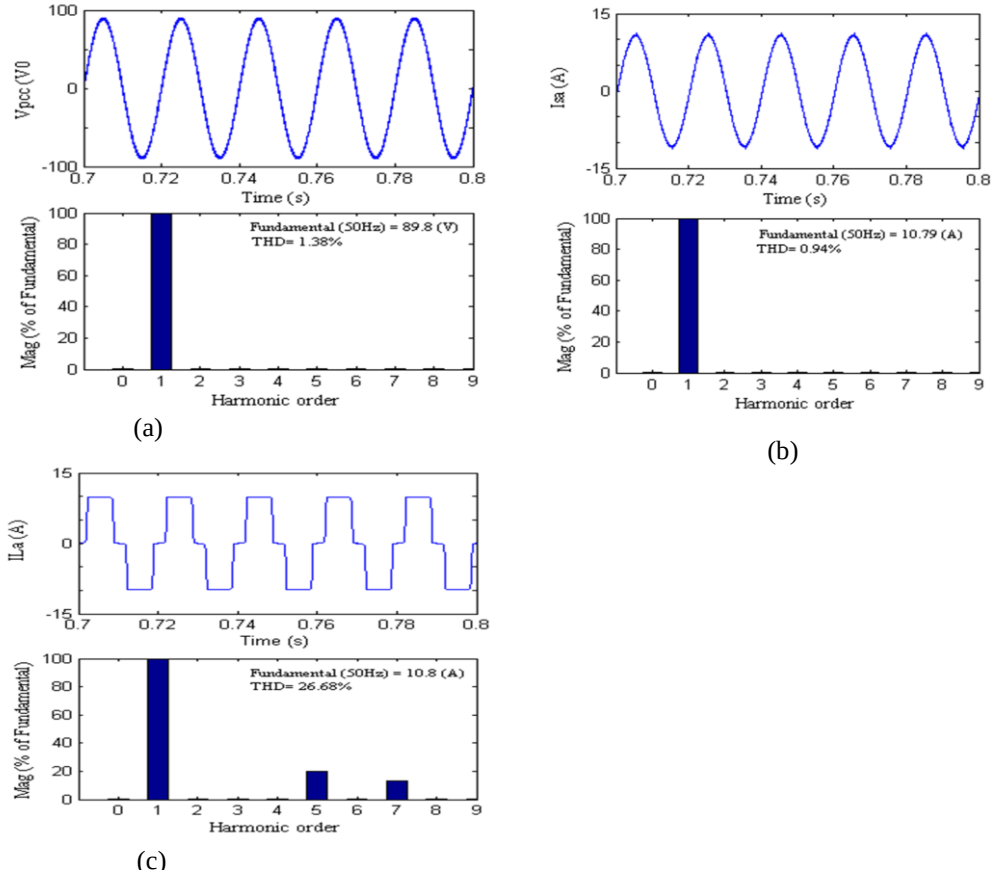

Fig. 2.6 Harmonic spectra of (a) PCC voltage v_{pcc} , (b) supply current i_{sa} and (c) load current i_{la} in voltage regulation mode for PBT

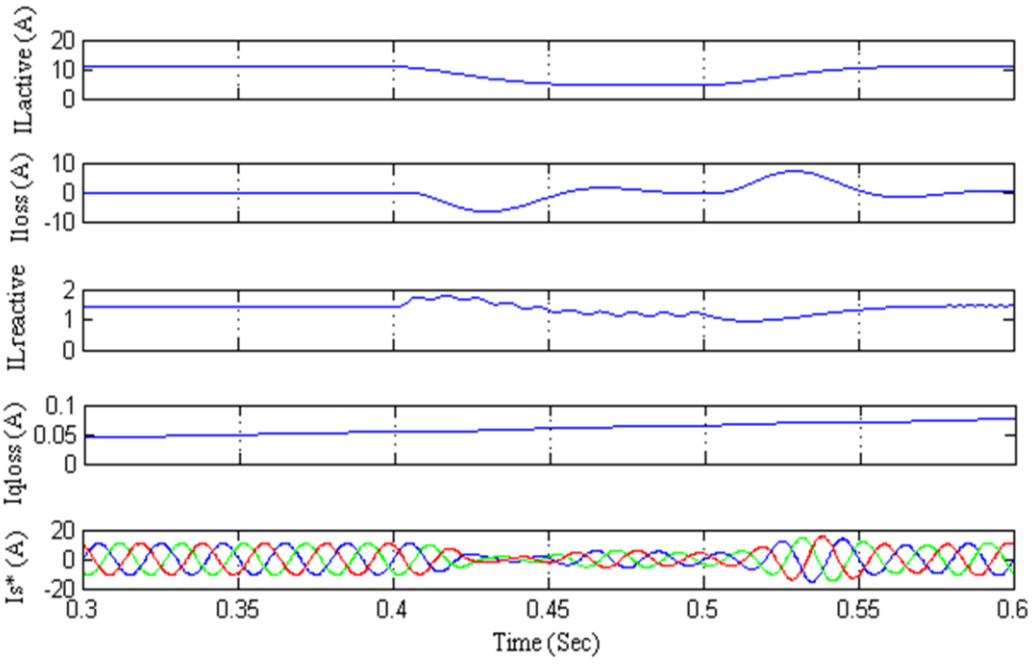

Fig.2. 7 Results for Intermediate signals for PBT

2.5.3 Instantaneous Reactive Power Theory

The instantaneous reactive power theory has been used for calculation of compensation current through long times and is still being used as conventional theory for reactive power compensation through shunt active filters. The instantaneous reactive power control algorithm uses αβ0 transformation that maps the instantaneous abc phase quantities to the instantaneous αβ0 quantities. The Clarke transformation of voltages is given as following

$$\begin{bmatrix} v_0 \\ v_\alpha \\ v_\beta \end{bmatrix} = \sqrt{\frac{2}{3}} \begin{bmatrix} \frac{1}{\sqrt{2}} & \frac{1}{\sqrt{2}} & \frac{1}{\sqrt{2}} \\ 1 & \frac{-1}{2} & \frac{-1}{2} \\ 0 & \frac{\sqrt{3}}{2} & \frac{\sqrt{3}}{2} \end{bmatrix} \begin{bmatrix} v_a \\ v_b \\ v_c \end{bmatrix} \tag{2.17}$$

Similarly three phase instantaneous currents can be transformed αβ0 and vice versa,

$$\begin{bmatrix} i_0 \\ i_\alpha \\ i_\beta \end{bmatrix} = \sqrt{\frac{2}{3}} \begin{bmatrix} \frac{1}{\sqrt{2}} & \frac{1}{\sqrt{2}} & \frac{1}{\sqrt{2}} \\ 1 & \frac{-1}{2} & \frac{-1}{2} \\ 0 & \frac{\sqrt{3}}{2} & \frac{\sqrt{3}}{2} \end{bmatrix} \begin{bmatrix} i_a \\ i_b \\ i_c \end{bmatrix} \tag{2.18}$$

The advantage of this transformation is that the separation of zero sequence component from the abc phase components. The αβ has no contribution of zero sequence component. In a balanced three phase three wire system there do not exist zero sequence component so that the evaluation of αβ voltages and currents are only required.

Three phase instantaneous power in terms of above defined Clarke transformation has inherent power invariant property thus the analysis of three phase instantaneous power is easily done.

$$P_{3\phi} = v_a\, i_a + v_b\, i_b + v_c\, i_c = v_\alpha i_\alpha + v_\beta i_\beta + v_0 i_0 \tag{2.19}$$

In the Clarke transformation the three phase active, reactive and zero sequence power is defined using the instantaneous αβ0 components.

$$\begin{bmatrix} p_0 \\ p \\ q \end{bmatrix} = \begin{bmatrix} v_0 & 0 & 0 \\ 0 & v_\alpha & v_\beta \\ 0 & v_\beta & -v_\alpha \end{bmatrix} \begin{bmatrix} i_0 \\ i_\alpha \\ i_\beta \end{bmatrix} \tag{2.20}$$

Since there are no zero sequence currents in balanced three phase three wire system the i_0 component is zero thus zero sequence power is always zero. Thus instantaneous active and reactive power is only present.

This instantaneous power theory can be used for shunt compensation of non-linear loads. The calculated real power and reactive of the load can be separated into its two components, first is average and second the oscillating part. Then the undesired component of the active and reactive power of the load that needs to be compensated is selected. The powers to be compensated are represented as p^* and q^* such that the compensator should draw current in such a way that it should produce exactly the inverse of the undesirable power drawn by the non-linear load. The source current is then the sum of load current and compensating current. The inverse transformation is applied form αβ to abc and the instantaneous values of three phase compensating reference currents are calculated as i_{ca}^*, i_{cb}^*, i_{cc}^*.

From the definition of active and reactive power in terms of $\alpha\beta$ components,

$$\begin{bmatrix} p \\ q \end{bmatrix} = \begin{bmatrix} v_\alpha & v_\beta \\ -v_\beta & v_\alpha \end{bmatrix} \begin{bmatrix} i_\alpha \\ i_\beta \end{bmatrix} \tag{2.21}$$

From the above relation it possible to write

$$\begin{bmatrix} i_\alpha \\ i_\beta \end{bmatrix} = \frac{1}{v_\alpha^2 + v_\beta^2} \begin{bmatrix} v_\alpha & -v_\beta \\ v_\beta & v_\alpha \end{bmatrix} \begin{bmatrix} p \\ q \end{bmatrix} \tag{2.22}$$

Here p and q are the powers to be compensated. These currents are then transformed from αβ to abc as reference currents. For reactive power compensation using DSTATCOM, only active power is used for calculation of reference currents which is filtered using a low pass filter on calculated active power so as to obtain only fundamental component, to this P_{loss} is added which is the power required for maintaining V_{dc} i.e. Dc link voltage at 200V. Finally these reference source currents are then compared with sensed source currents to get pulses by using HCC.

The overall control strategy is given in flow chart in the following figure 2. 8

2.5.4 Performance of System for IRPT

IRPT is simulated in Matlab/Simulink software. The control algorithm is tested for two modes of DSTATCOM namely power factor correction (PFC) mode and

Voltage regulation mode under nonlinear load. Gains for PI controller are obtained to be $k_p = 5$ and $k_i = 50$.

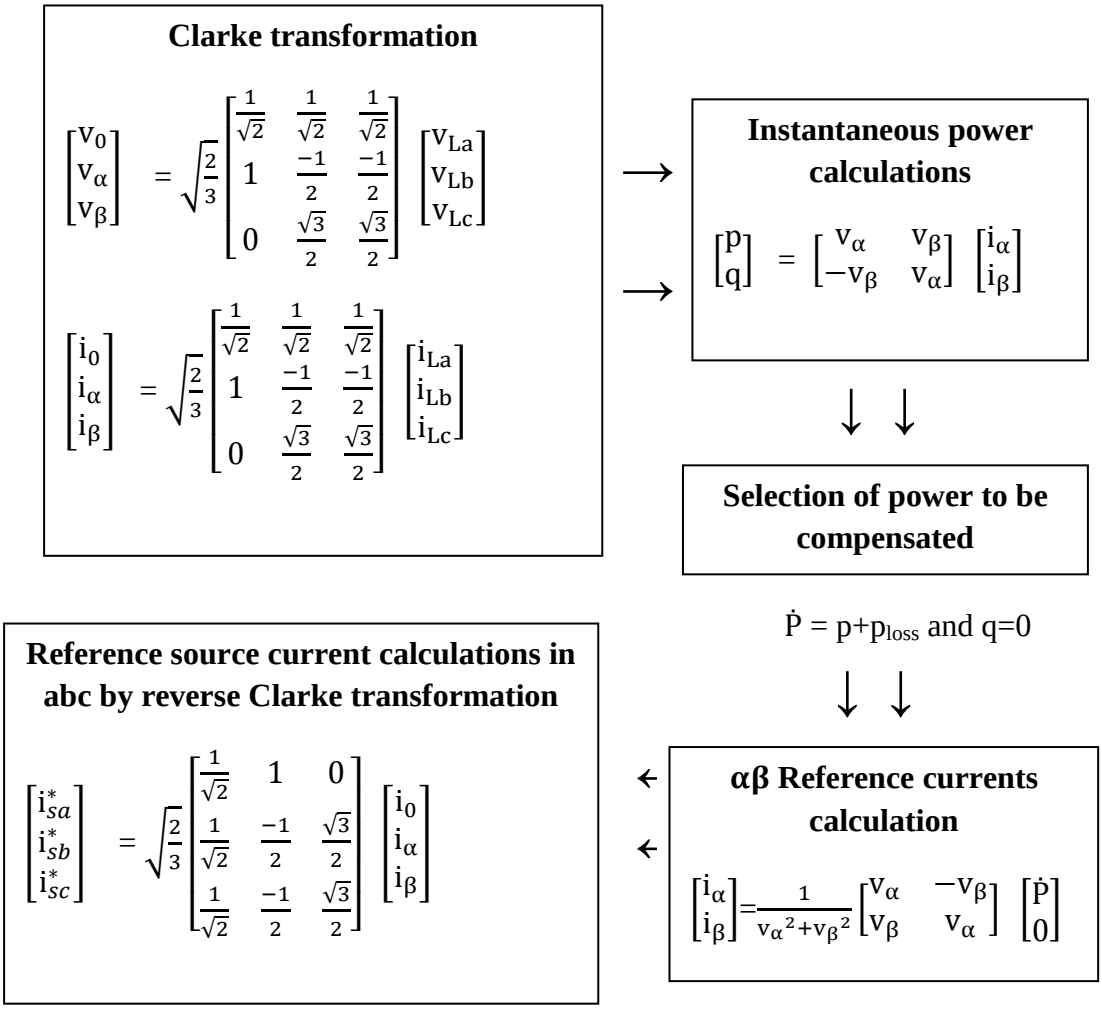

Fig.2.8 Overall control strategy for IRPT in PFC mode

2.5.4.1 Performance of DSTATCOM in PFC mode

In Fig.2.9 the PFC mode operation of DSTATCOM is shown under nonlinear load conditions. Results for different signals are obtained that includes, supply mains current (i_s), voltages at PCC (v_{pcc}), load currents (i_{la},i_{lb} , i_{lc}), DSTATCOM currents as i_{ca}, i_{cb} , i_{cc} and the Dc bus voltage (V_{dc}) are shown. The results show that the voltage of Dc bus is maintained at the reference value of 200 V. In the same figure steady state of the system is seen to be existed upto 0.6s and when unbalancing in phase 'a' from 0.6s to 1s is introduced, the DSTATCOM still maintains sinusoidal variation in supply currents.

In the following Fig.2.10, the harmonic analysis is shown, phase 'a' is taken of different signal for the harmonic spectrum. The result comprises of three signals namely supply current (i_{sa}), load current (i_{la}) and PCC voltage (v_{pcca}) in the power factor correction mode for nonlinear load. The results obtained provide the total harmonic distortion (THD) value of supply current i_{sa}, PCC voltage v_{pcca}, and load current i_{la}. Summarizing results for THD analysis suggest that THD in supply current is reduced to 1.82% when the load current still has THD of 26.68%. The THD values of the supply current for IRPT in PFC mode lies in the limits specified by IEEE-519 standards.

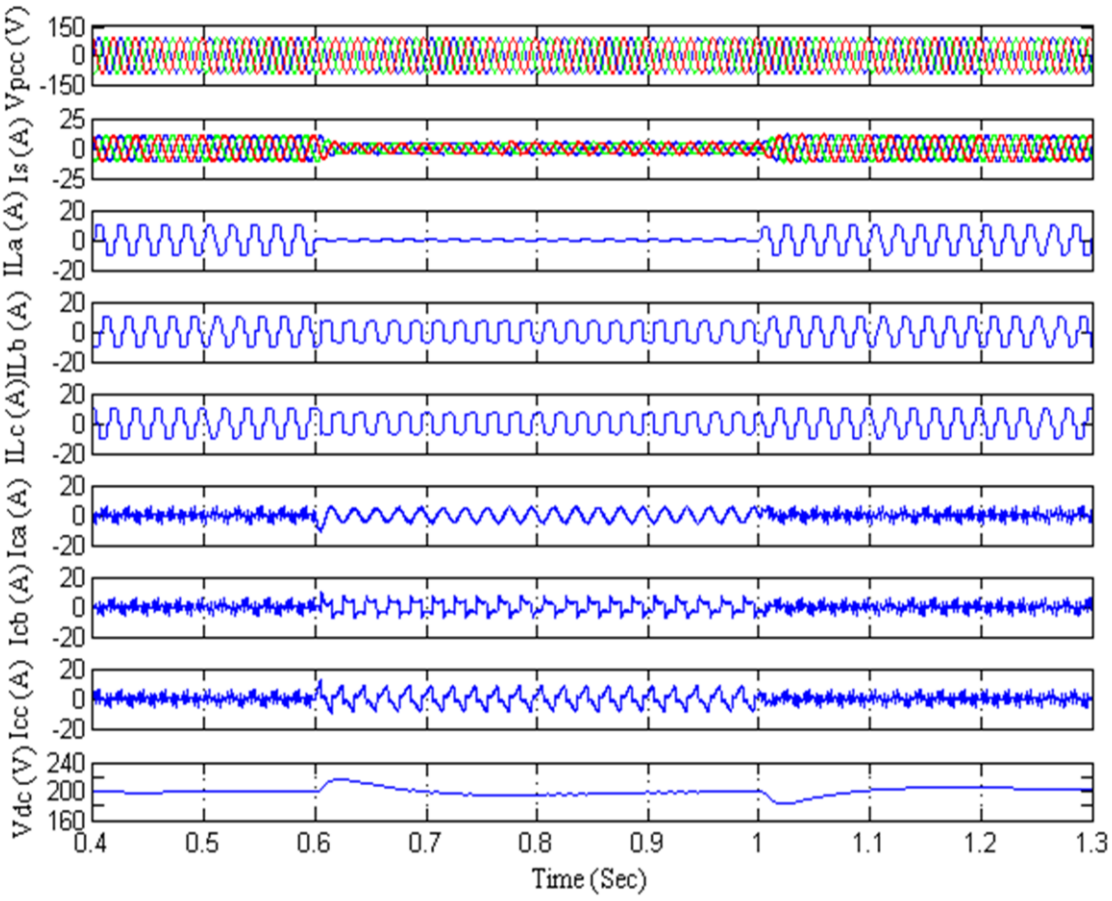

Fig.2.9 Performance of DSTATCOM for IRPT under PFC mode

2.5.4.2 Performance of DSTATCOM in Voltage Regulation mode

In Fig.2.11 the operation of DSTATCOM is shown for voltage regulation mode under nonlinear load condition. The results are obtained for different parameters like supply currents (i_s), load currents (i_{la} , i_{lb} , i_{lc}), PCC voltages (v_{pcc}), DSTATCOM currents (i_{ca} , i_{cb} , i_{cc}) and the Dc bus voltage (V_{dc}). The results show that

in addition to maintaining reference value of 200 V at Dc link, another PI controller is used to maintain the PCC voltage to the reference value of 89V. In the same figure up to 0.6 s the steady state of system is shown and when unbalancing is injected in phase 'a' for time interval 0.6 s to 1 s, the supply currents are well maintained to be sinusoidal but have a reduction in magnitude.

In the Fig.2.12 the harmonic analysis is shown, phase 'a' is taken of different signal for the harmonic spectrum. The result comprises of three signals namely supply current (i_{sa}), load current (i_{la}) and PCC voltage (v_{pcca}) in the power factor correction mode for nonlinear load. The results obtained provide the total harmonic

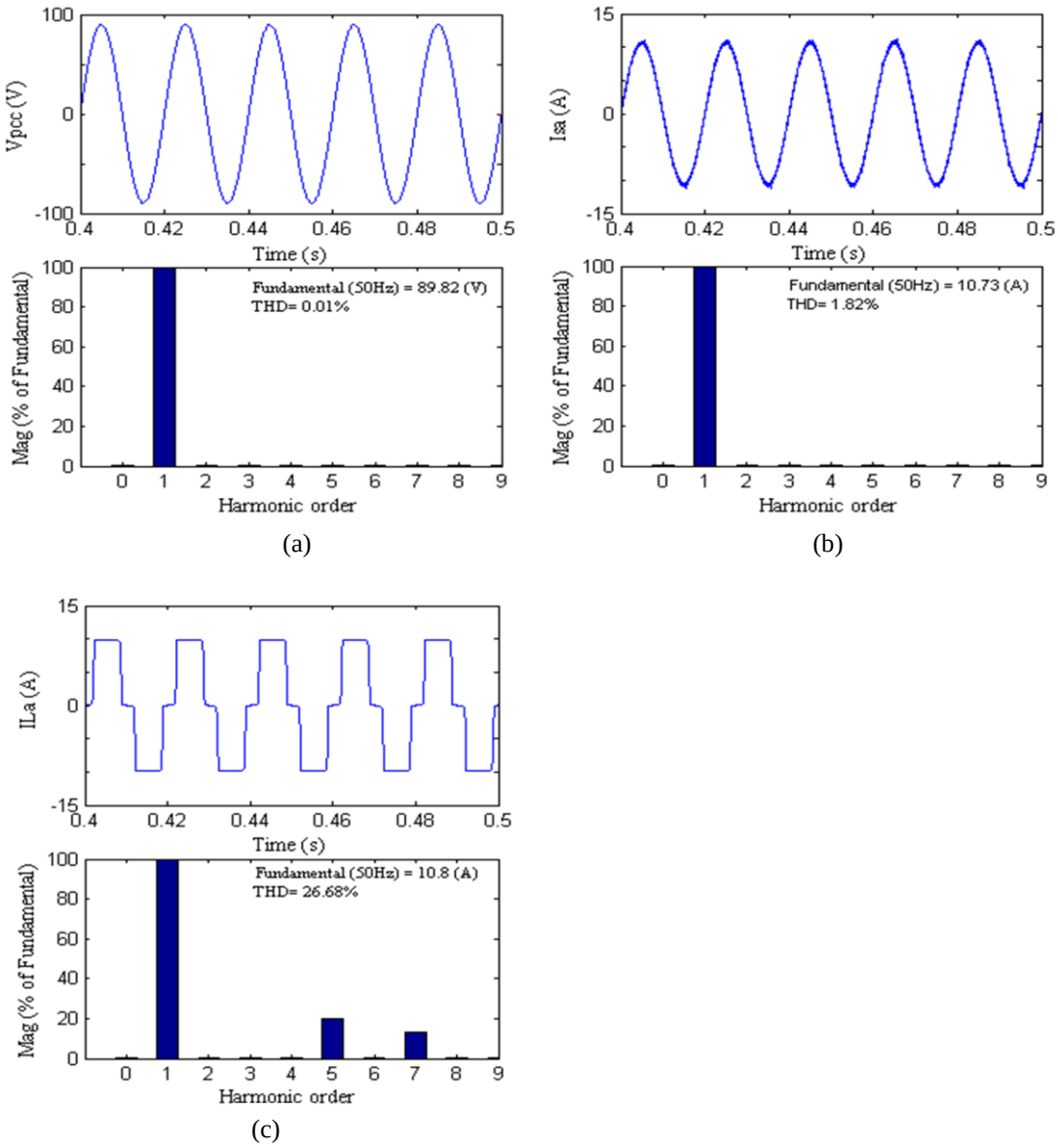

Fig. 2.10 Harmonic spectra of (a) PCC voltage v_{pcc} , (b) supply current i_{sa} and (c) load current i_{la} in PFC mode for IRPT

distortion (THD) value of supply current i_{sa}, PCC voltage v_{pcca}, and load current i_{la}. Summarizing results for THD analysis suggest that THD in supply current is reduced to 2% when the load current still has THD of 26.69%. The THD values of the supply current for IRPT in PFC mode lies in the limits specified by IEEE-519 standards.

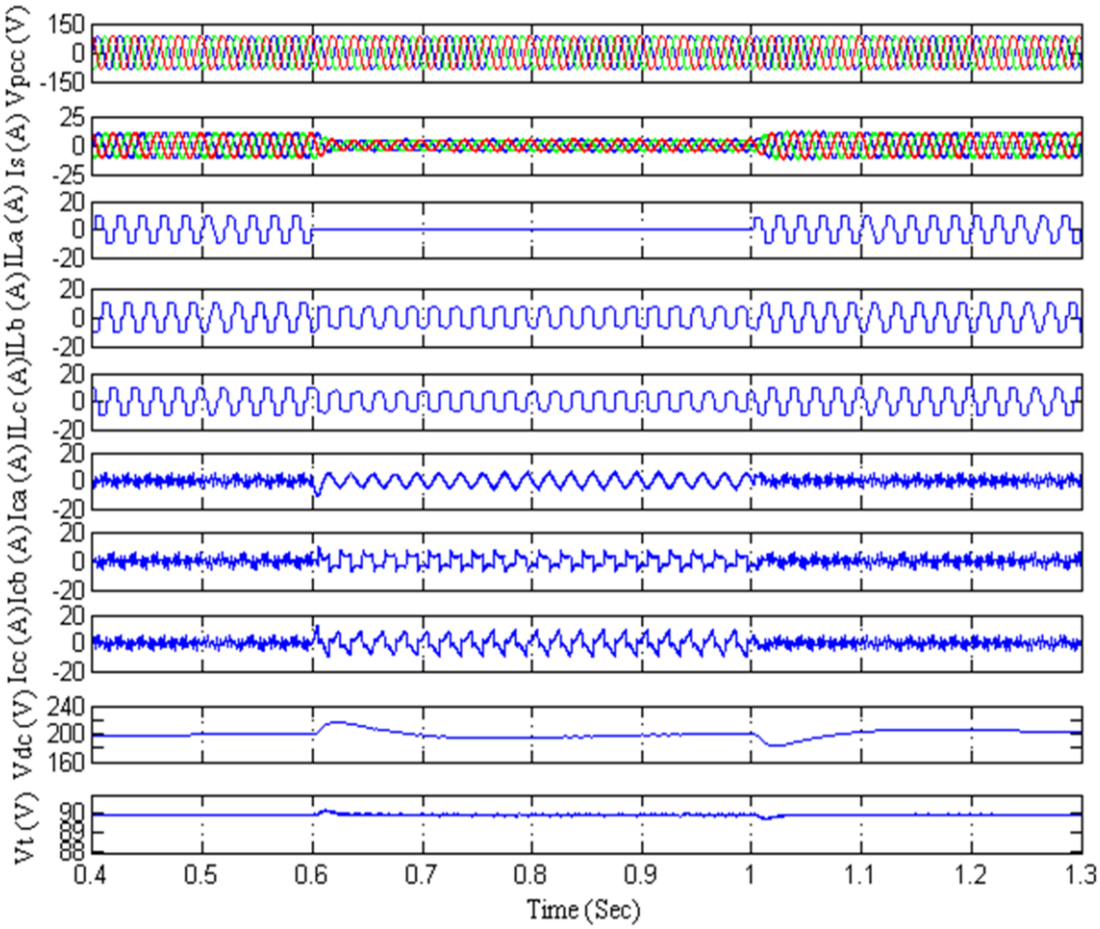

Fig. 2.11 Performance of DSTATCOM under voltage regulation mode for IRPT

2.5.4.3 Intermediate Results for IRPT

Intermediate results for Instantaneous Reactive Power Theory Power Balance Theory are given in Fig.2.13. The results are taken for alpha beta Voltages, alpha beta currents, reference alpha beta currents, power loss to maintain V_{dc} and final reference currents generated in abc form.

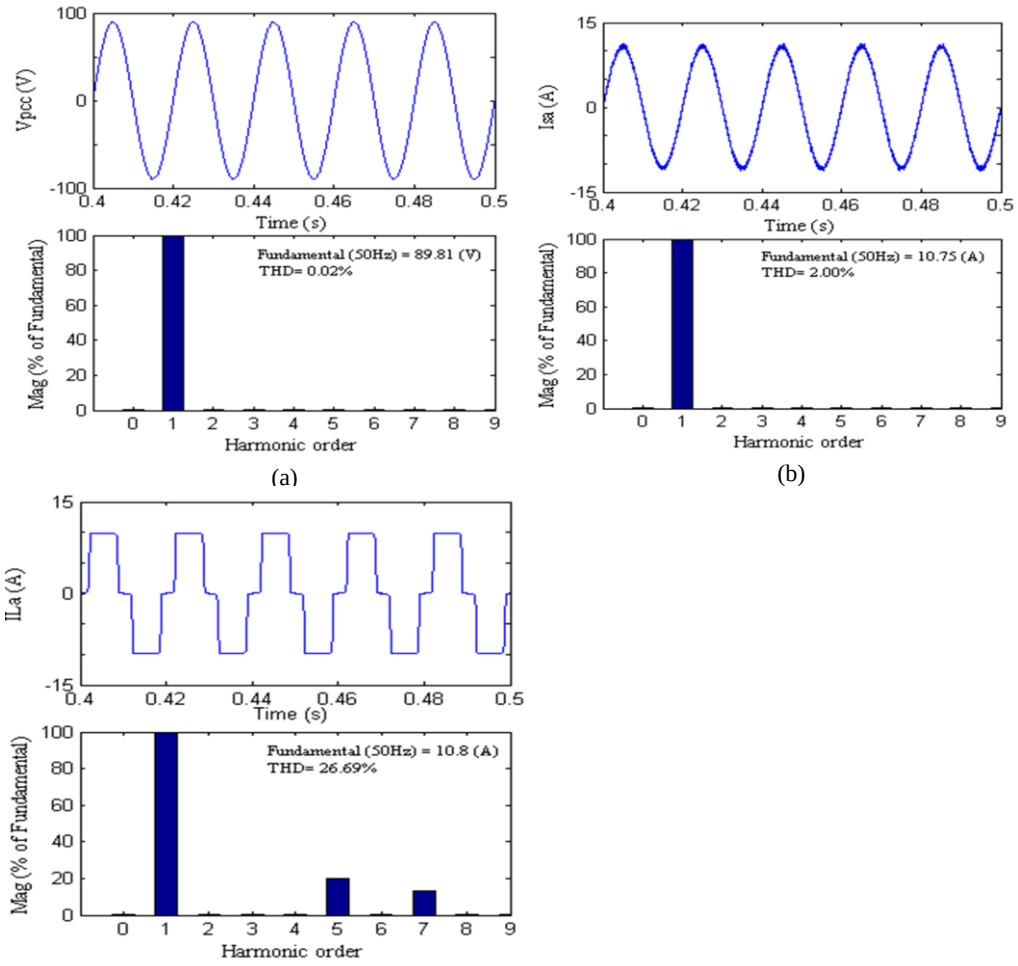

Fig. 2.12 Harmonic spectra of (a) PCC voltage v_{pcc} , (b) supply current i_{sa} and (c) load current i_{la} in voltage regulation mode for IRPT

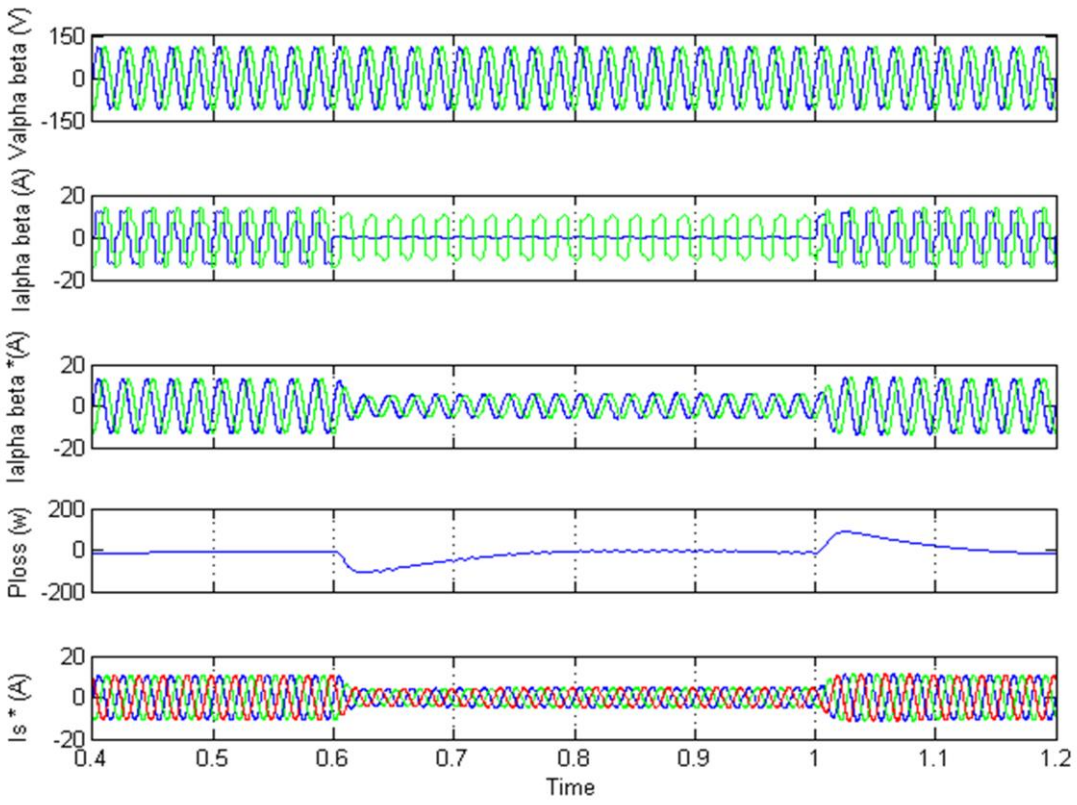

Fig.2.13 Results for Intermediate signals for IRPT

Table I Performance of DSTATCOM for PBT and IRPT

I PBT

Mode of Operation	Parameters	Magnitude and THD % of Parameters
Power factor correction mode	Supply current (A) Load current (A) PCC voltage (V)	10.71 A, 1.70% 10.8 A, 26.69% 89.81V, 0.33%
Voltage regulation mode	Supply current (A) Load current (A) PCC voltage (V)	10.79A, 0.94% 10.8A,26.68% 89.8V, 1.38%

II IRPT

Mode of Operation	Parameters	Magnitude and THD % of Parameters
Power factor correction mode	Supply current (A) Load current (A) PCC voltage (V)	10.73 A, 1.82% 10.8 A, 26.68% 89.82V, 0.01%
Voltage regulation mode	Supply current (A) Load current (A) PCC voltage (V)	10.75A, 2% 10.8A,26.69% 89.81V, 0.02%

2.6Conclusion

Conventional Power Balance theory and Instantaneous Reactive Power Theory have been studied in this chapter the results have been taken for improving several power quality features like power factor correction harmonic reduction load balancing and voltage regulation. Both the conventional schemes show satisfactory performance in improving some of these power quality features. The supply current THD is reduced to 1.70% using PBT algorithm and 1.82% For IRPT algorithm in PFC mode. Similarly for voltage regulation the two algorithms give a THD of 0.94% For PBT and 2% for IRPT in supply currents for the same value of load currents. These values are within the limits specified by IEEE-519 standards.

CHAPTER 3

SOME NEW ALGORITHMS FOR CONTROL OF DSTATCOM

3.1 General

Some new control algorithms for power quality improvement using DSTATCOM are investigated in this chapter. The first technique developed and analyzed is Linear Quadratic Regulator (LQR) based control algorithm that also involves use of power balance theory to generate reference currents. These reference and actual compensating currents are compared to generate error which is multiplied with LQR gain and finally PWM pulses are generated using carrier wave. The second algorithm designed and discussed is Composite Observer based control which uses a single composite observer structure to extract fundamental current from the load current is used. The third algorithm modeled and designed is based on Linear Proportional Resonant (PR) controller based algorithm for control of DSTATCOM. Design, modeling and analysis of the three new control algorithms is discussed in this chapter and the performance of the system in PFC mode is discussed and analyzed at the end of the chapter.

3.2 Linear Quadratic Regulator

Linear Quadratic Regulator (LQR) means regulating the settings of a controller governing either a machine or process that are found by using a mathematical algorithm which minimizes a cost function with weighting factors supplied by an engineer [17-19]. The "cost" function is usually defined as a sum of the deviations of key measurements from their desired values. In particular, this algorithm aims to find those controller settings that minimize the undesired deviations, like deviations from desired altitude or process temperature. Often the magnitude of the control action itself is included in this sum so as to keep the energy expended by the control action it limited.

In this work, LQR controller is designed to achieve dc bus voltage regulation and harmonics and reactive power compensation. The controller’s performance is affected by the weighting matrix, which is chosen by design engineers for satisfactory performance. The VSC is controlled as a single unit having multi-input

and multi-output system, the hysteresis current control technique is used to generate the gating pulses of the power devices.

A suitable control scheme is required to track the reference currents. Several control schemes have been proposed till date and one of the commonly used current controlled mode of the DSTATCOM such as hysteresis current control (HCC) is used. In systems with higher order HCC band to make actual currents closer to reference currents must be narrow or nearing to zero that result in perfect tracking, but very high switching frequency is required, which is undesirable. Literature survey [21] has shown that the LQR has better response dynamics and requires less control effort.

In LQR technique, the optimization of either a cost function or a performance index is done, that require the weights to the state variables by the design engineer to obtain desired performance of the system.

In commercial applications, a fixed switching frequency is preferred because it reduces the acoustic noise which is present with variable switching frequencies. Therefore LQR gains are used with the current error which is compared with constant switching frequency triangular wave of duty cycle such that the resultant PWM signal obtained tends current error to zero.

3.2.1 Design of LQR Controller

The current control mode is used along with LQR, in this technique, the current error is equated with a triangular carrier wave of fixed frequency and having duty cycle such that the resultant PWM signal tends the current error to zero value.

For LQR realization in the system, an equivalent circuit of system consisting DSTATCOM is used as shown in Fig.3.1. For analysis the DSTATCOM is considered as a voltage source in shunt connected to the system at PCC through coupling inductor (L) having leakage resistance (R).

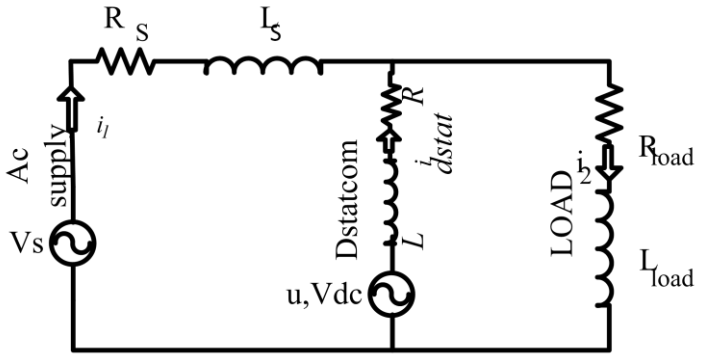

Fig.3.1. Simplified Circuit model of system

The state space modeling is done and state equation of the system is noted as

$$\dot{X} = AX + BU \tag{3.1}$$

where X is state vector for currents and an input vector U given as

$$X = \begin{pmatrix} i_1 \\ i_2 \end{pmatrix} \qquad U = \begin{pmatrix} v \\ u_c \end{pmatrix} \tag{3.2}$$

where i_1 and i_2 currents are the state variables for the system taken, v is input and u_c is state feedback variable. The system matrix A for the state variables and input variables matrix as B are given by following equations.

$$A = \begin{bmatrix} \frac{-(R+Rs)}{(L+Ls)} & 0 \\ 0 & \frac{-(R+R\,load)}{(L+L\,load)} \end{bmatrix} \tag{3.3}$$

$$B = \begin{bmatrix} \frac{1}{(L+Ls)} & 0 \\ 0 & \frac{Vdc}{(L+Ls)} \end{bmatrix} \tag{3.4}$$

The performance index for LQR in the system is represented by J and is given as

$$J = \int_0^\infty (x^T Q x + u^T R u)\, dt \tag{3.5}$$

where R and Q matrix are the weight matrix and state matrix respectively.

For the LQR system with DSTATCOM, control law is taken as u= -Kx , this is the outcome of minimization of the performance index. The linear control theory provides a solution for estimation of matrix gain K as per following equation

$$K = R^{-1} B^T P \tag{3.6}$$

where P is a state matrix found by solving the continuous Riccati equation given by

$$A^T P + PA - PBR^{-1}B^T P + Q = 0 \quad (3.7)$$

where R and Q are penalty matrix and weight matrix repectively. These Matrices have a general form as given below and contains only diagonal elements.

$$R = \begin{bmatrix} R_1 & 0 \\ 0 & R_2 \end{bmatrix} \quad ; \quad Q = \begin{bmatrix} W_1 & 0 \\ 0 & W_2 \end{bmatrix} \quad (3.8)$$

The entries of these matrices are taken suitably as per system consideration and the gain matrix is calculated using Matlab command in software. The gain matrix K is a diagonal matrix of order 2 x 2. The gains are obtained for the considered system.

The overall scheme used to generate pulses for VSC is given in Fig.3.2 below. The reference currents are generated using Power Balance Theory and which are compared with load currents to get reference compensating currents that is subtracted from actual compensating currents and multiplied with LQR gain. The pulses for VSC are generated by comparing the current error so obtained with a carrier wave of 5 kHz frequency.

3.2.2 Reference Current Generation

The conventional Power Balance Theory is used for generation of the reference currents. In this only active power component of the grid current is calculated hence Dc component of load current and loss current which is usually considered as the output of the PI controller for maintaining the DC link voltage of the DSTATCOM at

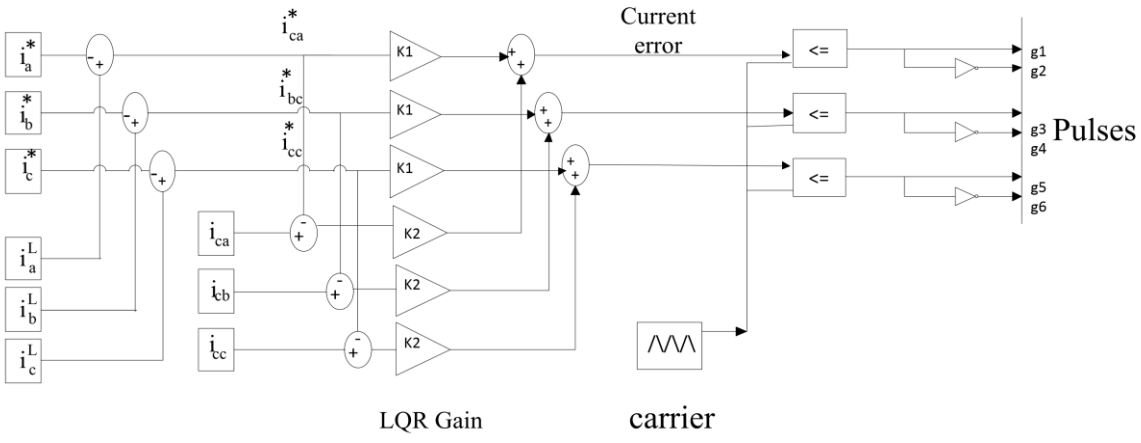

Fig.3.2 Overall control scheme for LQR

the desired value. The fundamental equations are same used in PBT and same are referred for estimation of the active power component of the grid currents.

The peak amplitude of the three phase voltages (v_{sa} , v_{sb}, v_{sc}) which are considered to be PCC voltage is calculated as,

$$V_t = [(2/3)(v_{sa}^2 + v_{sb}^2 + v_{sc}^2)]^{1/2} \quad (3.9)$$

Unit vectors that are in phase with phase voltages are calculated by,

$$u_{sa} = \frac{v_{sa}}{v_t}, \; u_{sb} = \frac{v_{sb}}{v_t}, \; u_{sc} = \frac{v_{sc}}{v_t} \quad (3.10)$$

P_L is the instantaneous value of active power of the connected load is calculated by,

$$P_L = (v_{sa}i_{La} + v_{sb}i_{Lb} + v_{sc}i_{Lc}) \quad (3.11)$$

P_L comprises of AC component and a DC component as discussed in PBT therefore again a Low Pass Filter (LPF) is used to filter out the value of DC component of the fundamental active power.

This further leads to the estimation of peak amplitude of the active power component of connected load as,

$$I_{L\,active} = (2/3)\,(P_L/V_t) \quad (3.12)$$

Another component of active power which is used for regulating the DC link voltage of VSC estimated through the output of PI controller that uses error between desired Dc link voltage and sensed Dc link voltage as

$$V_{dec(n)} = V^*_{dc(n)} - V_{dc(n)} \quad (3.13)$$

where $V^*_{dc(n)}$ is the desired Dc link voltage and $V_{dc(n)}$ is the sensed DC link voltage of the VSC.

The following equation gives the output of the PI controller as,

$$I_{loss(n)} = I_{loss(n-1)} + K_p\,[\,V_{decr(n)} - V_{decr(n-1)}\,] + K_i V_{decr(n)} \quad (3.14)$$

where $I_{loss(n)}$ is taken as the second component of the grid current as discussed earlier and K_p and K_i are the gains of the PI controller.

This output of PI controller when added with the Dc component of grid current gives us total active power component of the grid current i.e. I_{active}

$$I_{active} = I_{L\ active} + I_{loss(n)} \quad (3.15)$$

Thus reference currents are generated using the following equations,

$$I_{sa} = I_{active} * u_{sa}, I_{sb} = I_{active} * u_{sb}, I_{sc} = I_{active} \quad (3.16)$$

3.2.3 Performance of the System with LQR Controller

LQR is simulated in Matlab/Simulink software. The control algorithm is tested for two modes of DSTATCOM namely power factor correction (PFC) mode and Voltage regulation mode under nonlinear load.

3.2.3.1 Performance of DSTATCOM for PFC under load change

In Fig.3.3 the PFC mode operation of DSTATCOM is shown under nonlinear load conditions. Results for different signals are obtained that includes, supply mains current (i_s), voltages at PCC (v_{pcc}), load currents (i_{la},i_{lb} , i_{lc}), DSTATCOM currents as i_{ca}, i_{cb} , i_{cc} and the Dc bus voltage (V_{dc}) are shown. The results show that the voltage of Dc bus is maintained at the reference value of 200 V. In the same figure steady state of the system is seen to be existed upto 0.4s and when unbalancing in phase 'a' from 0.4s to 0.5s is introduced, the DSTATCOM still maintains sinusoidal variation in supply currents.

In the following Fig.3.4, the harmonic analysis is shown, phase 'a' is taken of different signal for the harmonic spectrum. The result comprises of three signals namely supply current (i_{sa}), load current (i_{la}) and PCC voltage (v_{pcca}) in the power factor correction mode for nonlinear load. The results obtained provide the total harmonic distortion (THD) value of supply current i_{sa}, PCC voltage v_{pcca}, and load current i_{la}. Summarizing results for THD analysis suggest that THD in supply current is reduced to 4.63% when the load current still has THD of 26.41%. The THD values of the supply current in PFC mode lies in the limits specified by IEEE-519 standards.

3.2.3.2 Performance of DSTATCOM under Voltage Regulation

In Fig.3.5 the operation of DSTATCOM is shown for voltage regulation mode under nonlinear load condition. The results are obtained for different parameters

like supply currents (i_s), load currents (i_{la} , i_{lb} , i_{lc}), PCC voltages (v_{pcc}), DSTATCOM currents (i_{ca} , i_{cb} , i_{cc}) and the Dc bus voltage (V_{dc}). The results show that in addition to maintaining reference value of 200 V at Dc link, another PI controller is used to maintain the PCC voltage to the reference value of 89V. In the same figure up to 0.4 s the steady state of system is shown and when unbalancing is injected in phase 'a' for time interval 0.4 s to 0.5 s, the supply currents are well maintained to be sinusoidal but have a reduction in magnitude.

In the Fig.3.6 the harmonic analysis is shown, phase 'a' is taken of different signal for the harmonic spectrum. The result comprises of three signals namely supply current (i_{sa}), load current (i_{la}) and PCC voltage (v_{pcca}) in the power factor correction mode for nonlinear load. The results obtained provide the total harmonic distortion (THD) value of supply current i_{sa}, PCC voltage v_{pcca}, and load current i_{la}. Summarizing results for THD analysis suggest that THD in supply current is reduced to 3.85% when the load current still has THD of 26.36%. The THD values of the supply current in PFC mode lies in the limits specified by IEEE-519 standards

K_1 = 0.7774 and K_2 = 31.5553 are the LQR gains obtained using following Matrix entries for the system for PFC mode is

$$A = \begin{bmatrix} \frac{-(0.2+0.1)}{(1+0.01)/1000} & 0 \\ 0 & \frac{-(0.2+13.3)}{(1+100)/1000} \end{bmatrix};$$

$$B = \begin{bmatrix} \frac{1}{(1+0.01)/1000} & 0 \\ 0 & \frac{200}{(1+100)/1000} \end{bmatrix};$$

$$Q = \begin{bmatrix} 1 & 0 \\ 0 & 1000 \end{bmatrix};$$

$$R = \begin{bmatrix} 1 & 0 \\ 0 & 1 \end{bmatrix}$$

K_1 = 0.7440 and K_2 = 31.5553 are obtained in voltae regulation mode and the system matrix used is as follows

$$A = \begin{bmatrix} \frac{-(0.2+0.1)}{(1+0.04)/1000} & 0 \\ 0 & \frac{-(0.2+13.3)}{(1+100)/1000} \end{bmatrix};$$

$$B = \begin{bmatrix} \frac{1}{(1+0.04)/1000} & 0 \\ 0 & \frac{200}{(1+100)/1000} \end{bmatrix};$$

$$Q = \begin{bmatrix} 1 & 0 \\ 0 & 1000 \end{bmatrix};$$

$$R = \begin{bmatrix} 1 & 0 \\ 0 & 1 \end{bmatrix}$$

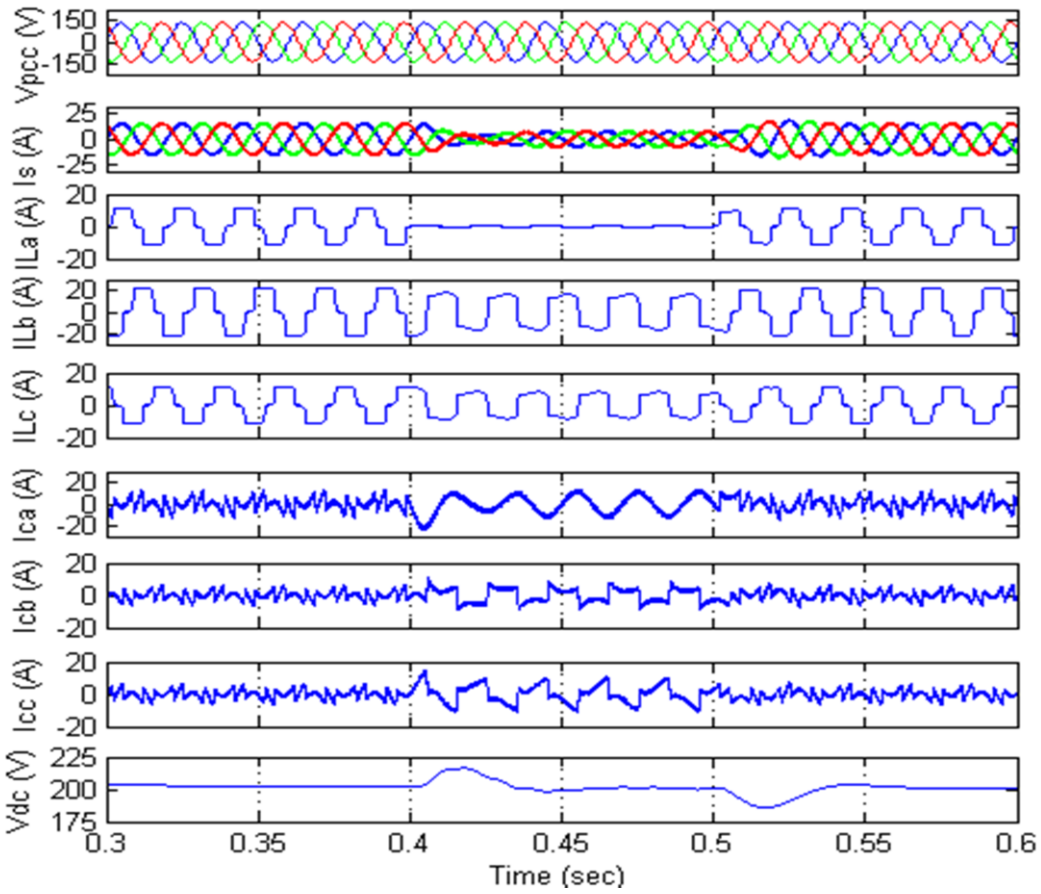

Fig.3.3 Performance of DSTATCOM under PFC mode for LQR

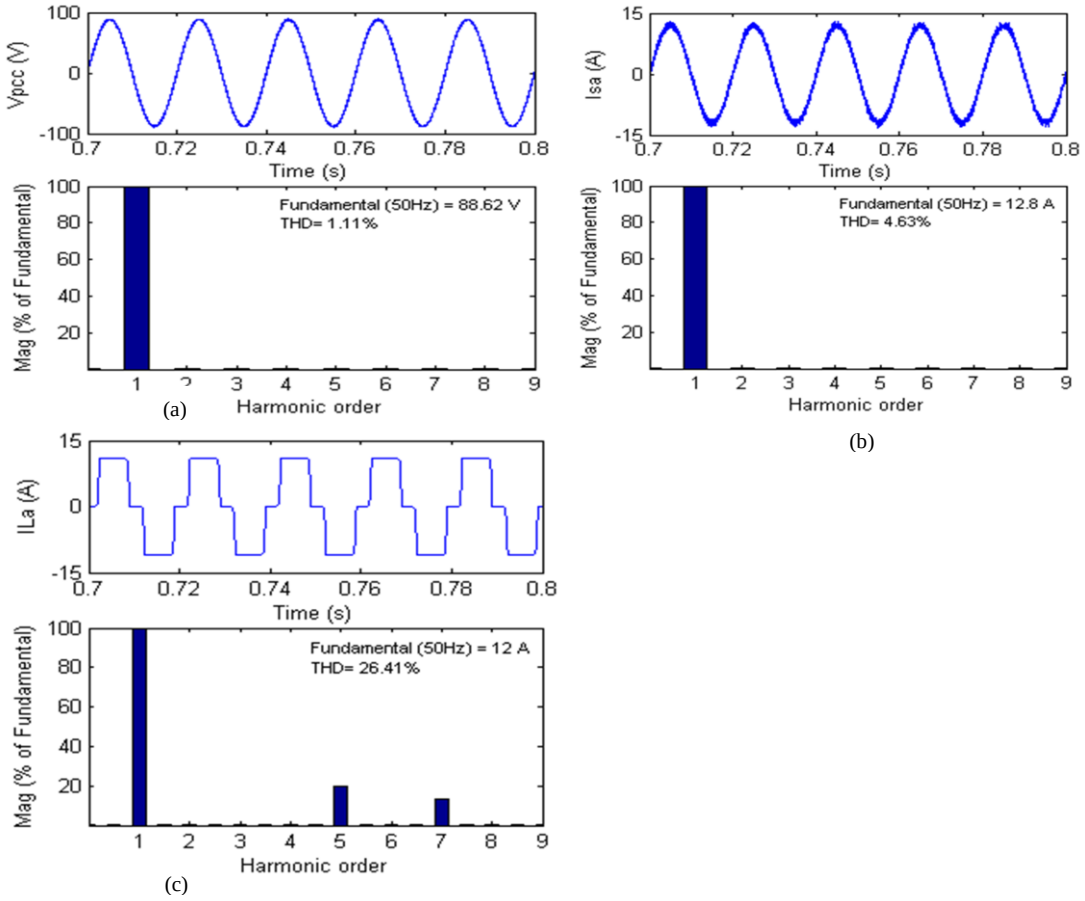

Fig.3.4 Harmonic spectra of (a) PCC voltage v_{pcca} ,(b) supply current i_{sa} , (c) load current i_{la} in PFC mode for LQR

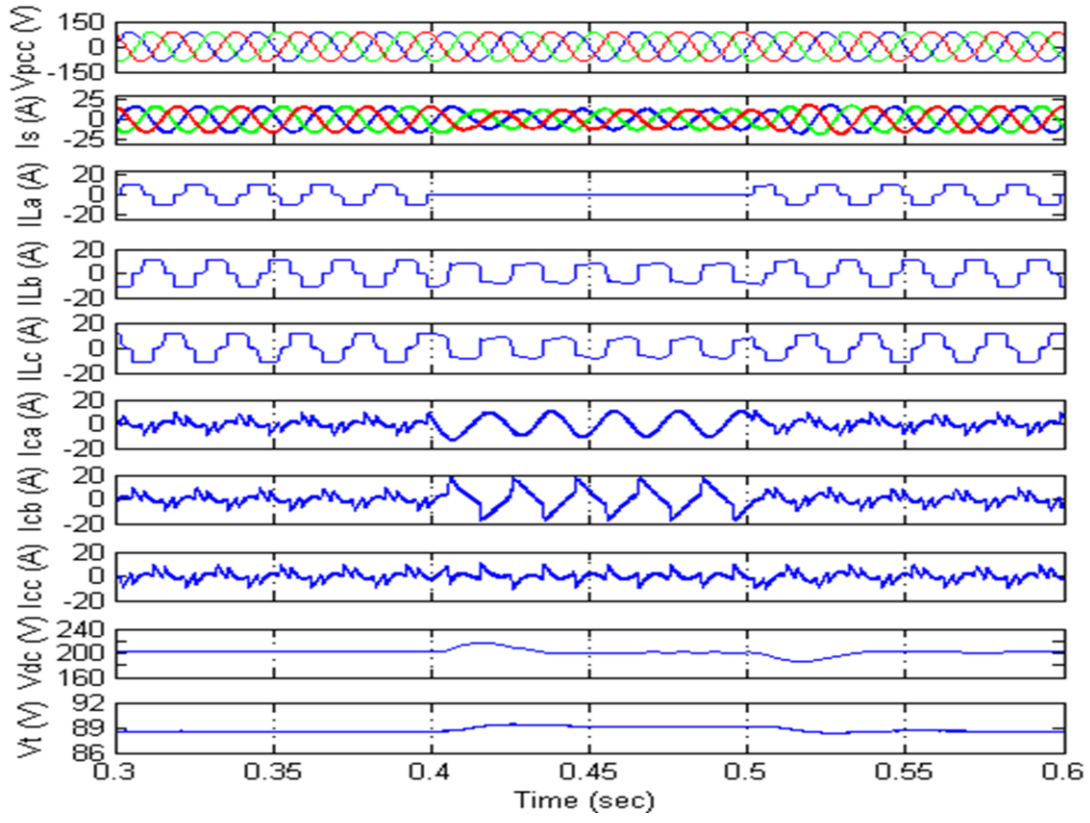

Fig.3.5. Performance of DSTATCOM in voltage regulation mode for LQR.

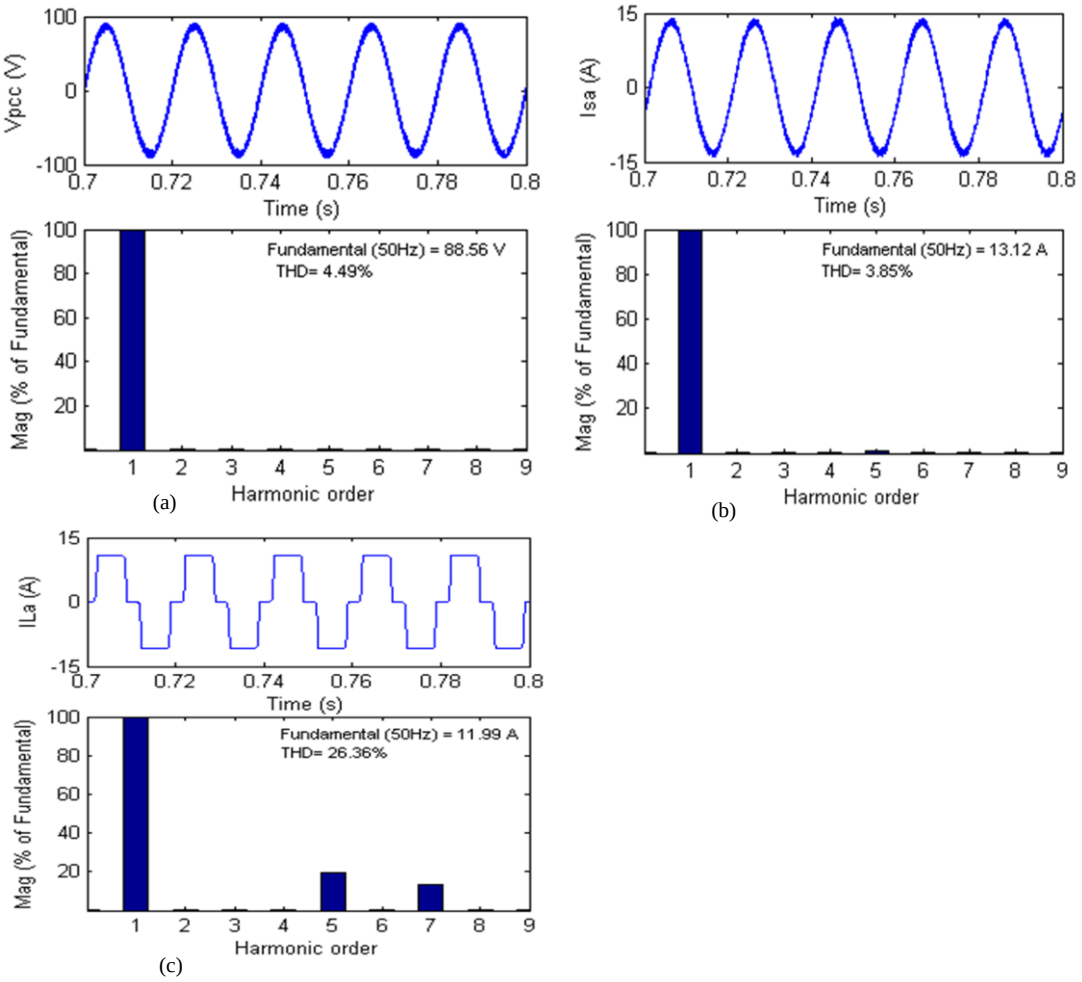

Fig.3.6 Harmonic spectra of (a) PCC voltage v_{pcca} ,(b) supply current i_{sa} , (c) load current i_{la} in voltage regulation mode for LQR

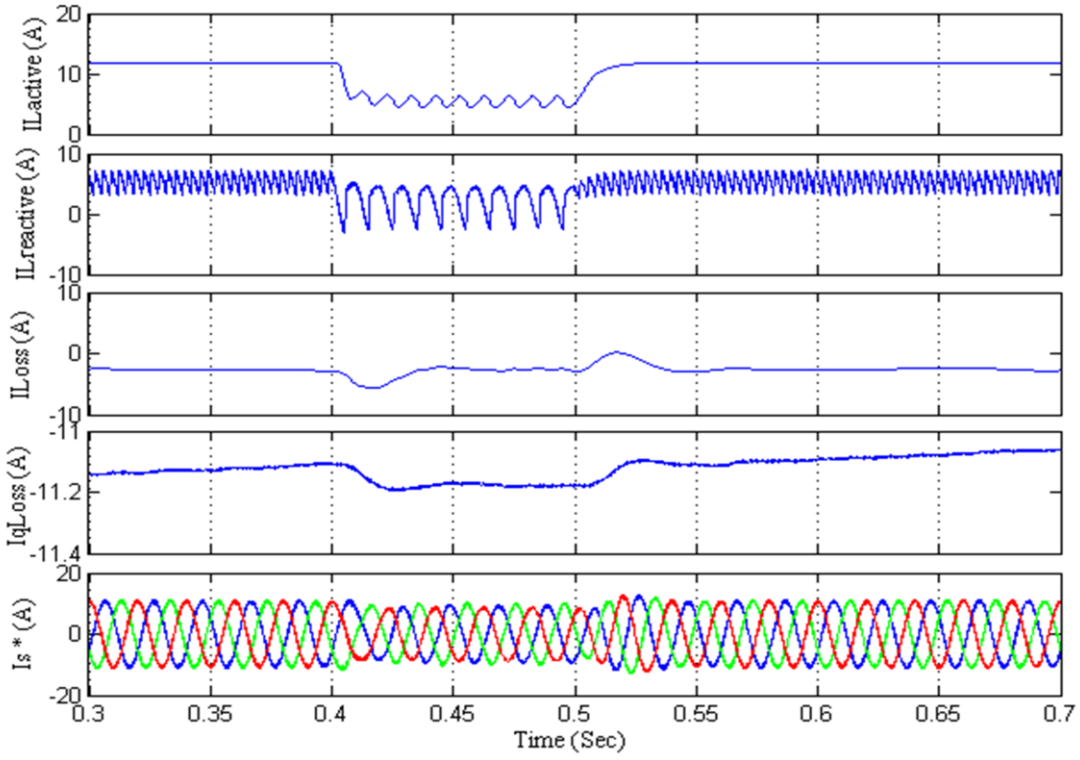

Fig.3. 7 Results for Intermediate signals for LQR

3.2.3.3 Intermediate Results for LQR

Intermediate results for LQR for power factor correction are given in Fig.3.7. The results are taken for fundamental component of active load current $I_{Lactive}$, fundamental component of reactive load current $I_{Lreactive}$, PI output for V_{dc} $I_{loss(n)}$, PI output for terminal voltage V_t $I_{qloss(n)}$ and reference currents generated i_s^*. It shows that the system is under steady state till 0.4s and unbalancing is introduced in phase a from 0.4s to 0.5s.

3.3 Composite Observer based Control Algorithm

These days advanced controllers are based on soft computing techniques such as fuzzy logic, adaptive algorithm based on neural network as back propagation, Lyapunov candidate-based algorithm which is developed using the Lyapunov stability theory, predictive current control, sliding mode observer-based control, control based on state observer and composite observer for harmonic extraction are getting popular. The composite observer-based control algorithm is used in three-phase system for extraction of harmonic current components and its implementation for three-phase shunt compensation.

This composite observer-based control algorithm is implemented in three-phase DSTATCOM for mitigation of power quality problems such as reactive power compensation, harmonic elimination, load balancing and neutral current compensation in three-phase distribution system. It is used for the extraction of fundamental component of load currents. These components of load currents are used for estimation of reference source currents to generate the gating pulses of insulated gate bipolar transistors used in Voltage Source Inverter (VSI) of DSTATCOM.

The advantages of this algorithm [36] are that it is less sensitive to supply frequency variation and there is low distortion in the extracted signal. It is considerably fast, accurate and robust with respect to time-varying harmonics and frequency. Its structure is simple, which requires only gain and integral blocks. Owing to these reasons, this control algorithm requires less computational time on a digital platform in real-time realization compared with traditional algorithms such as instantaneous reactive power theory (IRPT), Icos∅ control algorithm, addaline control

algorithm and single-phase p–q theory and so on. The control algorithm can also equally applicable in distorted and unbalanced supply system with minor modifications.

The block diagram of a control algorithm based on composite observer for extraction of load fundamental currents and subsequently their use in estimation of reference source currents is given in Fig.3.10. Three-phase point of common coupling (PCC) voltages (v_a, v_b, v_c), load currents (i_{La}, i_{Lb}, i_{Lc}), dc bus voltage (V_{dc}) of DSTATCOM are sensed as input signals to control algorithm. In-phase unit template of three-phase PCC voltages (u_a u_b, u_c) are estimated after dividing respective phase voltage with amplitude of three-phase PCC voltages (V_t) and consequently quadrature phase templates are generated (w_a w_b, w_c). The amplitude of PCC voltages and in-phase unit templates are computed.

The amplitude of the three phase voltages at the point of common coupling (PCC) represented as terminal voltage V_t is calculated as,

$$V_t = \left[\left(2/3\right)\left(v_a^2 + v_b^2 + v_c^2\right)\right]^{1/2} \tag{3.17}$$

in phase templates with phase voltages are calculated as,

$$u_{sa} = \frac{v_a}{v_t},\ u_{sb} = \frac{v_b}{v_t}, u_{sc} = \frac{v_c}{v_t} \tag{3.18}$$

quadrature phase templates to the phase voltages are derived as,

$$w_{sa} = \frac{v_a}{v_t},\ w_{sb} = \frac{v_b}{v_t}, w_{sc} = \frac{v_c}{v_t} \tag{3.19}$$

Periodic signal of frequency ω_1, rich in harmonics can be modeled as the sum of sine waves of frequency m.ω_1, emanating from subsystems as shown in Fig.3.8

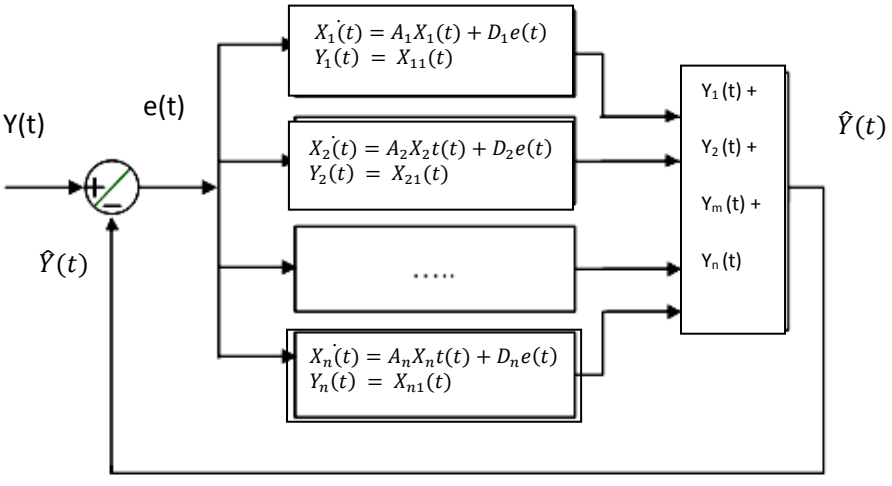

Fig. 3.8 Structure of Continuous Composite Observer

The composite 2N dimensional system describing the entire arrangement is described as

$$\dot{X} = A\,X \tag{3.20}$$

$$Y = C^T X \tag{3.21}$$

where

$$A = \begin{bmatrix} A_1 & \cdots & 0 \\ \vdots & \ddots & \vdots \\ 0 & \cdots & A_n \end{bmatrix} \tag{3.22}$$

and

$$[C]^T\ [1\ 0 \quad 1\ 0 \ldots \quad 1\ 0] \tag{3.23}$$

The composite [2N x 1] constant gain vector D, to be determined using the specified pole locations is:

$$D = [(D11, D12)\ (D21, D22)\ (Dm1, Dm2)\ (DN1, DN2)]^T \tag{3.24}$$

The closed loop poles are assumed to be equi-dominant and are located at $s = (-a\omega_1 + j\, m.\omega_1)$

The structure of a single unit of the composite observer is shown

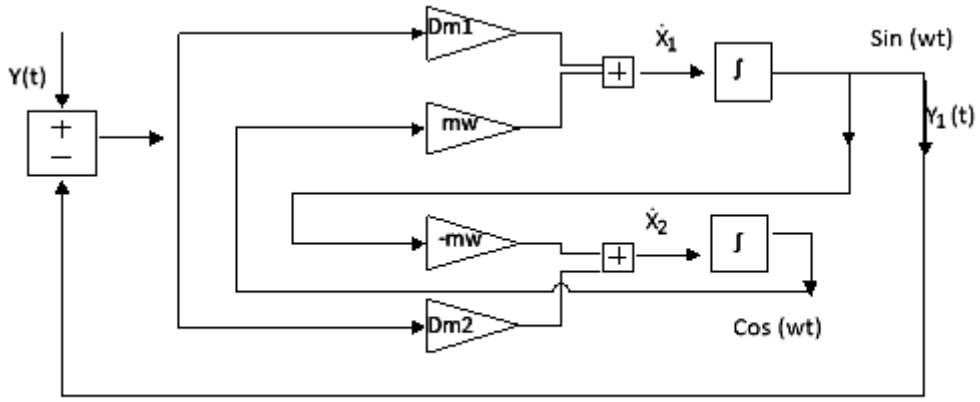

Fig. 3.9 Single Composite Observer structure

The observation speed and the bandwidth of the observer at the various notches $m\omega_1$, increase with the factor "a", the real part of the observer poles. The pole of the observer is lying in s-plane. Speed and bandwidth of observer at the various harmonics order increase with constant factor selected in the real-part of the observer poles.

Selected value of Dm_1, Dm_2 are to be evaluated for extraction of fundamental load current (i_L) as shown in Fig.3.9.

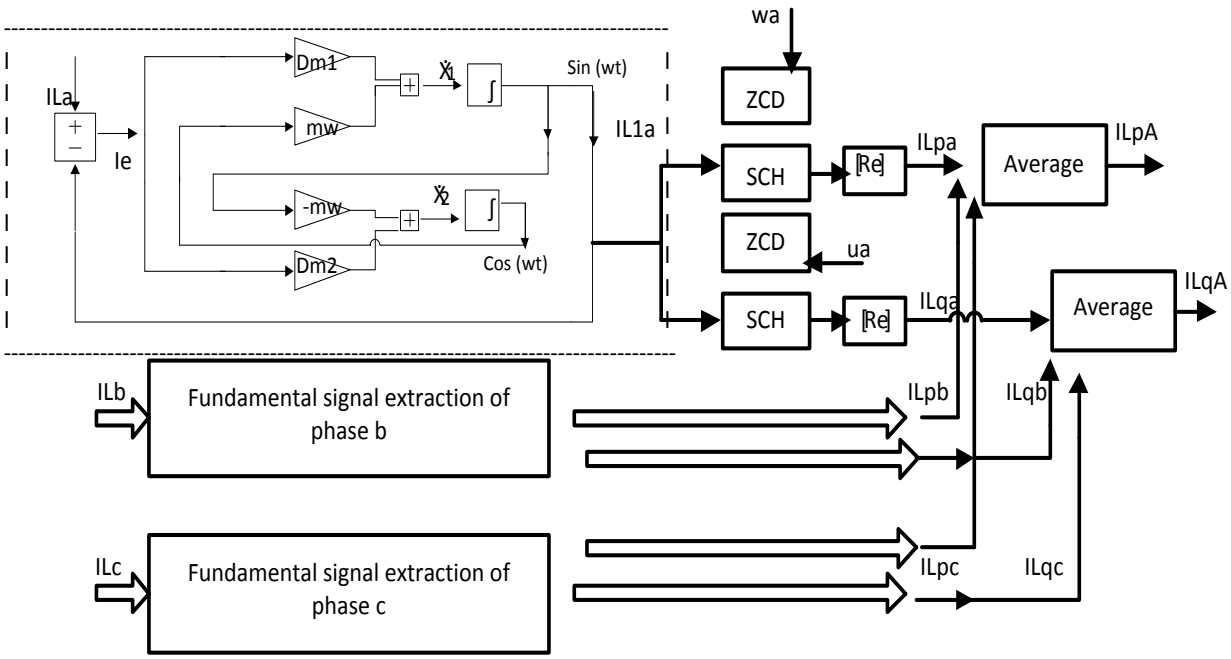

Fig. 3.10 fundamental current extraction using composite observer

3.3.1 Harmonic Extraction

The composite observer algorithm may also be used for extraction of different harmonics. It is done so by using same single composite observer structure, the only modification is for extracting a particular harmonic of order 'm', the 'mw' varies as the angular frequency of the component to be extracted i.e. for extraction of fifth and seventh harmonic the mw is written as 5w and 7w, where w is fundamental angular frequency of the system. The fifth and seventh harmonic extracted from the load is shown in the Fig. 3.11.

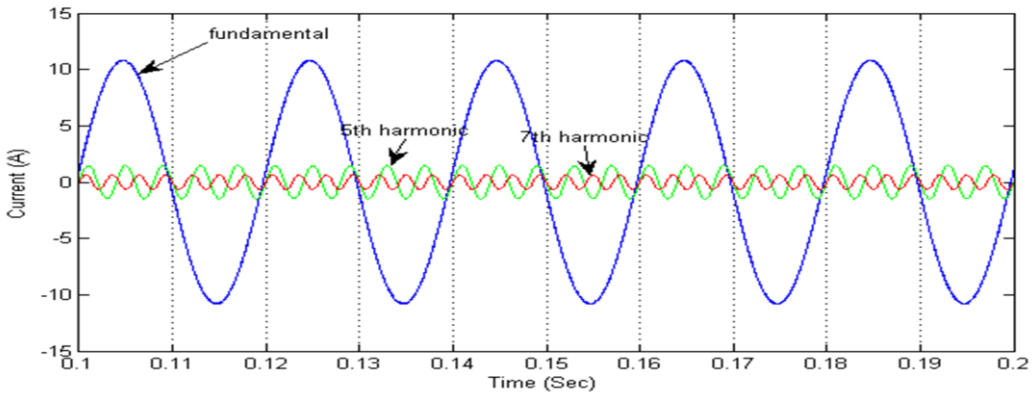

Fig. 3.11 Fifth and seventh harmonic extracted from the load current using composite observer

3.3.2 Performance of System using Composite Observer

This stated algorithm is implemented in Matlab/Simulink software. The performance is tested for two modes of operation of DSTATCOM i.e. power factor correction (PFC) mode and voltage regulation mode.

3.3.2.1 Performance of DSTATCOM for PFC mode

In Fig.3.12 the PFC mode operation of DSTATCOM is shown under nonlinear load conditions. Results for different signals are obtained that includes, supply mains current (i_s), voltages at PCC (v_{pcc}), load currents (i_{la},i_{lb} , i_{lc}), DSTATCOM currents as i_{ca}, i_{cb} , i_{cc} and the Dc bus voltage (V_{dc}) are shown. The results show that the voltage of Dc bus is maintained at the reference value of 200 V. In the same figure steady state of the system is seen to be existed upto 0.4s and when unbalancing in phase 'a' from 0.4s to 0.5s is introduced, the DSTATCOM still maintains sinusoidal variation in supply currents.

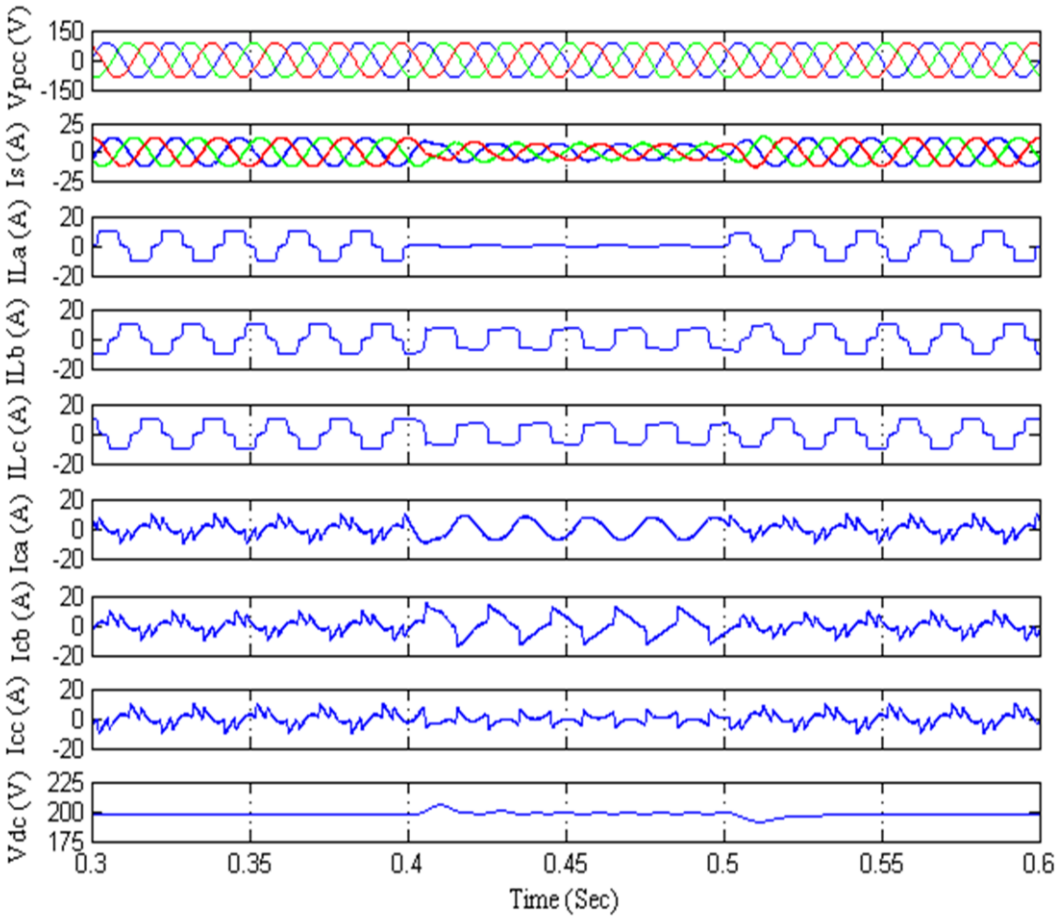

Fig. 3.12 Performance of DSTATCOM under PFC mode with composite observer

In the subsequent Fig.3.13, the harmonic analysis is shown phase 'a' is taken of different signal for the harmonic spectrum. The result comprises of three signals namely supply current (i_{sa}), load current (i_{la}) and PCC voltage (v_{pcca}) in the power factor correction mode for nonlinear load. The results obtained provide the total harmonic distortion (THD) value of supply current i_{sa}, PCC voltage v_{pcca}, and load current i_{la}. Summarizing results for THD analysis suggest that THD in supply current is reduced to 1.28% when the load current still has THD of 26.69%. The THD values of the supply current for PBT in PFC mode lies in the limits specified by IEEE-519 standards.

3.3.2.2 Performance of DSTATCOM in Voltage Regulation mode

In Fig.3.14 the operation of DSTATCOM is shown for voltage regulation mode under nonlinear load condition. The results are obtained for different parameters like supply currents (i_s), load currents (i_{la} , i_{lb} , i_{lc}), PCC voltages (v_{pcc}), DSTATCOM currents (i_{ca} , i_{cb} , i_{cc}) and the Dc bus voltage (V_{dc}). The results show that in addition to maintaining reference value of 200 V at Dc link, another PI controller is used to maintain the PCC voltage to the reference value of 89V. In the same figure up to 0.4 s the steady state of system is shown and when unbalancing is injected in phase 'a' for time interval 0.4 s to 0.5 s, the supply currents are well maintained to be sinusoidal but have a reduction in magnitude.

In the Fig.3.15 the harmonic analysis is shown, phase 'a' is taken of different signal for the harmonic spectrum. The result comprises of three signals namely supply current (i_{sa}), load current (i_{la}) and PCC voltage (v_{pcca}) in the power factor correction mode for nonlinear load. The results obtained provide the total harmonic distortion (THD) value of supply current i_{sa}, PCC voltage v_{pcca}, and load current i_{la}. Summarizing results for THD analysis suggest that THD in supply current is reduced to 0.81% when the load current still has THD of 26.68%. The THD values of the supply current for PBT in PFC mode lies in the limits specified by IEEE-519 standards.

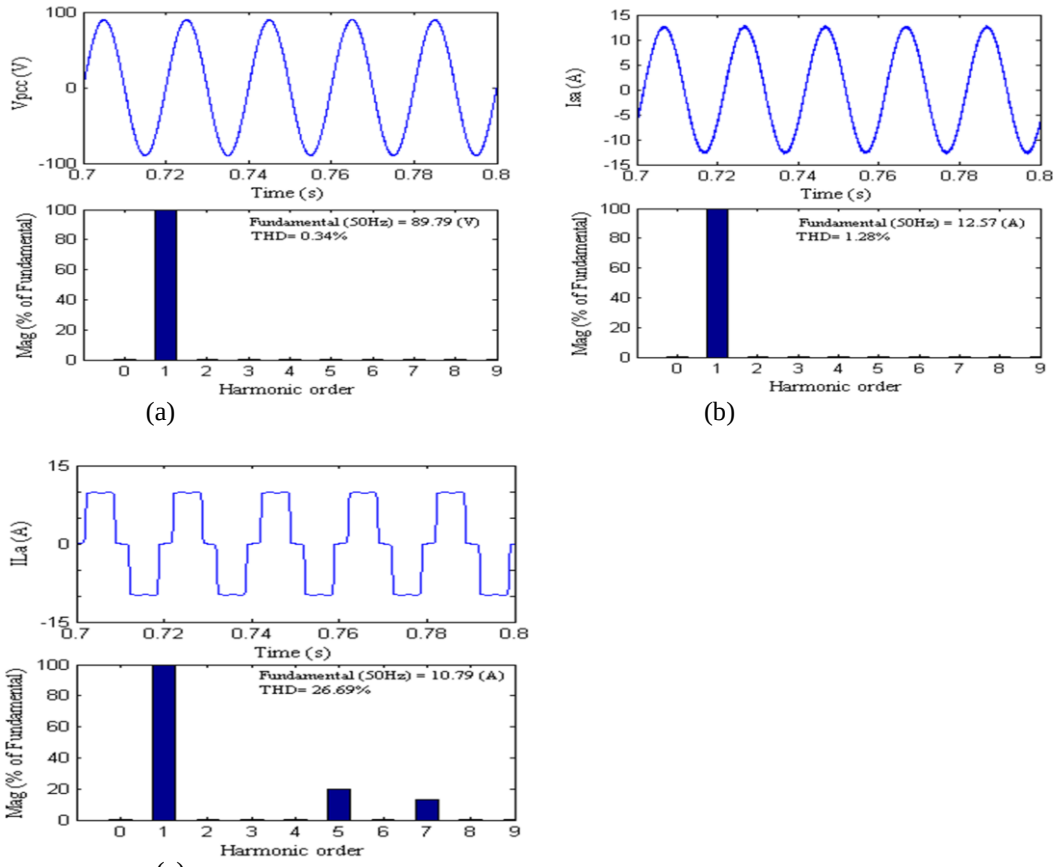

Fig.3.13 Harmonic spectra of (a) PCC voltage v_{pcca} ,(b) supply current i_{sa} , (c) load current i_{la} in PFC mode for Composite Observer

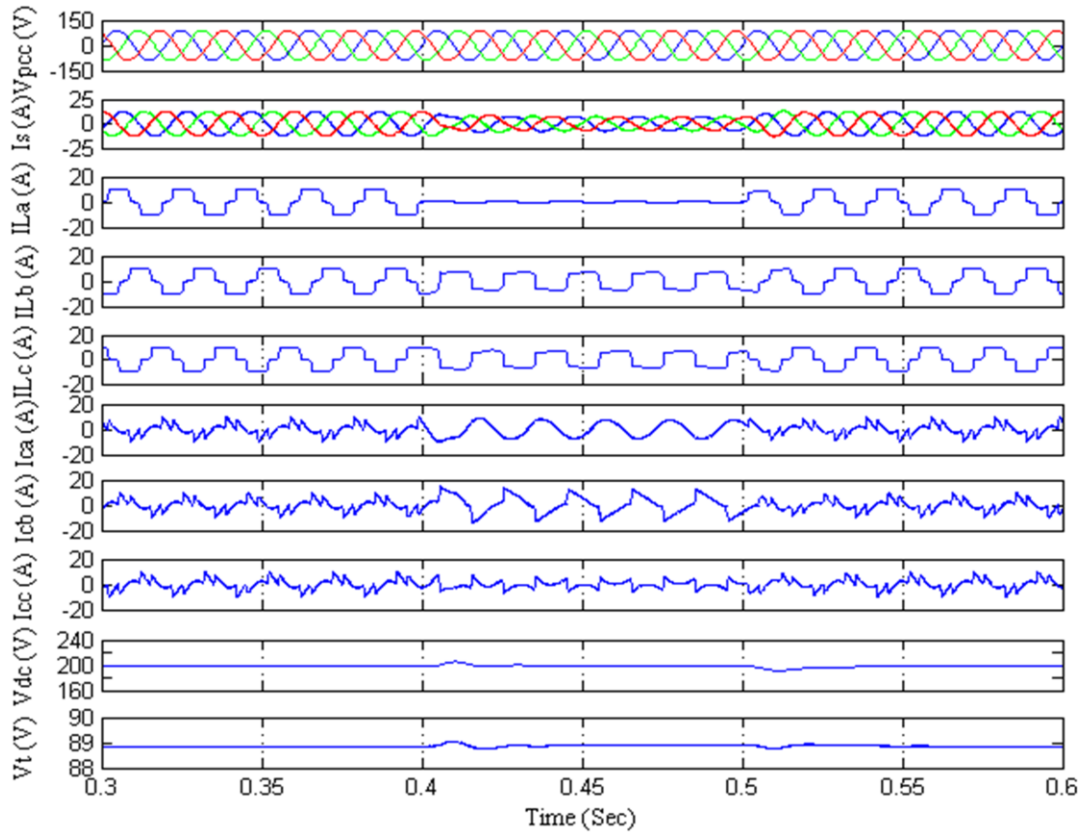

Fig.3.14. Performance of DSTATCOM in voltage regulation mode for Composite Observer.

3.3.2.3 Intermediate Results for Composite Observer

Intermediate results for Composite Observer are given in Fig.3.16. The results are taken for fundamental component of active load current I_{Lp}, fundamental component of reactive load current I_{Lq} and reference currents generated i_s^*.

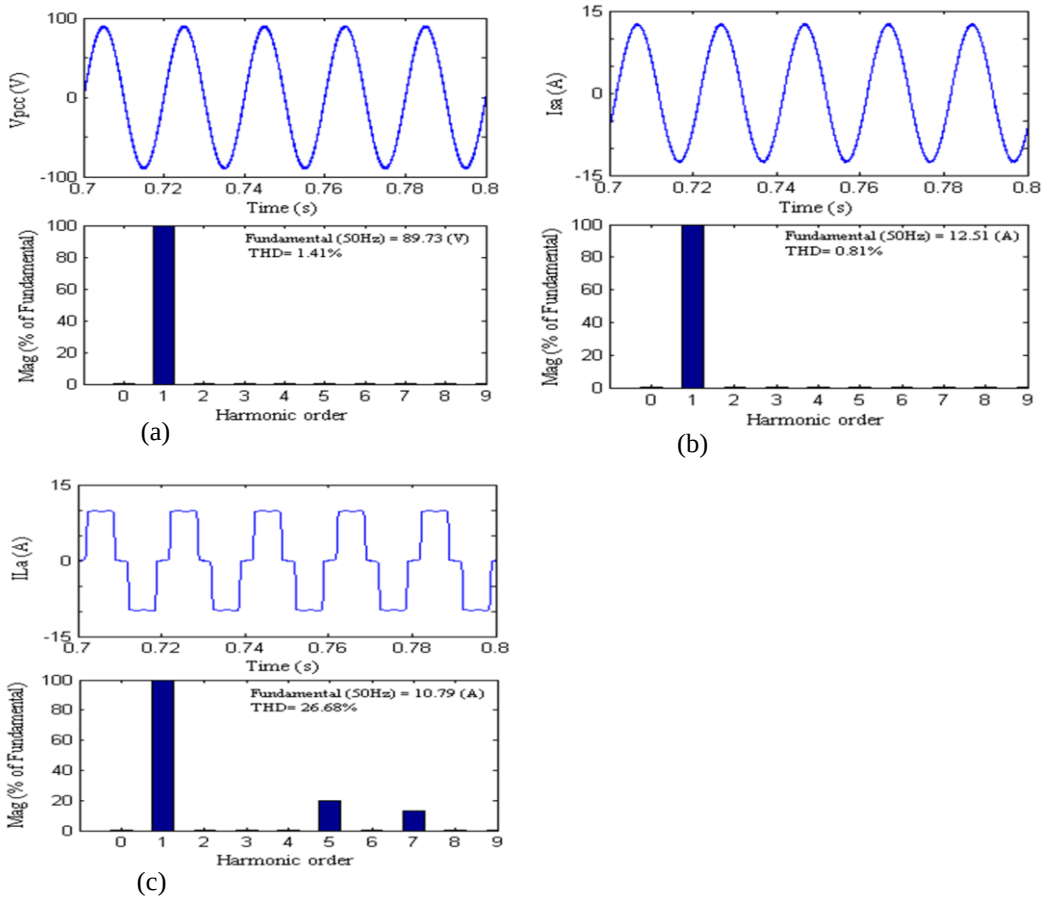

Fig.3.15 Harmonic spectra of (a) PCC voltage v_{pcca} ,(b) supply current i_{sa} , (c) load current i_{la} in ZVR mode for Composite Observer

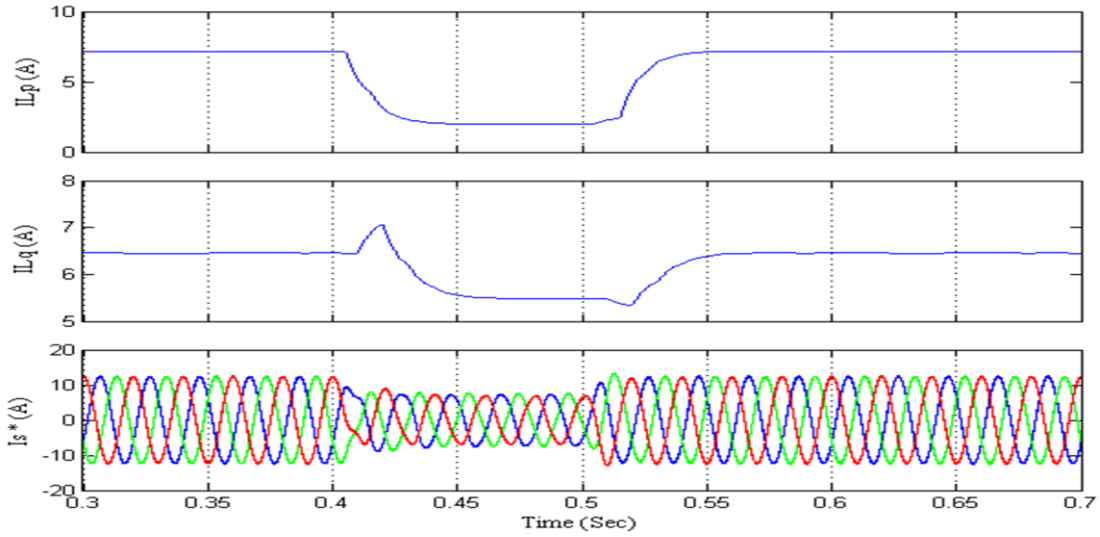

Fig.3.16 Results for Intermediate signals for Composite Observer

3.4 Proportional Resonant Controller

The conventional PI controllers have a drawback that they cannot track non dc or sinusoidal references without error. Therefore, to overcome these drawbacks, proportional resonant (PR) controllers have been proposed in many recent works. The PR controller essentially introduces an infinite gain at a selected resonant frequency for eliminating steady state error at that frequency. Hence, multiple PR controllers can be used for selectively compensating low order harmonics.

Recent applications of PR controllers can be found in grid connected three phase active power filters. Another advantage of PR controller over PI is the unique feature of compensating both positive and negative sequence components simultaneously. Experiments conducted on single phase active power filter controlled using digital PR controller using two integrators have been conducted. Once the PR controller is designed, digital implementation of PR controllers can be performed using discretization methods.

The design and implementation of PR controller for selective harmonic extraction is given in detail. Fundamental, fifth and seventh order harmonics are extracted using PR filters and the fundamental component of load current is utilized further for reference current generation. A simplified current control technique is presented and simulation results using Matlab based models are presented in the subsequent section.

3.4.1 Design and Realization of PR based filters

The design and realization of PR based filters for harmonic analysis, fundamental extraction and subsequent use in compensation is now described below.

Using the Clarke's transformation, three-phase currents can be transformed from abc-αβ components using the Eqs. (3.25) - (3.26)

$$i_{\alpha=}\sqrt{\frac{2}{3}}\left[i_{La}-\frac{i_{Lb}}{2}-\frac{i_{Lc}}{2}\right] \tag{3.25}$$

$$i_{\beta=}=\frac{1}{\sqrt{2}}[i_{Lb}-i_{Lc}] \tag{3.26}$$

where i_{La}, i_{Lb} and i_{Lc} are the three-phase load currents and i_{α}, i_{β} are the αβ components of load currents.

PR based filter with an ideal gain is expressed as in Eq(3.27)

$$G_c(s) = k_p + \frac{2k_r s}{s^2+\omega^2} \tag{3.27}$$

where $G_c(s)$ represents the controller transfer function in's' domain and k_p, k_r and w denote the proportional gain, integral gain and angular frequency in rad/sec respectively.

with a non-ideal gain, the PR based filter is expressed as

$$G_c(s) = k_p + \frac{2k_r\omega_c s}{s^2+2\omega_c s+\omega^2} \tag{3.28}$$

where w_c denotes the cutoff angular frequency in rad/sec.

The Bode plots for the ideal and non-ideal PR filter are depicted in Fig.3.17. It is observed that Bode plot for ideal PR filter shows an infinite gain at the fundamental frequency (50Hz) for which it is tuned. The Bode plot for the non-ideal PR filter gives a correspondingly lower gain at the tuned frequency of 50Hz. The design parameters chosen for both the filters have cutoff frequency w_c=15rad/s, w=314rad/s,

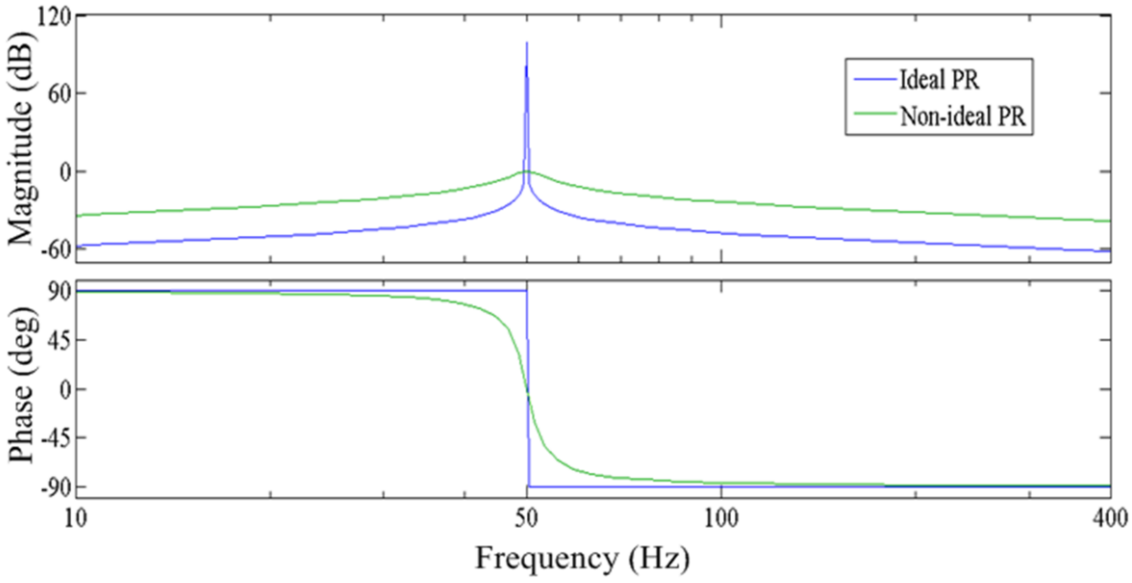

Fig.3.17 Bode plots for Ideal and non-ideal PR filter

kp=0.1 and k_r=1.02.

The transfer function $G_c(s)$ for resonant based filter tuned to 5^{th} and 7^{th} harmonics can be represented as

$$G_c(s) = k_p + \sum_{n=5,7} \frac{2k_r\omega_c s}{s^2+2\omega_c s+(n*w)^2} \quad (3.29)$$

where k_p and k_r denotes the proportional and resonant gains.

The complete transfer function of the PR controller used for the extraction of fundamental, 5th and 7th order harmonics can now be depicted as

$$G_h(s) = k_p + \sum_{h=1,5,7} \frac{2k_r\omega_c s}{s^2+2\omega_c s+(h\omega^2)} \quad (3.30)$$

The Bode plot for multiple PR controller represented in Eq(3.30) has been depicted in Fig.3.18. The figure shows now three peaks corresponding to 50Hz, 250Hz and 350Hz respectively for which the filter has been designed.

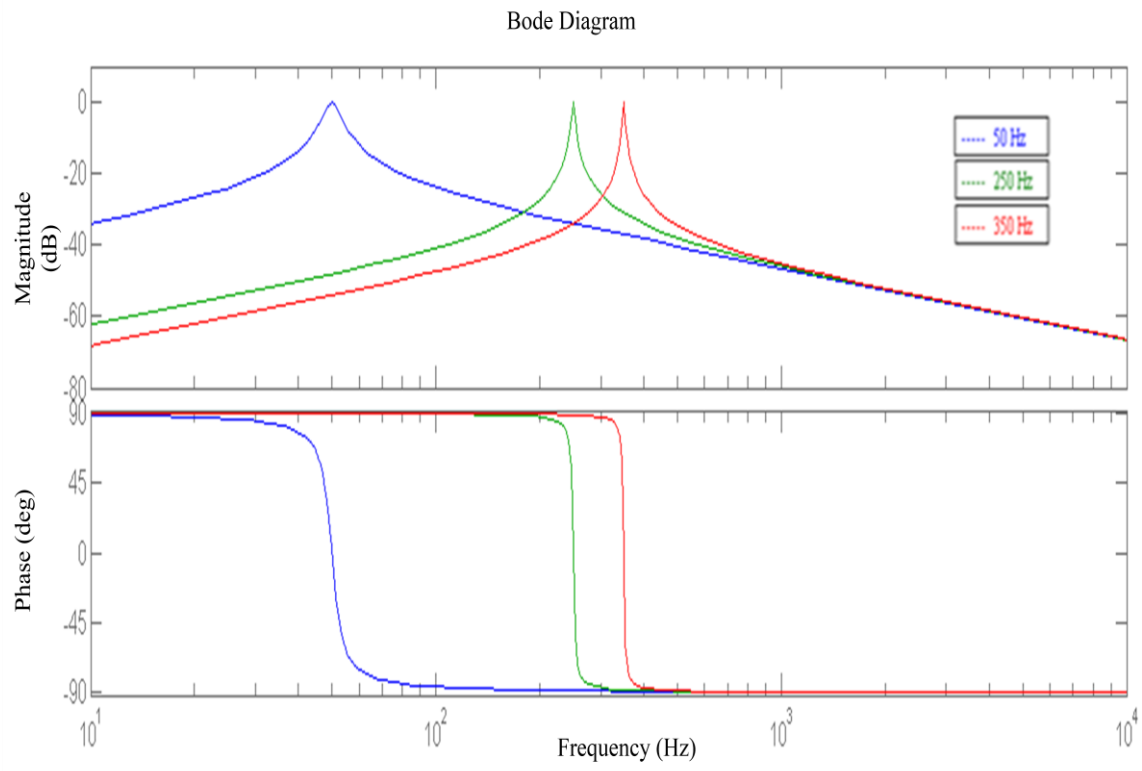

Fig.3.18 Bode plot for PR filter tuned to 50, 250 and 350 Hz

The distorted load current is decomposed into α-β components to obtain i_α, i_β and then passed through PR filters to extract 'nth' order of harmonic. The fundamental αβ components $i_{\alpha1}, i_{\beta1}$ are

$$i_{\alpha1} = (k_p + \frac{2k_r\omega_c s}{s^2+2\omega_c s+\omega^2})i_\alpha \quad (3.31)$$

$$i_{\beta1} = (k_p + \frac{2k_r\omega_c s}{s^2+2\omega_c s+\omega^2})i_\beta \quad (3.32)$$

The fundamental components ($i_{\alpha 1,}$ $i_{\beta 1}$) are then transformed in *abc* domain to obtain reference currents.

$$\begin{bmatrix} i_{sa} \\ i_{sb} \\ i_{sc} \end{bmatrix} = \sqrt{\frac{2}{3}} \begin{bmatrix} \frac{1}{\sqrt{2}} & 1 & 0 \\ \frac{1}{\sqrt{2}} & \frac{-1}{2} & \frac{\sqrt{3}}{2} \\ \frac{1}{\sqrt{2}} & \frac{-1}{2} & \frac{\sqrt{3}}{2} \end{bmatrix} \begin{bmatrix} i_0 \\ i_\alpha \\ i_\beta \end{bmatrix} \tag{3.33}$$

These currents are then used to calculate the fundamental weight of load current by using Eq.(3.34)

$$I_{Lp} = \sqrt{\frac{2}{3}\left(i_{sa}^2 + i_{sb}^2 + i_{sc}^2\right)} \tag{3.34}$$

This fundamental component extracted using PR filters tuned to 50Hz is perfectly sinusoidal. On the same lines, PR filter tuned to 5th and 7th harmonic have been utilized for selective harmonic extraction; however for closed loop shunt compensation only the fundamental weight component is used further.

3.4.2 Generation of Reference Supply Currents

The peak amplitude of the three phase voltage at the point of common coupling (PCC) terminal is calculated as,

$$V_t = \left[\left({}^{2}/_{3}\right)\left(v_a^2 + v_b^2 + v_c^2\right)\right]^{1/2} \tag{3.35}$$

in phase unit templates with phase voltages are obtained as,

$$u_{sa} = \frac{v_a}{v_t},\ u_{sb} = \frac{v_b}{v_t}, u_{sc} = \frac{v_c}{v_t} \tag{3.36}$$

The component of the active power current required to maintain Dc link voltage is estimated by PI controller output whose input is the error in voltage between reference DC link voltage and its sensed DC link voltage.

$$V_{dec}(n) = V^*_{dc(n)} - V_{dc(n)} \tag{3.37}$$

in the above difference equation, $V^*_{dc(n)}$ is the DC link voltage and $V_{dc(n)}$ is the sensed DC link voltage.

As discussed earlier in chapter 2, the PI controller output is the second component of current required to maintain the DC link voltage.

$$I_{loss(n)} = I_{loss(n-1)} + K_p\left[V_{decr(n)} - V_{decr(n-1)}\right] + K_i V_{decr(n)} \tag{3.38}$$

where $I_{loss(n)}$is considered as the loss component that needs to be met from the grid to maintain the DC link voltage which is the output of PI controller haiving gains as K_p and K_i.

The total active power component of the grid currents I_{active} is estimated by adding $I_{loss(n)}$ and I_{Lp} as,

$$I_{active} = I_{Lp} + I_{loss(n)} \tag{3.39}$$

The reference grid currents (i_{sa}^*, i_{sb}^* and i_{sc}^*) which are in phase to PCC voltage are estimated as,

$$i_{sa}^* = I_{active} \times u_{sa}, i_{sb}^* = I_{active} \times u_{sb}, i_{sc}^* = I_{active} \times u_{sc} \tag{3.40}$$

The reference currents (i_{sa}^*, i_{sb}^* and i_{sc}^*) are compared with the actual supply currents (i_{sa}, i_{sb} and i_{sc}) and the errors thus generated are passed over the pulse width modulated (PWM) current controller to generate six pulses for the control of shunt compensator.

3.4.3 Digital PR Filter Design

The analog PR filter shown in Eq(3.28) has be discretized for real time implementation. Since, the resonant controllers have high gains and narrow band, the implementation of digital PR filter is another important step. The process is sensitive and depends on suitable discretization method adopted and hence discretization is performed using bilinear transformation

$$s = \frac{2(1 - z^{-1})}{T_s(1+z^{-1})} \tag{3.41}$$

where T_s is sampling time

For a sampling time T_s=50μs, w_c=15rad/sec, the transfer function of the PR filter tuned for the fundamental frequency $F_1(z)$is

$$F_1(z) = \frac{0.0007494z^2 - 0.0007494}{z^2 - 1.998z + 0.9985} \tag{3.42}$$

On the same lines, with w_c=15rad/sec, the transfer function of the PR filter tuned for the 5^{th} harmonic $F_5(z)$is

$$F_5(z) = \frac{0.0007483z^2 - 2.22e^{-16}z - 0.0007483}{z^2 - 1.992z + 0.9985} \tag{3.43}$$

On the same lines, with w_c=15rad/sec, the transfer function of the PR filter tuned for the 7th harmonic $F_7(z)$is

$$F_7(z) = \frac{0.0007472z^2+4.441e^{-16}z-0.0007472}{z^2-1.986z+0.9985} \quad (3.44)$$

3.4.4 Performance of the System with PR Controller

PR model is simulated in Matlab/Simulink environment. The operation of DSTATCOM is tested for two modes i.e. power factor correction (PFC) mode and voltage regulation mode. The values of k_p and k_r are taken to be 0.1 And 1.02 in the transfer fuinction mentioned in equation (3.28).

3.4.4.1 Performance of PR Controller for Harmonic Extraction

Fig.3.19 shows the harmonics extracted using PR filters from the load current. PR filters have been designed and simulated to extract 5th and 7th harmonic along with the fundamental component of the load current. The waveforms depict the component magnitudes of 1st, 5th and 7th as a function of time and the relationship between different harmonic components is clearly evident.

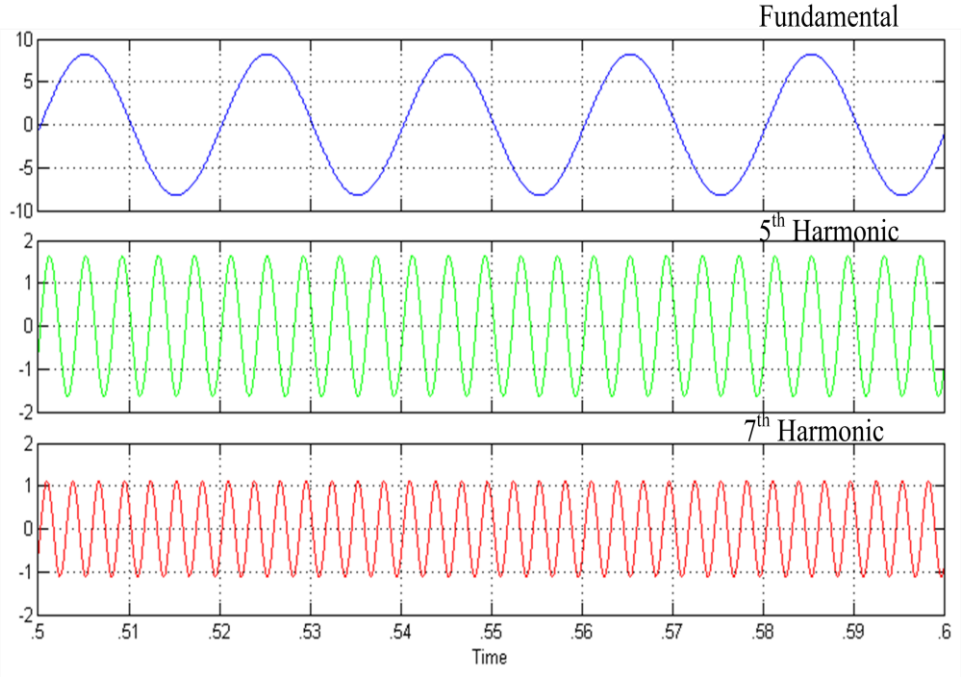

Fig.3.19 Harmonic extraction using PR filter

3.4.5.1 Performance of DSTATCOM for PFC mode

In Fig.3.20 the PFC mode operation of DSTATCOM is shown under nonlinear load conditions. Results for different signals are obtained that includes, supply mains current (i_s), voltages at PCC (v_{pcc}), load currents (i_{la},i_{lb} , i_{lc}), DSTATCOM currents as i_{ca}, i_{cb} , i_{cc} and the Dc bus voltage (V_{dc}) are shown. The results show that the voltage of Dc bus is maintained at the reference value of 200 V. In the same figure steady state of the system is seen to be existed upto 0.6s and when unbalancing in phase 'a' from 0.6s to 1s is introduced, the DSTATCOM still maintains sinusoidal variation in supply currents.

In the following Fig.3.21, the harmonic analysis is shown, phase 'a' is taken of different signal for the harmonic spectrum. The result comprises of three signals namely supply current (i_{sa}), load current (i_{la}) and PCC voltage (v_{pcca}) in the power factor correction mode for nonlinear load. The results obtained provide the total harmonic distortion (THD) value of supply current i_{sa}, PCC voltage v_{pcca}, and load current i_{la}. Summarizing results for THD analysis suggest that THD in supply current is

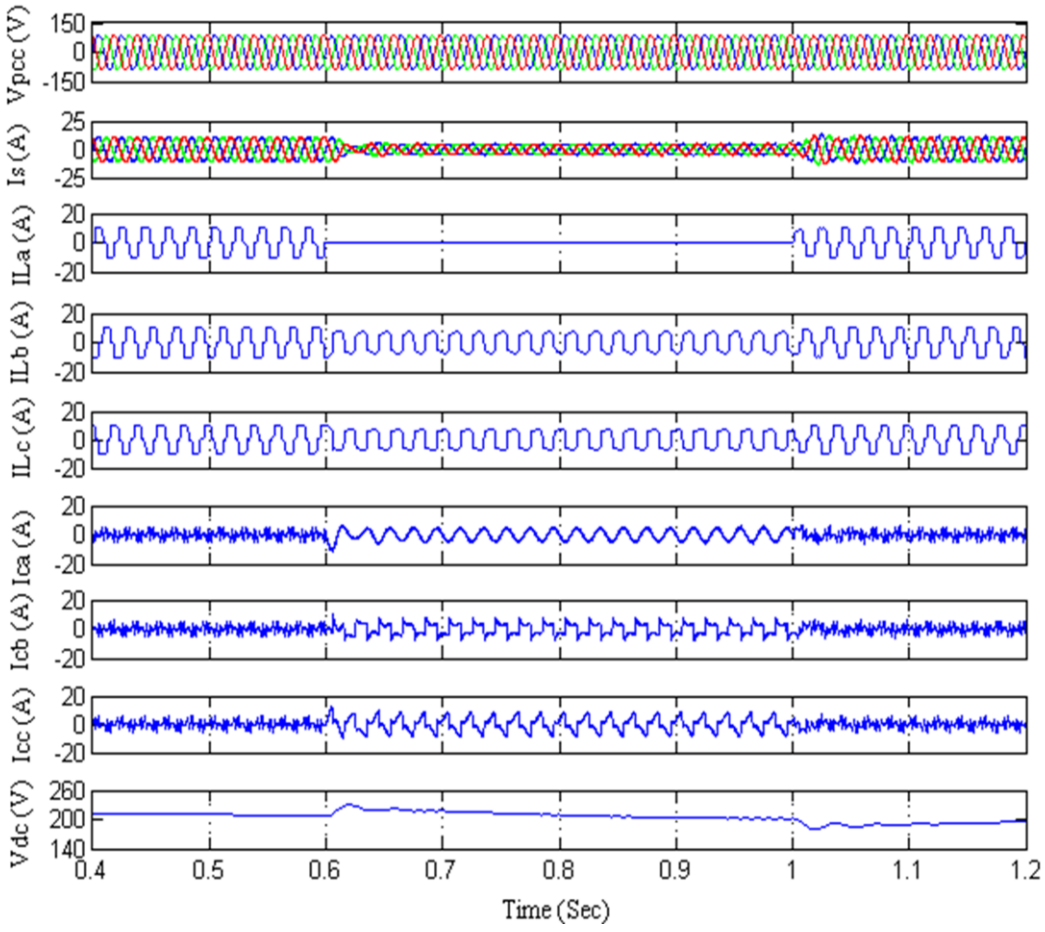

Fig.3.20 Performance of DSTATCOM under PFC mode with PR filter

reduced to 1.53% when the load current still has THD of 26.68%. The THD values of the supply current for PBT in PFC mode lies in the limits specified by IEEE-519 standards.

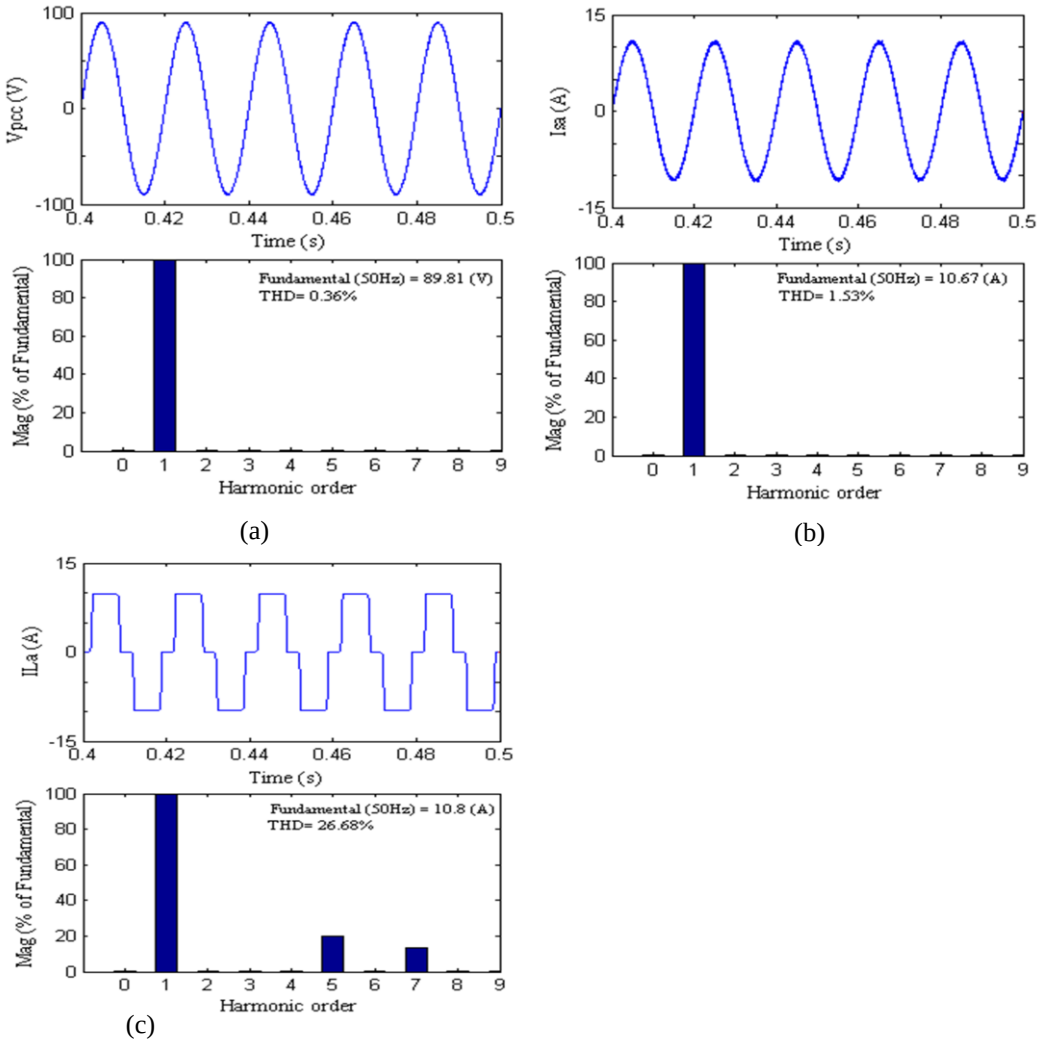

Fig.3.21 Harmonic spectra of (a) PCC voltage v_{pcca} ,(b) supply current i_{sa} , (c) load current i_{la} in PFC mode for PR filter

3.4.5.2 Performance of DSTATCOM in voltage regulation

In Fig.3.22 the operation of DSTATCOM is shown for voltage regulation mode under nonlinear load condition. The results are obtained for different parameters like supply currents (i_s), load currents (i_{la} , i_{lb} , i_{lc}), PCC voltages (v_{pcc}), DSTATCOM currents (i_{ca} , i_{cb} , i_{cc}) and the Dc bus voltage (V_{dc}). The results show that in addition to maintaining reference value of 200 V at Dc link, another PI controller is

used to maintain the PCC voltage to the reference value of 89V. In the same figure up to 0.6 s the steady state of system is shown and when unbalancing is injected in phase 'a' for time interval 0.6 s to 1 s, the supply currents are well maintained to be sinusoidal but have a reduction in magnitude..

In the Fig.3.23 the harmonic analysis is shown, phase 'a' is taken of different signal for the harmonic spectrum. The result comprises of three signals namely supply current (i_{sa}), load current (i_{la}) and PCC voltage (v_{pcca}) in the power factor correction mode for nonlinear load. The results obtained provide the total harmonic distortion (THD) value of supply current i_{sa}, PCC voltage v_{pcca}, and load current i_{la}. Summarizing results for THD analysis suggest that THD in supply current is reduced to

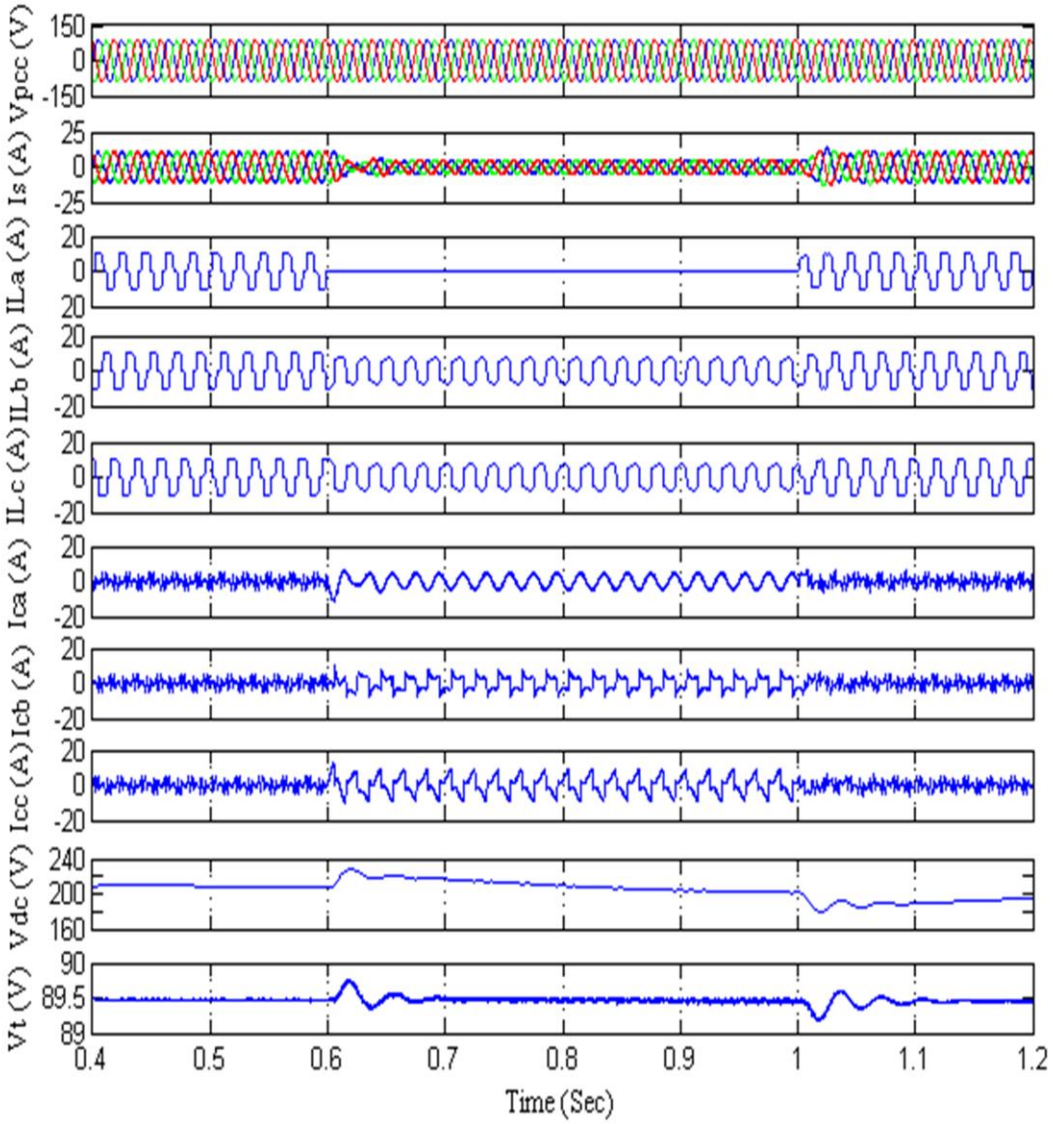

Fig.3.22 Performance of DSTATCOM under voltage regulation mode with PR filter

0.80% when the load current still has THD of 26.68%. The THD values of the supply current for PBT in PFC mode lies in the limits specified by IEEE-519 standards

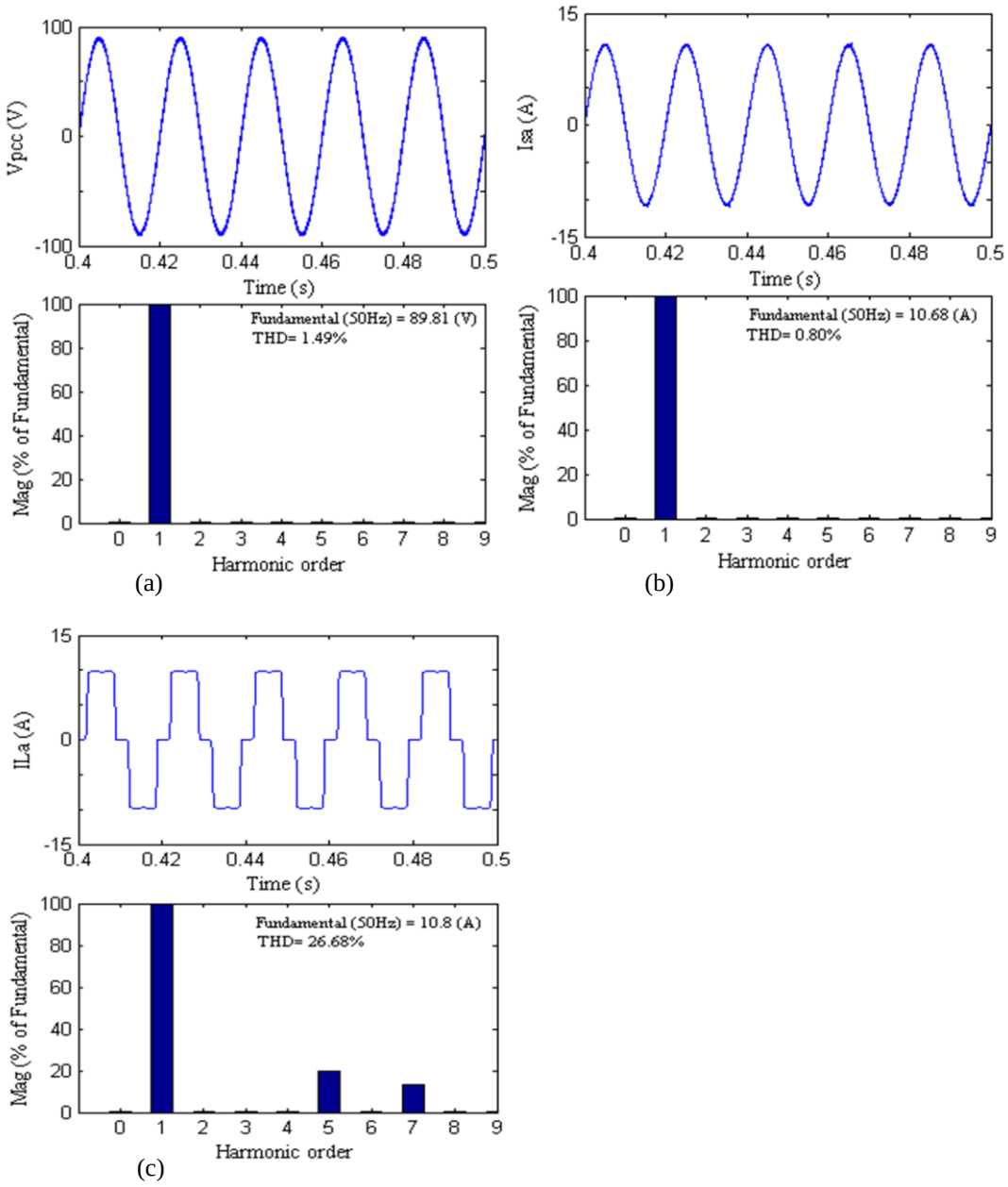

Fig.3.23 Harmonic spectra of (a) PCC voltage v_{pcca} ,(b) supply current i_{sa} , (c) load current i_{la} in voltage regulation mode for PR filter

3.4.5.3 Intermediate Results for PR filter

Intermediate results for PR filter are given in Fig.3.24. The results are taken for fundamental component for alpha and beta current before and after the filter i.e. first plot shows alpha current component of load and output of filter, second plot is for beta current of load and output of filter and third plot is for reference currents generated i_s^*. The system operates under steady state till 0.6s and unbalancing is introduced from 0.6s to 1s.

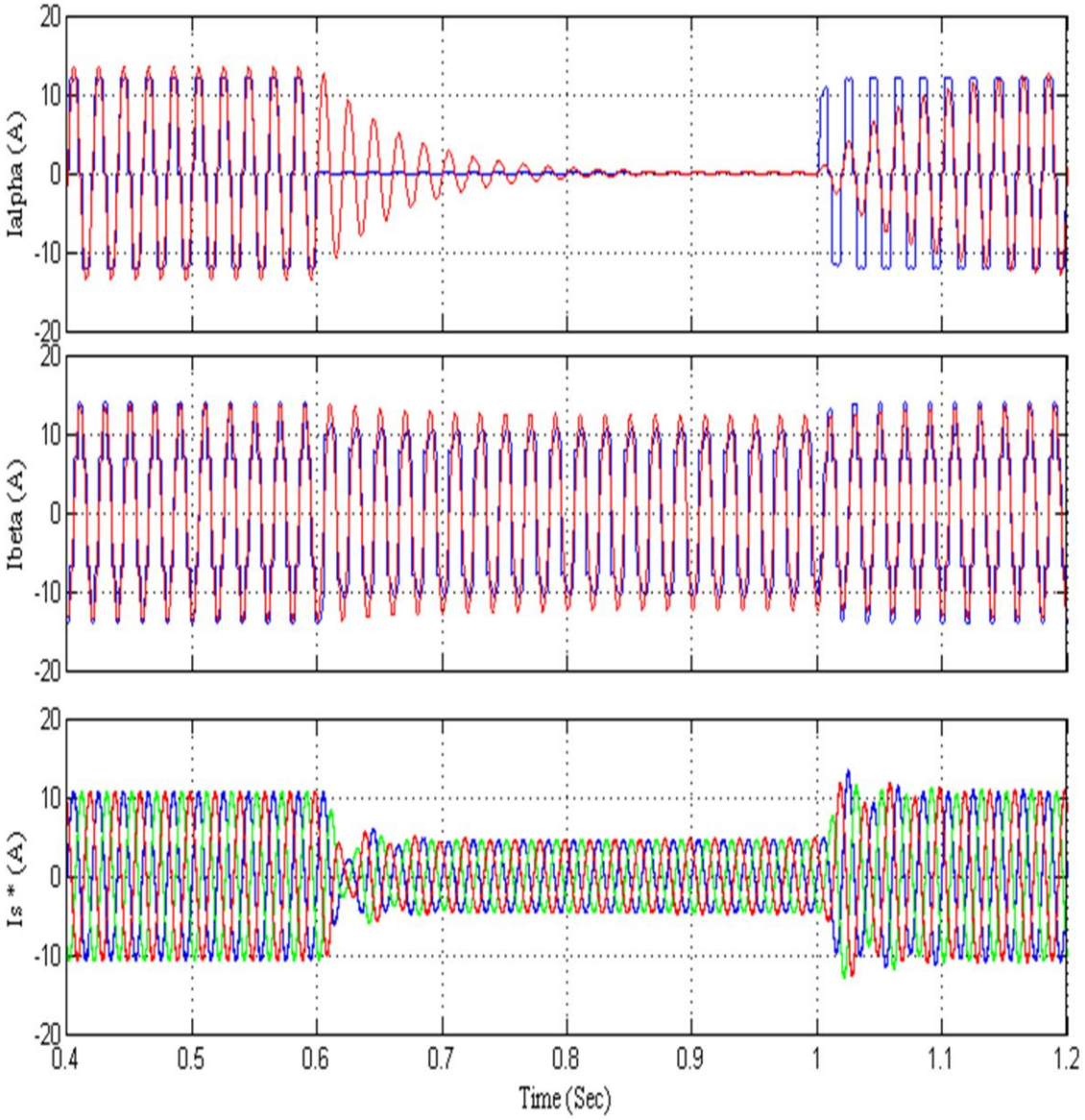

Fig.3.24 Results for Intermediate signals for PR filter

Table II Performance of DSTATCOM for LQR, CO, PR based controllers

I Linear Quadratic Regulator

Mode of Operation	Parameters	Parameters Magnitude and their THD %
Power factor correction mode	Supply current (A) Load current (A) PCC voltage (V)	10.71 A, 1.70% 10.8 A, 26.69% 89.81V, 0.33%
Voltage regulation mode	Supply current (A) Load current (A) PCC voltage (V)	10.79A, 0.94% 10.8A,26.68% 89.8V, 1.38%

II Composite Observer algorithm

Power factor correction mode	Supply current (A) Load current (A) PCC voltage (V)	12.57 A, 1.28% 10.79 A, 26.69% 89.79V, 0.34%
Voltage regulation mode	Supply current (A) Load current (A) PCC voltage (V)	12.51A, 0.81% 10.79A,26.68% 89.73V, 1.41%

III Proportional Resonant algorithm

Power factor correction mode	Supply current (A) Load current (A) PCC voltage (V)	10.67 A, 1.53% 10.8 A, 26.68% 89.81V, 0.36%
Voltage regulation mode	Supply current (A) Load current (A) PCC voltage (V)	10.68A, 0.80% 10.8A,26.68% 89.81V, 1.49%

3.5Conclusion

Three new algorithms have been considered for control of DSTATCOM which include Linear Quadratic Regulator (LQR), Composite Observer Based Control algorithm and last the Proportional Resonant (PR) filter based control algorithm for harmonic compensation in non-linear loads. Modeling, design and analysis of the system with these controllers has been discussed in detail. In LQR, the matrix, gains are calculated as $K_1 = 0.7774$ and $K_2 = 31.5553$ for PFC mode and $K_1 = 0.7440$ and K_2

= 31.5553 for voltage regulation mode. In Composite Observer based control algorithm, the fundamental component of load current has been estimated which has been used further for reference current calculations. In PR filter there is a possibility of harmonic extraction, not just fundamental but harmonics too. Digital PR filter for real time implementation has also been designed. A suitable discretization method such as bilinear transformation is adopted for discretization. All the three control schemes proposed for the control of DSTATCOM in three phase three wire system give satisfactory performance in mitigation of several power quality problems.

CHAPTER 4

ANALYSIS OF DSTATCOM UNDER DISTORTED SUPPLY VOLTAGE

4.1General

The analysis of DSTATCOM under non-ideal voltage scenarios for two different control algorithms is done in this chapter. First, power balance theory is tested for the unbalanced supply voltage scenario and thereafter Instantaneous reactive power theory is analyzed for load compensation with non-linear loads under the unbalanced supply condition. The three phase voltages considered are distorted and considered as non-ideal voltages. These three phase non-ideal voltages are filtered out to extract the positive sequence voltages which are then used in further calculations. A control algorithm based on Perfect harmonic compensation is discussed which also involves the use of Band-pass filter for filtering out the fundamental voltage component.

4.2Power Balance Theory under Distorted Supply Conditions

Power Balance Theory (PBT) based control algorithm derives the reference grid currents to achieve the power quality improvement at AC mains using power calculation from PCC voltage and load current. For synchronization, the calculation of unit templates in phase with source voltages and in phase quadrature with source voltage are derived, which are finally multiplied to the active current component calculated from power calculations. This whole process uses PCC voltage as the reference voltage for calculations; therefore in case the supply voltage is distorted its performance declines and the schemes do not work well under these circumstances. A solution in this case involves the extraction and use of positive sequence voltages from the distorted supply voltage and further calculations are performed using the filtered voltages.

In case of distorted supply the voltage is first filtered using positive sequence filter which is developed as per the Fortesque theorem based on symmetrical components. The method of symmetrical components is used to simplify analysis of unbalanced three-phase power systems under both normal and abnormal conditions. The most use of this transformation is made in the analysis of faults in power systems in

which the three phase voltages are transformed into three mutually independent set of voltages namely positive, negative and zero sequence voltages. In a three-phase system, the three phases can be resolved into three sets of phasors, one set has the same phase sequence as the original voltages of the system positive sequence, another set has the reverse phase sequence as negative sequence, and the third set the has the three phasors in phase with each other as zero sequence.

Three-phase voltages V_a, V_b, V_c can be given as sum of three symmetrical phasors as following

$$\begin{bmatrix} V_a \\ V_b \\ V_c \end{bmatrix} = \begin{bmatrix} V_{a0} \\ V_{b0} \\ V_{c0} \end{bmatrix} + \begin{bmatrix} V_{a1} \\ V_{b1} \\ V_{c1} \end{bmatrix} + \begin{bmatrix} V_{a2} \\ V_{b2} \\ V_{c2} \end{bmatrix} \quad (4.1)$$

With â defined as the operator that shifts the original vector by 120° forward, $\hat{a} = e^{(2/3)i}$

from the definition of symmetrical components,

$V_a = V_0 + V_1 + V_2$

$V_b = V_0 + \hat{a}^2 V_1 + \hat{a} V_2$

$V_c = V_0 + \hat{a} V_1 + \hat{a}^2 V_2$

$$\begin{bmatrix} V_a \\ V_b \\ V_c \end{bmatrix} = \begin{bmatrix} 1 & 1 & 1 \\ 1 & \hat{a}^2 & \hat{a} \\ 1 & \hat{a} & \hat{a}^2 \end{bmatrix} \begin{bmatrix} V_0 \\ V_1 \\ V_2 \end{bmatrix} \quad (4.2)$$

Conversely, the sequence components generated from phase voltages can be written as

$$\begin{bmatrix} V_0 \\ V_1 \\ V_2 \end{bmatrix} = 1/3 \begin{bmatrix} 1 & 1 & 1 \\ 1 & \hat{a} & \hat{a}^2 \\ 1 & \hat{a}^2 & \hat{a} \end{bmatrix} \begin{bmatrix} V_a \\ V_b \\ V_c \end{bmatrix} \quad (4.3)$$

Thus positive sequence voltage can therefore be calculated as

$$V_1 = 1/3 (V_a + \hat{a} V_b + \hat{a}^2 V_c) \quad (4.4)$$

This filtered voltage is then used further for basic calculations involved in PBT

The basic equations for estimating active power components of grid currents are same as used in chapter 2 so it is redundant to explain those equations again here therefore simply equations are written which are involved as,

$$V_t = [(2/3)(v_{sa}^2 + v_{sb}^2 + v_{sc}^2)]^{1/2} \quad (4.5)$$

$$u_{sa} = \frac{v_{sa}}{v_t}, u_{sb} = \frac{v_{sb}}{v_t}, u_{sc} = \frac{v_{sc}}{v_t} \quad (4.6)$$

$$P_L = (v_{sa}\, i_{La} + v_{sb}\, i_{Lb} + v_{sc}\, i_{Lc}) \quad (4.7)$$

After power calculation, active component of current is filtered using LPF

$$I_{L\ active} = (2/3)\ (P_L/V_t) \quad (4.8)$$

$$V_{dec(n)} = V^*_{dc(n)} - V_{dc(n)} \quad (4.9)$$

$$I_{loss(n)} = I_{loss(n-1)} + K_p\ [\ V_{decr(n)} - V_{decr(n-1)}\ ] + K_i V_{decr(n)} \quad (4.10)$$

This is the required output of PI controller where $I_{loss(n-1)}$ is considered to be second component of rid currents that is required to maintain Dc link voltage, the PI controller has K_p and K_i as their gains.

This output of PI is then added to active component of current so as to obtain fundamental active power component of the grid currents i.e. I^*_{active}

$$I^*_{active} = I_{L\ active} + I_{loss(n)} \quad (4.11)$$

$$I^*_{sad} = I^*_{active} * u_{sa}\ ,\ I^*_{sbd} = I^*_{active} * u_{sb}\ ,\ I^*_{scd} = I^*_{active} * u_{sc} \quad (4.12)$$

These reference grid currents along with sensed grid currents are fed to PWM current controller to generate gating signals for IGBTs of VSC. For only power factor correction to unity, active power components of grid currents are taken as reference grid currents.

4.2.1 System Performance with PBT under Distorted Supply Grid

The modified PBT based control algorithm for distorted supply voltage conditions is simulated in Matlab/Simulink. The performance of DSTATCOM is tested for its power factor correction (PFC) mode. Results are shown for steady-state as well as dynamic performance of DSTATCOM. The filtered PCC voltage has reduced THD after using Positive sequence extractor. The performance of DSTATCOM shows satisfactorily results and the supply current THD gets reduced to below 5% levels as per IEEE-519 standards. The results for PFC mode obtained are discussed below.

In Fig.4.1 the PFC mode operation of DSTATCOM is shown under nonlinear load conditions in distorted supply conditions. Results for different signals are obtained that includes, supply mains current (i_s), voltages at PCC (v_{pcc}), load currents (i_{la},i_{lb} , i_{lc}), DSTATCOM currents as i_{ca}, i_{cb} , i_{cc} and the Dc bus voltage (V_{dc}) are shown. The results show that the voltage of Dc bus is maintained at the reference value of 200 V. In the same figure steady state of the system is seen to be existed upto 0.4s and when unbalancing in phase 'a' from 0.4s to 0.6s is introduced, the DSTATCOM still maintains sinusoidal variation in supply currents.

The Fig.4.2 shows the results for distorted PCC voltage with supply currents, it can be seen that though the PCC voltage contains harmonics and is distorted but the supply currents are close to sinusoidal. The supply current THD has a value close to 4.99% and some peaks can be seen in the supply currents indicating that the algorithm is not very good for distorted supply voltage scenario.

In the Fig.4.3 the harmonic spectra analysis of phase 'a' of filtered PCC voltage (v_{pccaf}) and distorted PCC voltage (v_{pcca}), supply current (i_{sa}) and load current (i_{la}) in power factor correction mode is obtained. The total harmonic distortion (THD) of i_{sa} and i_{la} are 4.99% and 24.86%, respectively. Results show that supply current has a THD of 4.99% when the THD in load current is 24.86%. The THD values of the supply current lies within the limit of IEEE-519 standards. The PCC voltage v_{pcca}, has THD of 4.90% which is reduced to 0.01% so as to obtain satisfactorily results by using positive sequence voltage extractor.

The supply voltage used in the simulation results was distorted by including the effect of harmonics (5^{th} and 7^{th}). The three phase voltages are given as below:

$$\left.\begin{aligned} v_a(t) &= 110\sin(wt) + 5\sin(5wt) + 2\sin(7wt) \\ v_b(t) &= 110\sin(wt\text{-}120^0) + 5\sin(5wt\text{-}120^0) + 2\sin(7wt\text{-}120^0) \\ v_c(t) &= 110\sin(wt\text{-}240^0) + 5\sin(5wt\text{-}240^0) + 2\sin(7wt\text{-}240^0) \end{aligned}\right\} \quad (4.13)$$

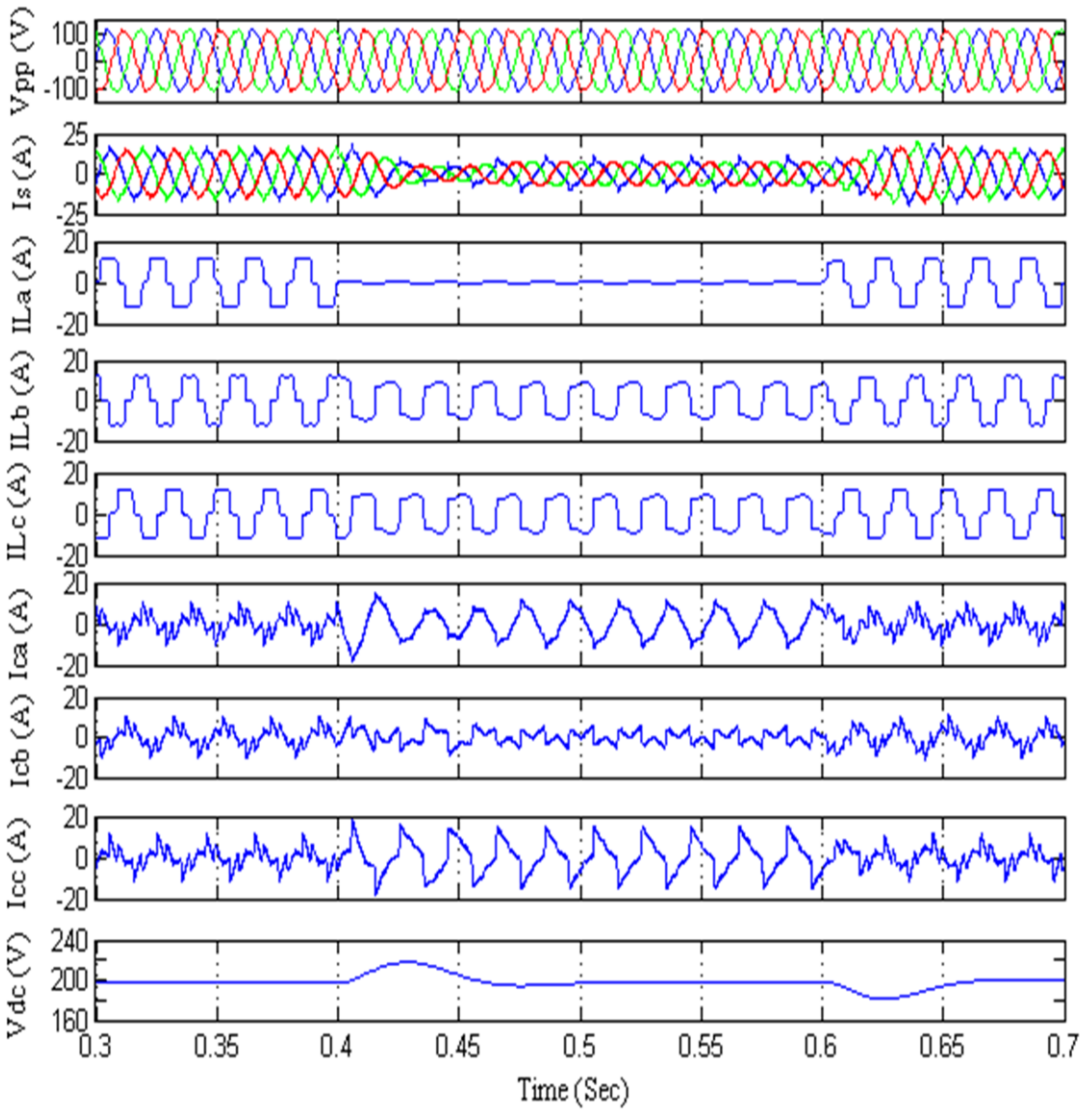

Fig. 4.1 Performance of DSTATCOM under PFC mode for distorted supply with PBT

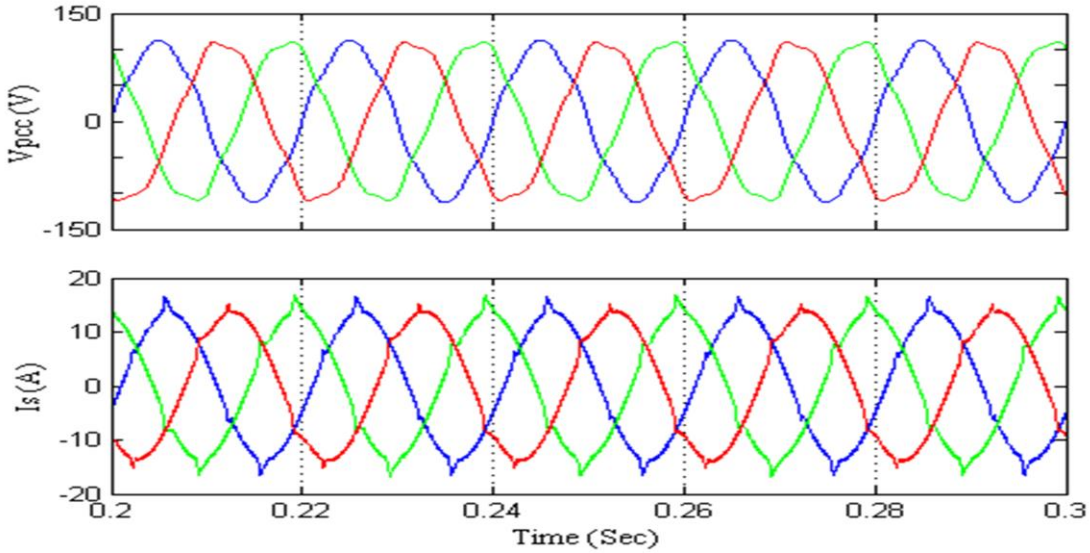

Fig.4.2 Supply voltage and supply currents for PBT under distorted supply

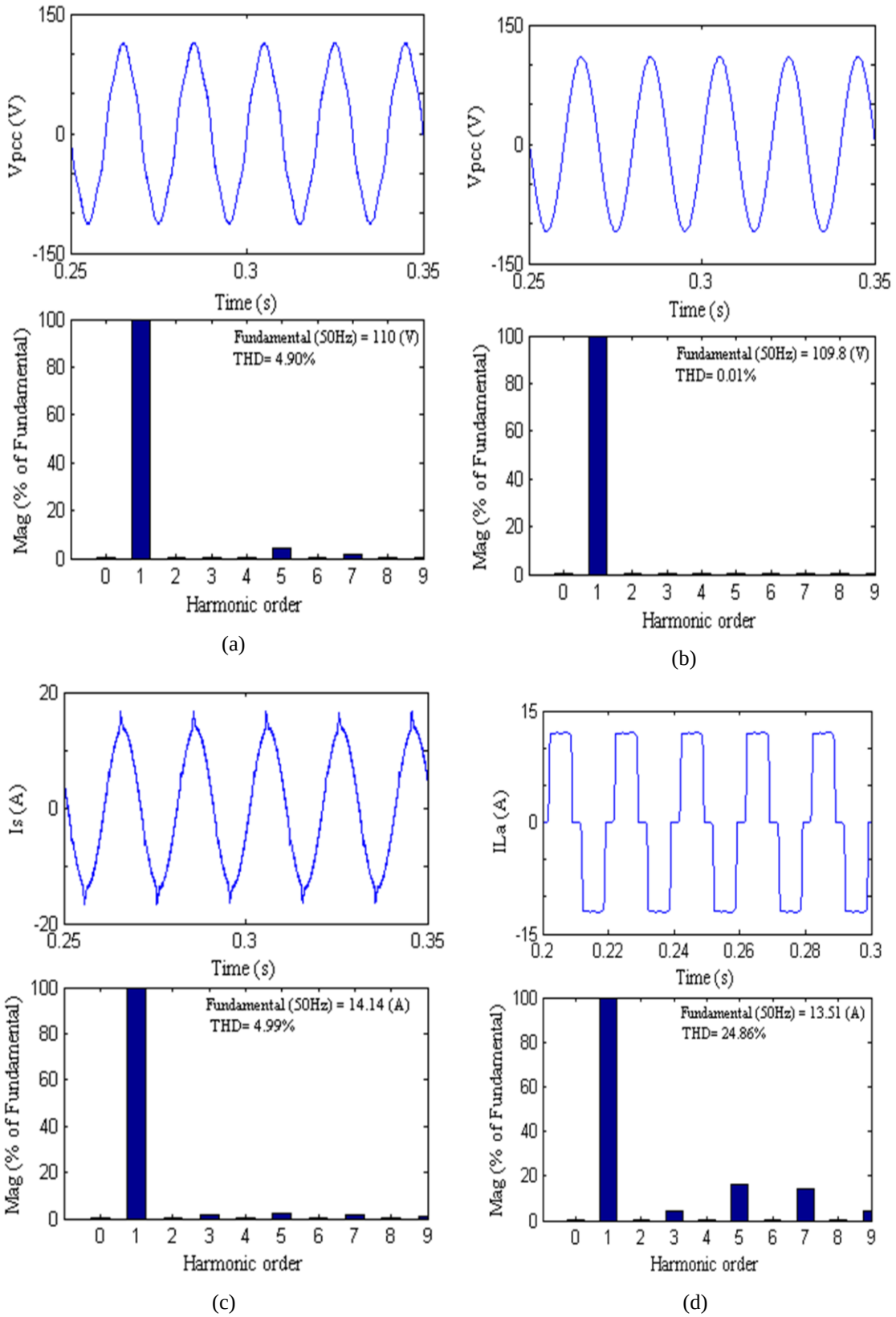

Fig. 4.3 Harmonic spectra of (a) Distorted PCC voltage v_{pcca} , (b) filtered PCC voltage (c) supply current i_{sa} , (d) load current i_{la} in PFC mode for PBT in distorted supply

4.3 Instantaneous Reactive Power Theory under Distorted Supply Condition

The instantaneous reactive power theory has been used for calculation of compensation current since a long time and it is still being used as conventional theory for reactive power compensation for shunt active filters. This theory considers supply mains voltage to be ideal source which is used in the reference current calculation process. It is observed that this algorithm proves out to be working well for load compensation under a set of balanced three phase voltages, however, under the more realistic scenario; this theory fails to provide effective results when the supply mains voltage is distorted

However if the distorted supply mains is filtered to extract the positive sequence voltage and this filtered voltage is then used for compensation current calculations; still it is observed that the performance is very effective in regard to reduction in source current THD is concerned.

The instantaneous reactive power control algorithm [74] uses αβ0 transformation that maps the instantaneous abc phase quantities to the instantaneous αβ0 quantities. The Clarke transformation of voltages is given as following

$$\begin{bmatrix} v_0 \\ v_\alpha \\ v_\beta \end{bmatrix} = \sqrt{\frac{2}{3}} \begin{bmatrix} \frac{1}{\sqrt{2}} & \frac{1}{\sqrt{2}} & \frac{1}{\sqrt{2}} \\ 1 & \frac{-1}{2} & \frac{-1}{2} \\ 0 & \frac{\sqrt{3}}{2} & \frac{\sqrt{3}}{2} \end{bmatrix} \begin{bmatrix} v_a \\ v_b \\ v_c \end{bmatrix} \tag{4.14}$$

Similarly three phase instantaneous currents can be transformed αβ0 and vice versa,

$$\begin{bmatrix} i_0 \\ i_\alpha \\ i_\beta \end{bmatrix} = \sqrt{\frac{2}{3}} \begin{bmatrix} \frac{1}{\sqrt{2}} & \frac{1}{\sqrt{2}} & \frac{1}{\sqrt{2}} \\ 1 & \frac{-1}{2} & \frac{-1}{2} \\ 0 & \frac{\sqrt{3}}{2} & \frac{\sqrt{3}}{2} \end{bmatrix} \begin{bmatrix} i_a \\ i_b \\ i_c \end{bmatrix} \tag{4.15}$$

The advantage of this transformation is that the separation of zero sequence components from the abc phase components. In a balanced three phase three wire system, zero sequence component does not exist so that the evaluation of αβ voltages and currents are only required.

Three phase instantaneous power in terms of above defined Clarke transformation has inherent power invariant property thus the analysis of three phase instantaneous power is easily done.

$$P_{3\phi} = v_a\, i_a + v_b\, i_b + v_c\, i_c \;=\; v_\alpha i_\alpha + v_\beta i_\beta + v_0 i_0 \tag{4.16}$$

In the Clarke transformation, the three phase active, reactive and zero sequence power is defined using the instantaneous αβ0 components.

$$\begin{bmatrix} p_0 \\ p \\ q \end{bmatrix} = \begin{bmatrix} v_0 & 0 & 0 \\ 0 & v_\alpha & v_\beta \\ 0 & v_\beta & -v_\alpha \end{bmatrix} \begin{bmatrix} i_0 \\ i_\alpha \\ i_\beta \end{bmatrix} \tag{4.17}$$

Since there are no zero sequence currents in balanced three phase three wire system the i_0 component is zero thus zero sequence power is always zero. Thus instantaneous active and reactive power is only present.

This instantaneous power theory can be used for shunt compensation of non-linear loads. The calculated real power and reactive of the load can be separated into its two components, average and the oscillating part. Then the undesired component of the active and reactive power of the load that needs to be compensated is selected. The powers to be compensated are represented as p^* and q^* such that the compensator should draw current in such a way that it should produce exactly the inverse of the undesirable power drawn by the non-linear load.

The inverse transformation is applied form αβ to abc and the instantaneous values of three phase compensating reference currents are calculated as i_{ca}^*, i_{cb}^*, i_{cc}^*.

From the definition of active and reactive power in terms of αβ components,

$$\begin{bmatrix} p \\ q \end{bmatrix} = \begin{bmatrix} v_\alpha & v_\beta \\ -v_\beta & v_\alpha \end{bmatrix} \begin{bmatrix} i_\alpha \\ i_\beta \end{bmatrix} \tag{4.18}$$

From the above relation it possible to write

$$\begin{bmatrix} i_\alpha \\ i_\beta \end{bmatrix} = \frac{1}{v_\alpha^2 + v_\beta^2} \begin{bmatrix} v_\alpha & -v_\beta \\ v_\beta & v_\alpha \end{bmatrix} \begin{bmatrix} p \\ q \end{bmatrix} \tag{4.19}$$

Here p and q are the powers to be compensated. These currents are then transformed from αβ to abc as reference currents for the compensator. For reactive

power compensation using DSTATCOM, only active power is used for calculation of reference currents which is filtered using a low pass filter on calculated active power so as to obtain only the fundamental component of load current.

In distorted supply voltage case, the calculation of reference currents can be done using PCC voltage which is filtered by a band pass filter, however power calculation is done with PCC voltage containing harmonics. These reference currents along with sensed grid currents are fed to PWM based hysteresis current controller to generate gating signals for IGBTs of VSC.

The overall control strategy is given in flow chart in the following Figure 4.4

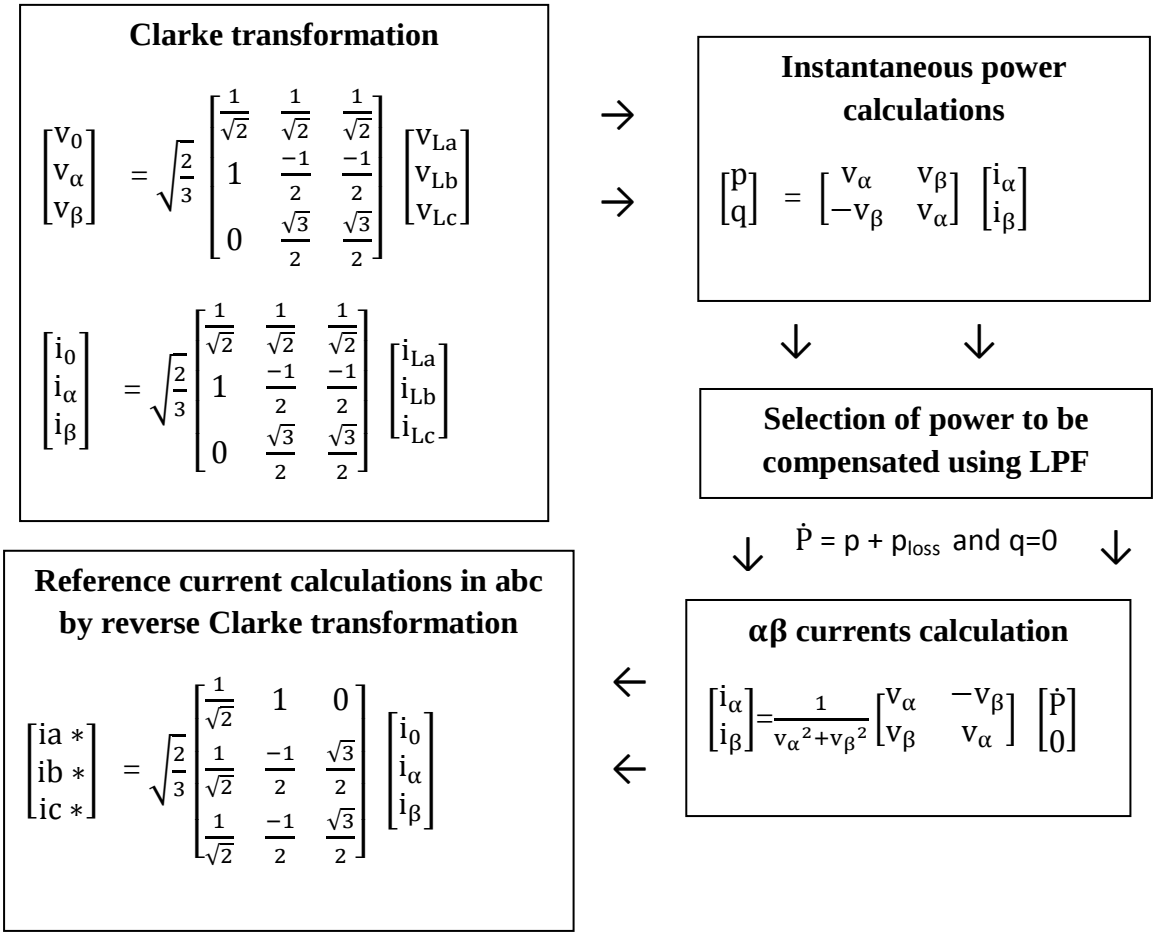

Fig.4.4 Overall control strategy for IRPT in PFC mode

4.3.1 Performance of the System with IRPT algorithm under Distorted Supply Grid

The IRPT simulation model for distorted supply voltage is made in Matlab/Simulink. The performance of DSTATCOM is tested for power factor

correction (PFC) mode under nonlinear load in distorted supply scenario. Band pass filter has been designed to filter PCC voltage. Although compensation V_{dc} takes larger time to stabilize, the performance of DSTATCOM shows satisfactorily results still IRPT in distorted supply case to obtain perfect harmonic.

A band-pass filter is a device that passes frequencies within a certain range and rejects frequencies outside that range. An example of an analogue electronic band-pass filter is an RLC circuit. An ideal band pass filter would have a completely flat pass band i.e. with no gain or attenuation throughout the range and would completely attenuate all frequencies outside the pass band. In practice, no band pass filter is ideal. The filter does not attenuate all frequencies outside the desired frequency range completely; in particular, there is a region just outside the intended pass band where frequencies are attenuated, but not rejected. The bandwidth of the filter is simply the difference between the upper and lower cutoff frequencies. The shape factor is the ratio of bandwidths measured using two different attenuation values to determine the cutoff frequency known as 3dB frequencies. The response of a practical Band pass filter is shown in Fig.4.5 below.

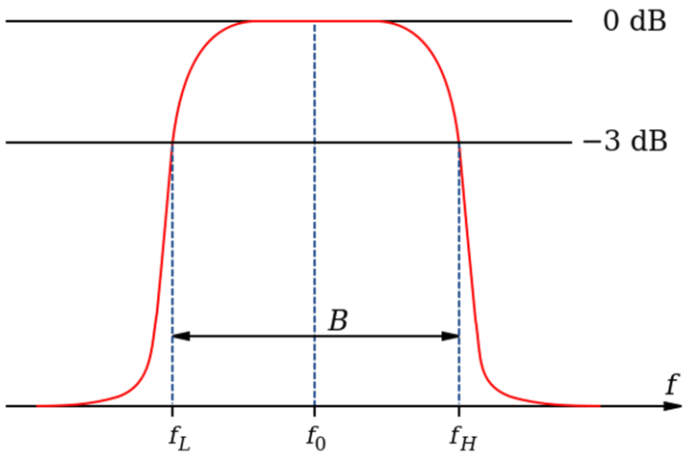

Fig.4.5 Band Pass filter characteristics

In Fig.4.6 the PFC mode operation of DSTATCOM is shown under nonlinear load conditions in distorted supply conditions. Results for different signals are obtained that includes, supply mains current (i_s), voltages at PCC (v_{pcc}), load currents (i_{la},i_{lb} , i_{lc}), DSTATCOM currents as i_{ca}, i_{cb} , i_{cc} and the Dc bus voltage (V_{dc}) are shown. The results show that the voltage of Dc bus is maintained at the reference value of 200

V. In the same figure steady state of the system is seen to be existed upto 0.4s and when unbalancing in phase ‘a’ from 0.4s to 0.6s is introduced, the DSTATCOM still maintains sinusoidal variation in supply currents.

Fig. 4.7 shows the distorted PCC voltage with supply currents, it can be seen that though the PCC voltage contains harmonics and is distorted but the supply currents tend to remain sinusoidal.

The Fig.4.8 shows harmonic spectra analysis of filtered PCC voltage (v_{pccaf}) and distorted PCC voltage (v_{pcca}), supply current (i_{sa}) and load current (i_{la}) each of phase ‘a’ in unity power factor mode under nonlinear load. The total harmonic distortion (THD) of i_{sa} and i_{la} are 4.78% and 24.87%, respectively. It is observed from these results that a 4.78% THD is obtained in supply current when the THD in load current is 24.87%. The THD values of the supply current lies in the limits of IEEE-519 standards. The PCC voltage v_{pcca}, has THD of 4.90% which is reduced to 0.01% so as to obtain satisfactorily results.

The supply voltage used is given as below

$$\left.\begin{aligned} v_a(\mathrm{t}) &= 110\sin(\mathrm{wt}) + 5\sin(5\mathrm{wt}) + 2\sin(7\mathrm{wt}) \\ v_b(\mathrm{t}) &= 110\sin(\mathrm{wt}\text{-}120) + 5\sin(5\mathrm{wt}\text{-}120) + 2\sin(7\mathrm{wt}\text{-}120) \\ v_c(\mathrm{t}) &= 110\sin(\mathrm{wt}\text{-}240) + 5\sin(5\mathrm{wt}\text{-}240) + 2\sin(7\mathrm{wt}\text{-}240) \end{aligned}\right\} \quad (4.20)$$

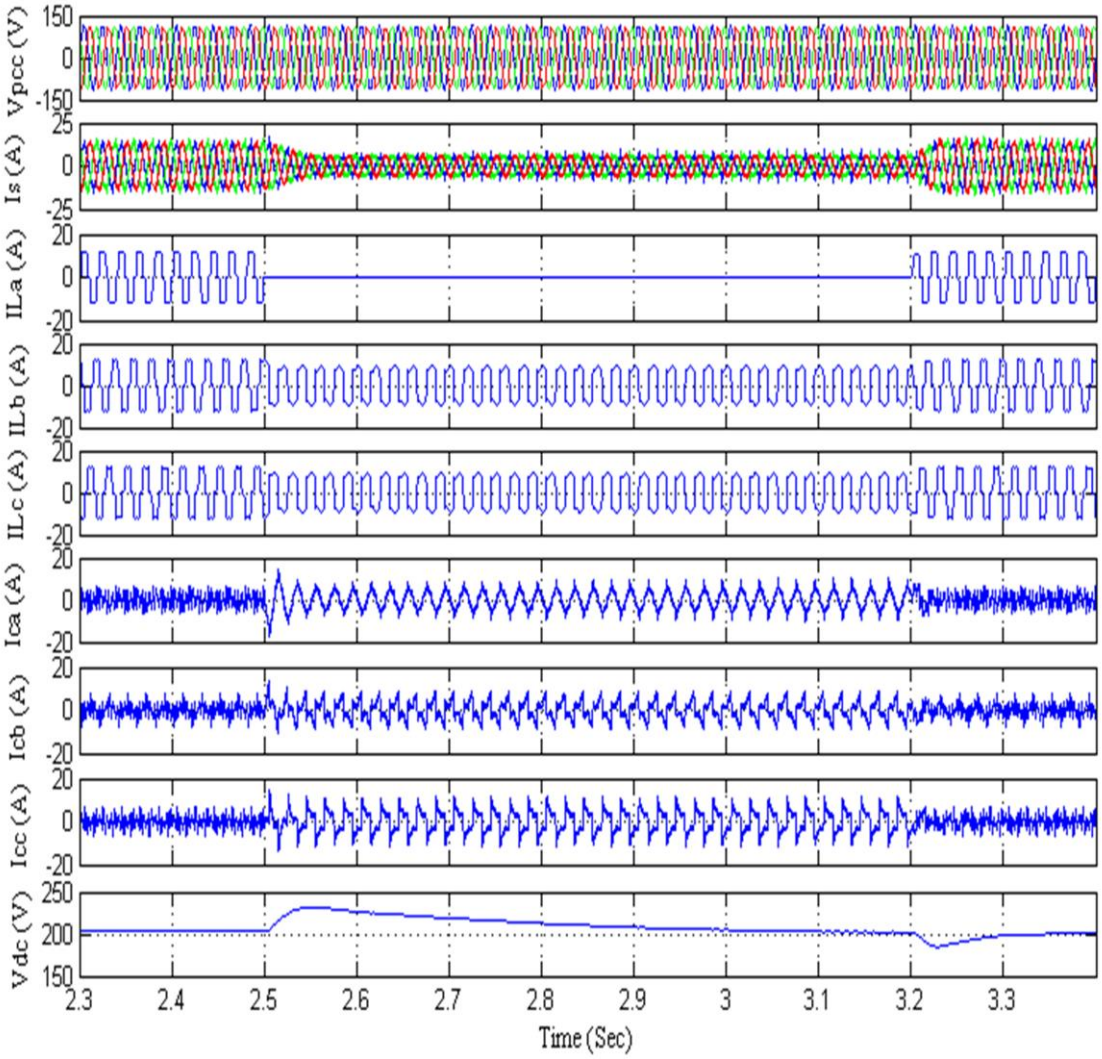

Fig. 4.6 Performance of DSTATCOM under PFC mode for IRPT in distorted supply

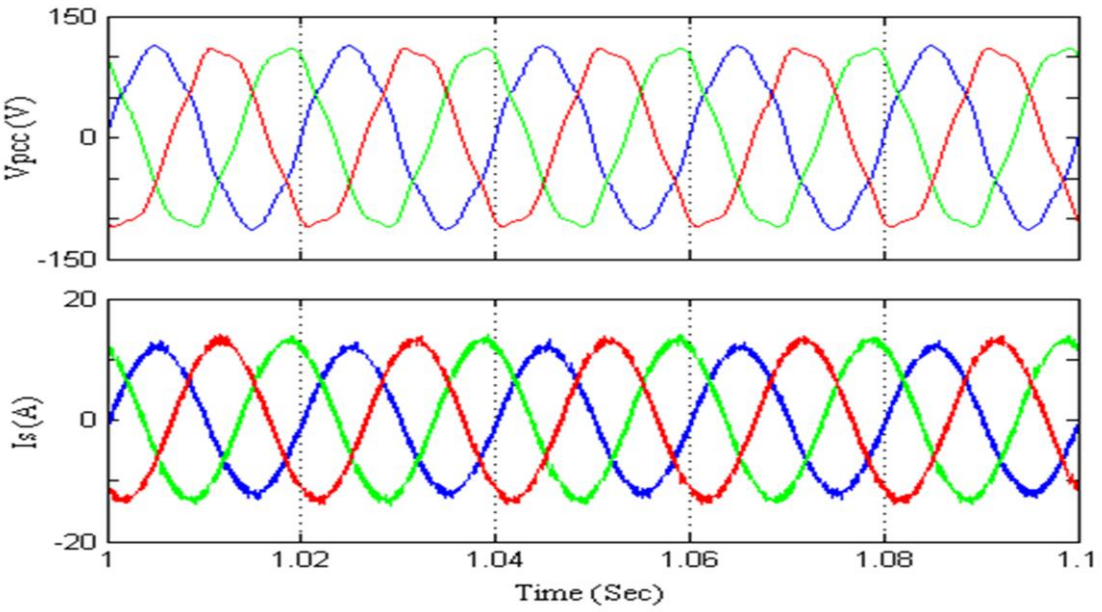

Fig.4.7 Supply voltage and supply currents for IRPT in distorted supply

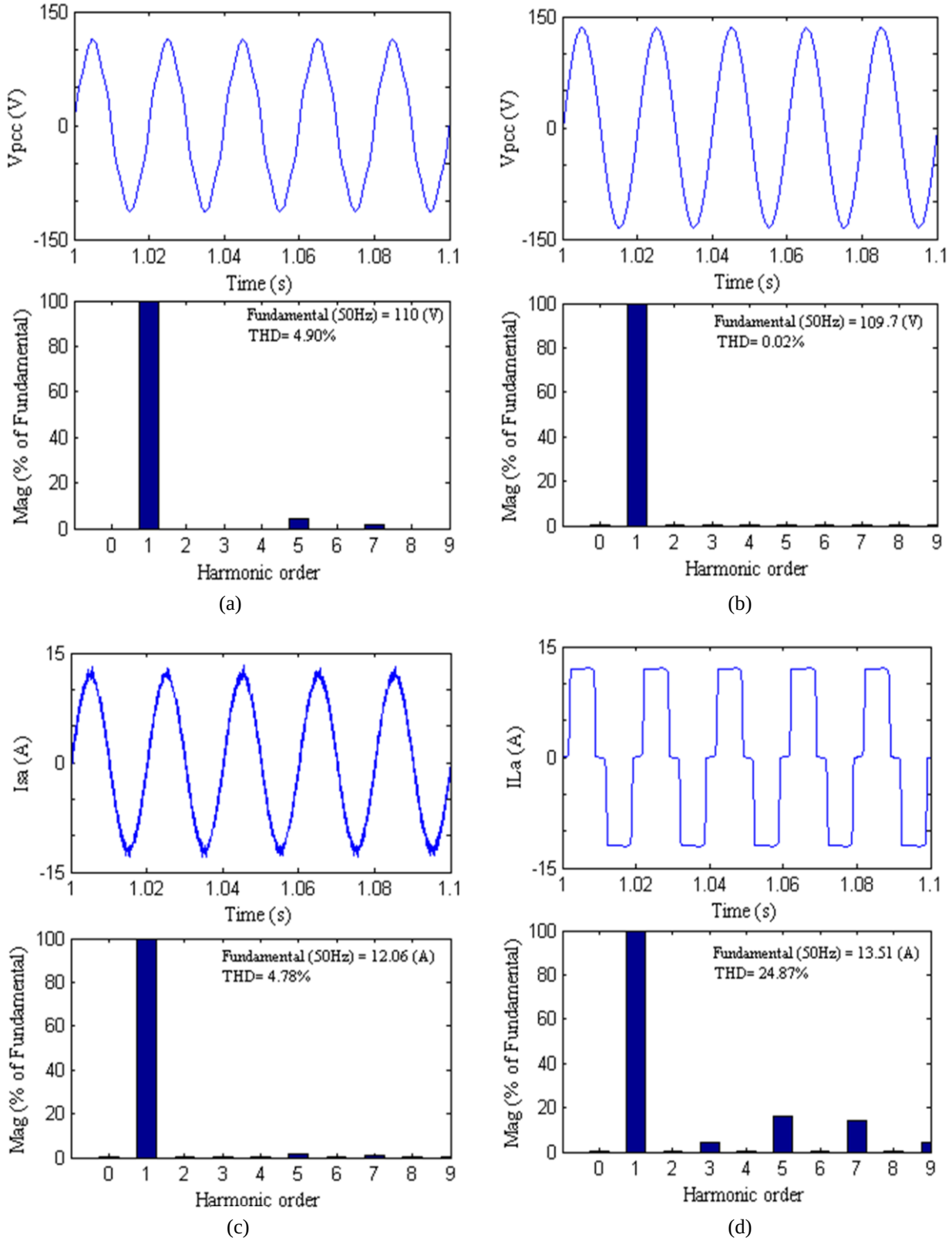

Fig.4.8 Harmonic spectra of (a) Distorted PCC voltage v_{pcca} , (b) filtered PCC voltage (c) supply current i_{sa} , (d) load current i_{la} in PFC mode for IRPT in distorted supply

Table III Performance of DSTATCOM for PBT and IRPT under distorted supply

I PBT

Mode of Operation	Parameters	Parameters Magnitude and their THD %
Power factor correction	Supply current (A) Load current (A) PCC voltage (V) Filtered PCC voltage (V)	14.14 A, 4.99% 13.51 A, 24.86% 109.8V, 4.90% 109.8V, 0.01%

II IRPT

Power factor correction	Supply current (A) Load current (A) PCC voltage (V) Filtered PCC voltage (V)	12.06A, 4.78% 13.51A,24.87% 109.7V, 4.90% 109.7V, 0.02%

4.4Conclusion

Power Balance Theory and Instantaneous Reactive Power Theory have been used for long time for harmonic compensation under ideal supply voltage conditions. But in this chapter the case of distorted supply mains is studied. Direct application of conventional PBT and IRPT schemes with unbalanced supply mains does not give satisfactorily results and it was observed during simulations hence both the schemes were modified to give good performance under distorted supply. In case of distorted mains for Power Balance Theory PCC voltage is filtered using Positive sequence extraction and is used for subsequent reference current calculations. This filtration improves the performance in the power factor correction mode of DSTATCOM. On the other hand, Instantaneous Reactive Power Theory has been used for perfect harmonic compensation by designing and using a band pass filter to filter out the PCC voltages. This improves the performance of DSTATCOM the simulation results show that with these modifications the conventional algorithms can now be used in the case if even in the distorted supply mains. The supply current has a THD of 4.99% for PBT and 4.78% for IRPT in power factor correction mode under the same load conditions and supply distortions. The performance of modified IRPT is observed to be slightly better the modified PBT.

CHAPTER 5

Modeling and Simulation of Grid Connected Permanent Magnet Synchronous Generator Wind Turbine

5.1 General

In this chapter, a control algorithm for the direct-driven wind turbine PMSG systems is studied and simulated. The direct-driven wind turbine PMSGs do not have the gearbox between the wind turbine and the PMSG rotor shaft, which avoids the mechanical power losses caused by the gearbox. Moreover, the removal of the gearbox also helps in reducing the cost of the system. The overall configuration of a direct-drive wind turbine PMSG system is shown in Figure 5.1.

This figure shows the system is composed of a wind turbine PMSG, a rectifier, and an inverter. The wind turbine PMSG transforms the mechanical power from the wind into the electrical power, while the rectifier converts the AC power into DC power and controls the speed of the PMSG. The controllable inverter helps in converting the DC power to variable frequency and magnitude AC power. With the voltage oriented control algorithm, the inverter also possesses the ability to control the active and reactive powers injected into the grid.

The overall control scheme is developed in Matlab/Simulink, the wind connected PMSG model is taken as preset model and is used to integrate with the grid system having a common DC link voltage between two voltage source converters (VSC). The control algorithms involved in the two VSC's has been studied and results are obtained for the open loop operation of the scheme.

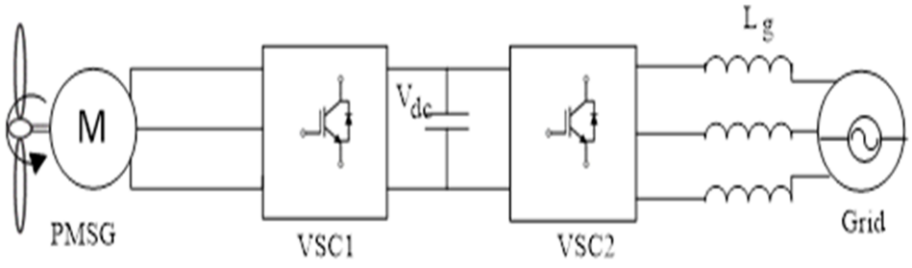

Fig.5.1 System configuration for Grid connected wind turbine based PMSG

5.2 Wind Turbine Connected Permanent Magnet Synchronous Generator

The preset model of wind connected PMSG is used for the simulation purpose; however the modeling of PMSG is done using dq-axis synchronously rotating reference frame. The basic equations involved are given below and equivalent circuit diagram in dq frame is also represented in Fig. 5.2.

The dq0 or Park's transformation is a mathematical transformation which aims to simplify the analysis of synchronous machinery models, and was first introduced by R.H.Park in 1929. In the three-phase systems like permanent magnet synchronous machines (PMSM), the phase quantities which include stator voltages, stator currents, and flux linkages are time varying quantities. By applying Park's transformation, which is in essence the projection of the three phase quantities onto a rotating two axes reference frame, the AC quantities are transformed to DC quantities which are independent of time.

The abc to dq0 transformation is given by

$$\begin{bmatrix} v_d \\ v_q \\ v_0 \end{bmatrix} = \sqrt{\frac{2}{3}} \begin{bmatrix} \cos\theta_r & \cos(\theta_r - \frac{2\pi}{3}) & \cos(\theta_r + \frac{2\pi}{3}) \\ -\sin\theta_r & -\sin(\theta_r - \frac{2\pi}{3}) & -\sin(\theta_r + \frac{2\pi}{3}) \\ \frac{\sqrt{2}}{2} & \frac{\sqrt{2}}{2} & \frac{\sqrt{2}}{2} \end{bmatrix} \begin{bmatrix} v_a \\ v_b \\ v_c \end{bmatrix} \quad (5.1)$$

and inverse transformation is given by

$$\begin{bmatrix} v_a \\ v_b \\ v_c \end{bmatrix} = \sqrt{\frac{2}{3}} \begin{bmatrix} \cos\theta_r & -\sin\theta_r & \frac{\sqrt{2}}{2} \\ \cos(\theta_r - \frac{2\pi}{3}) & -\sin(\theta_r - \frac{2\pi}{3}) & \frac{\sqrt{2}}{2} \\ \cos(\theta_r + \frac{2\pi}{3}) \frac{\sqrt{2}}{2} & -\sin(\theta_r + \frac{2\pi}{3}) & \frac{\sqrt{2}}{2} \end{bmatrix} \begin{bmatrix} v_d \\ v_q \\ v_0 \end{bmatrix} \quad (5.2)$$

Using Eqs (5.1) and (5.2), we can represent the stator voltages, stator currents or flux linkages of the AC machines. Considering that under balanced conditions, v_0=0, the voltage function of the PMSM in the dq-axes reference frame can be expressed as follows

$$v_{ds} = R_s i_{ds} + L_d \frac{di_{ds}}{dt} - w_e L_q i_{qs} \quad (5.3)$$

$$v_{qs} = R_s i_{qs} + L_q \frac{di_{qs}}{dt} + w_e L_d i_{ds} + w_e \emptyset_r \quad (5.4)$$

where, $v_{ds}$and v_{qs} are the instantaneous stator voltages in the dq-axes reference frame, and $i_{ds}$and i_{qs} are the instantaneous stator currents in the dq-axes reference frame, L_d and L_q are the d-axis and q-axis inductances, and w_e is the electrical angular speed of the rotor, while $\emptyset_r$ is the peak value of the phase flux linkage due to the rotor-mounted PMs. According to expressions (5.3) and (5.4), the equivalent circuits of the PMSM in the dq-axes reference frame can be drawn as shown in Fig.5.2.

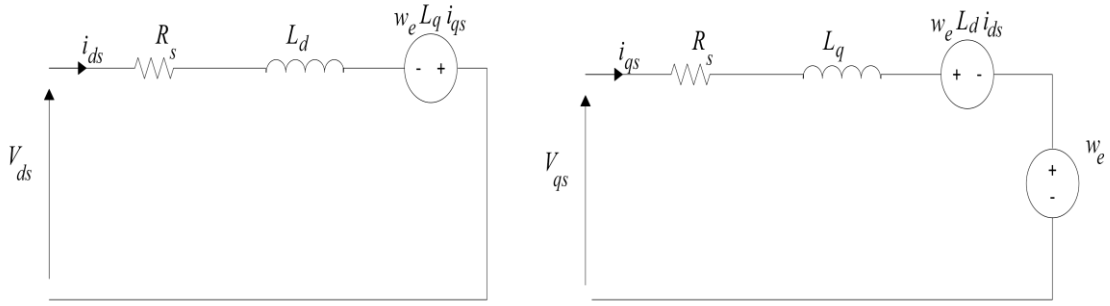

Fig.5.2. Equivalent circuits of PMSM in d and q frame.

5.2.1 Generator Side Converter Control

In wind turbine PMSG systems, three system variables need to be strictly controlled [66] which are : the optimal power generated by the PMSG at different wind speed levels;) the active and reactive power injected into the grid; the DC bus voltage of the back to back converter. Figure 5.1 shows a direct-drive wind turbine PMSG fed by a back-to-back converter. In this system, the generator-side converter regulates the speed of the PMSG to implement the MPPT control. Meanwhile, the grid-connected converter controls the active and reactive power injected into the grid.

In MPPT mode, when the wind speed is greater than the cut-in speed, the wind turbine system starts to work and generate electrical power. Because the wind speed is in a relatively low range in the MPPT mode, the power captured by the wind turbine is below its rated value, the MPPT control needs to be applied to ensure a maximum efficiency of power capture. The MPPT mode ends when the wind speed is greater than the rated wind speed, (12m/s).

The expression of the mechanical power captured by the wind turbine is given as

$$P_{turbine} = \frac{1}{2} \rho \pi r^2 C_p(\lambda, \beta) V_w^3 \quad (5.5)$$

where $C_p(\lambda, \beta)$ is power coefficient, V_W is wind speed , λ is tip speed ratio, r is turbine blade radius and ρ is air denity.

As shown in equation (5.5), to control the captured mechanical power,$P_{turbine}$, at given wind speed, V_W, the only controllable term is the power coefficient,$C_p(\lambda, \beta)$. In the MPPT operation mode, the pitch angle is usually kept at zero degree. In order to achieve the peak power coefficient value in the zero degree pitch angle is used, the tip speed ratio needs to be controlled at the optimal value. From expression (5.5), the control of the tip speed ratio is actually the control of the rotor speed of the PMSG.

The wind speed information is sensed by a sensor and sent to a microcontroller, from which reference speed of the PMSG can be calculated according to the optimal tip speed ratio. Consequently, the generator speed will reach its reference value in the static state, and then the MPPT control is achieved.

5.2.2 Field Oriented Control based Generator-Side Converter Control

The torque equation of PMSM is given by

$$T_e = \frac{3}{2}\left(\frac{p}{2}\right)(\emptyset_r i_{qs} + (L_d - L_q) i_{qs} i_{ds} \quad (5.6)$$

where p is no of poles, $\emptyset_r$ is rms flux density, L_d and L_q are the d and q axis inductance of the stator.

For surface mounted PMSM $L_d = L_q$ i.e. d and q axis inductances are equal thus the torque equation is reduced to

$$T_e = \frac{3}{2}\left(\frac{p}{2}\right) \emptyset_r i_{qs} \quad (5.7)$$

In order to achieve the maximum torque per ampere, the d-axis current is set at zero ($i_{ds} = 0$). In expression (5.7),$\emptyset_r$ is the flux linkage due to the permanent magnets which is a constant. Thus, there will be a linear relationship between the electromagnetic torque and the q-axis current,i_{qs}, such that the electromagnetic torque can be easily controlled by regulating the q-axis current. In the FOC approach coupled

to the optimal tip speed ratio based MPPT, control strategy is applied as the control algorithm for the generator-side power converter.

In Figure 5.3, there are three feedback loops in the control system which is: (a) the speed control loop, (b) the d-axis current control loop, and (c) the q axis current control loop. In the speed loop, at every sampling time, the actual speed of the generator sensed by an encoder mounted on the shaft of the rotor is compared to its reference value, which in turn is generated by the optimal tip speed ratio control, and then the error is sent to a PI controller which will output the reference q-axis current, i_q^*.

The d-axis reference current i_d^* is always set at zero. To acquire the feedback current signals, three-phase stator currents are sensed and transformed into the dq-axes reference frame according to Park's transformation. The reference stator voltages are then being achieved by PI controllers in the dq-axes current control loops. Here, the space vector pulse width modulation (SVPWM) approach is to be applied as the modulation strategy in this system, because it generates less harmonic distortion in the output stator voltages/currents and provides more efficient use of the DC supply voltages than the conventional sinusoidal pulse width modulation (SPWM). The outputs of the SVPWM model are six PWM signals to control the ON/OFF state of the six IGBT switches in the generator-side converter. This SVPWM approach is being investigated and will be used for generating pulses of both converter 1 and 2. At present only control algorithm is designed and open loop results are taken for intermediate signals.

The block diagram depicting the generator side control is given below.

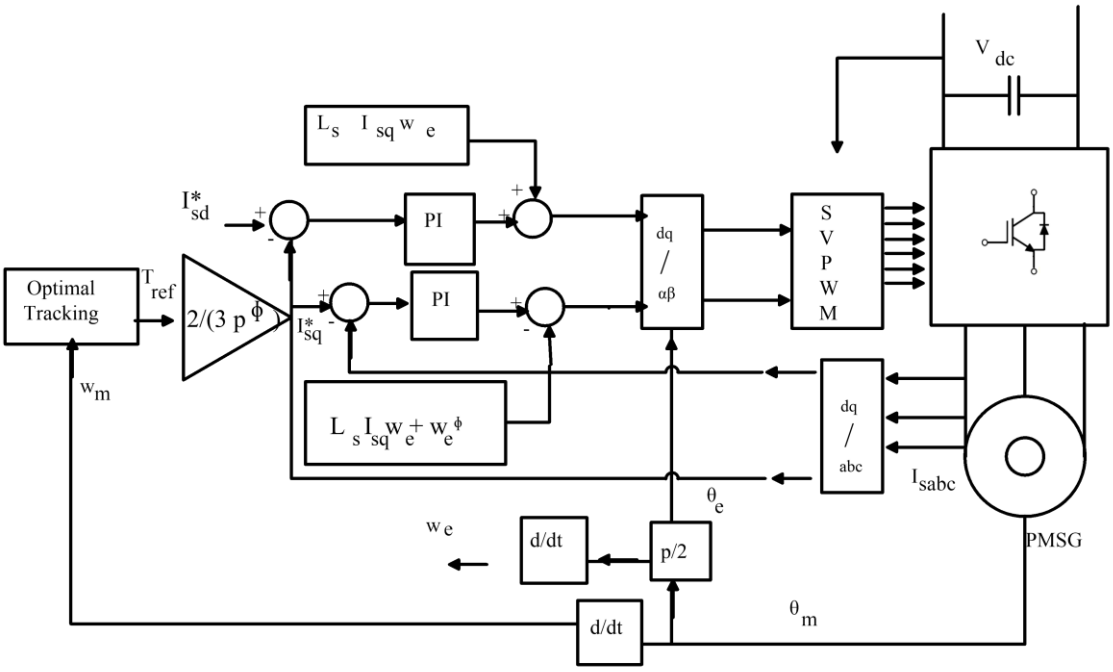

Fig. 5.3 Overall control of PMSG side converter

5.2.2.1 Calculations

The Parameters of PMSG and wind turbine is given below.

PMSG: 6 kW, 415 V, 25 Hz, p=10, stator phase resistance = 0.425 ohm, armature inductance = 0.000835 H, Flux linkage = 0.433 weber, Rated speed = 152.85 rad/s

Turbine: Nominal mechanical power= 8500 W, wind speed= 12 m/s, maximum power at base speed= 0.8 pu

The mechanical torque on the rotor shaft can be calculated as:

$T_m = P_{turbine} / w_m = 8500/152.85 = -55.61$ Nm

The torque is denoted as a negative value because the PMSM is working in the generator mode. When the system reaches the steady state, the mechanical torque is equal to the electromagnetic torque. The q-axis current can be calculated as follows using eq. (5.7).

$$T_e = T_m = \frac{3}{2}\left(\frac{p}{2}\right) \emptyset_r i_{qs}$$

$i_{qs}*$ = (55.61*2)/(3*5*0.433*1.414) = -12.11 A

This reference value of the quadrature current is subtracted from sensed value and then fed through PI controller to regulate it to the desired value.

5.3Grid side Converter Control

The objective of the grid side converter control is to stabilize the dc link voltage at its nominal value 750 V. Choosing the DC link voltage (V_{dc}) is related to the value of the line to line rms voltage seen in the grid side ($V_{g\text{-}ll}$). V_{dc} =1.633$V_{g\text{-}ll}$ [69].

Consequently, it has to be ensured that the active power generated by the generator is fed to the grid but the capacitor voltage always varies during wind turbine operation [70]. It is mentioned in the literature that there are several control strategies used to perform grid side converter depending on the reference frame used to perform control strategies. Here, the synchronous reference frame control strategy is studied. The dynamic model of the grid connection in reference frame rotating synchronously with the grid voltage is given as follows [67]:

$$V_{gd} = V_{id} - R\,I_{gd} - L\frac{dI_{gd}}{dt} - Lw_g I_{gq} \tag{5.8}$$

$$V_{gq} = V_{iq} - R\,I_{gd} - L\frac{dI_{gq}}{dt} - Lw_g I_{gd} \tag{5.9}$$

where L and R are the grid inductance and resistance, respectively. V_{id} and V_{iq} are the inverter voltage components. If the reference frame is oriented along the supply voltage, the grid vector voltage is

$$V = V_{gd} + j0\,V_{id} \tag{5.10}$$

Active and reactive power can be expressed as follows [67].

$$P = \frac{3}{2}V_{gd}I_{gd} \tag{5.11}$$

$$Q = \frac{3}{2}V_{gd}I_{gq} \tag{5.12}$$

It could be seen from above equations that we can control the active and reactive powers by respectively changing the d and q-current components. Also in order to

transfer all the active power generated by the wind turbine the dc-link voltage must remain constant [70], as explained in the following constraint [71].

$$C\frac{dV_{dc}}{dt} = \frac{P_t}{V_{dc}} - \frac{P_g}{V_{dc}} \tag{5.13}$$

where subscript ‘g’ refers to the grid and ‘t’ refers to the wind turbine.

Based on (68), if the two powers (the wind turbine power and the grid power) are equal there will be no change in the dc-link voltage. The control strategy of the grid side converter is studied.

5.4Some Intermediate open loop results for the Grid connected PMSG

Few of the intermediate results are taken both for PMSG are discussed in this section. Grid side and hence overall control algorithm for operation of Grid connected Permanent Magnet Synchronous Generator is still to be implemented. Some results on PMSG side are given in Fig.5.6 which shows the output voltage, currents, power of wind turbine based PMSG system. In Fig.5.7 the PMSG side voltage and current are shown. In Fig.5.8 shows the conversion of PMSG voltages and currents to dq0 form.

The Mtalab/Simulink model of the system is shown in Fig.5.4 and generator side converter implementation in Fig.5.5

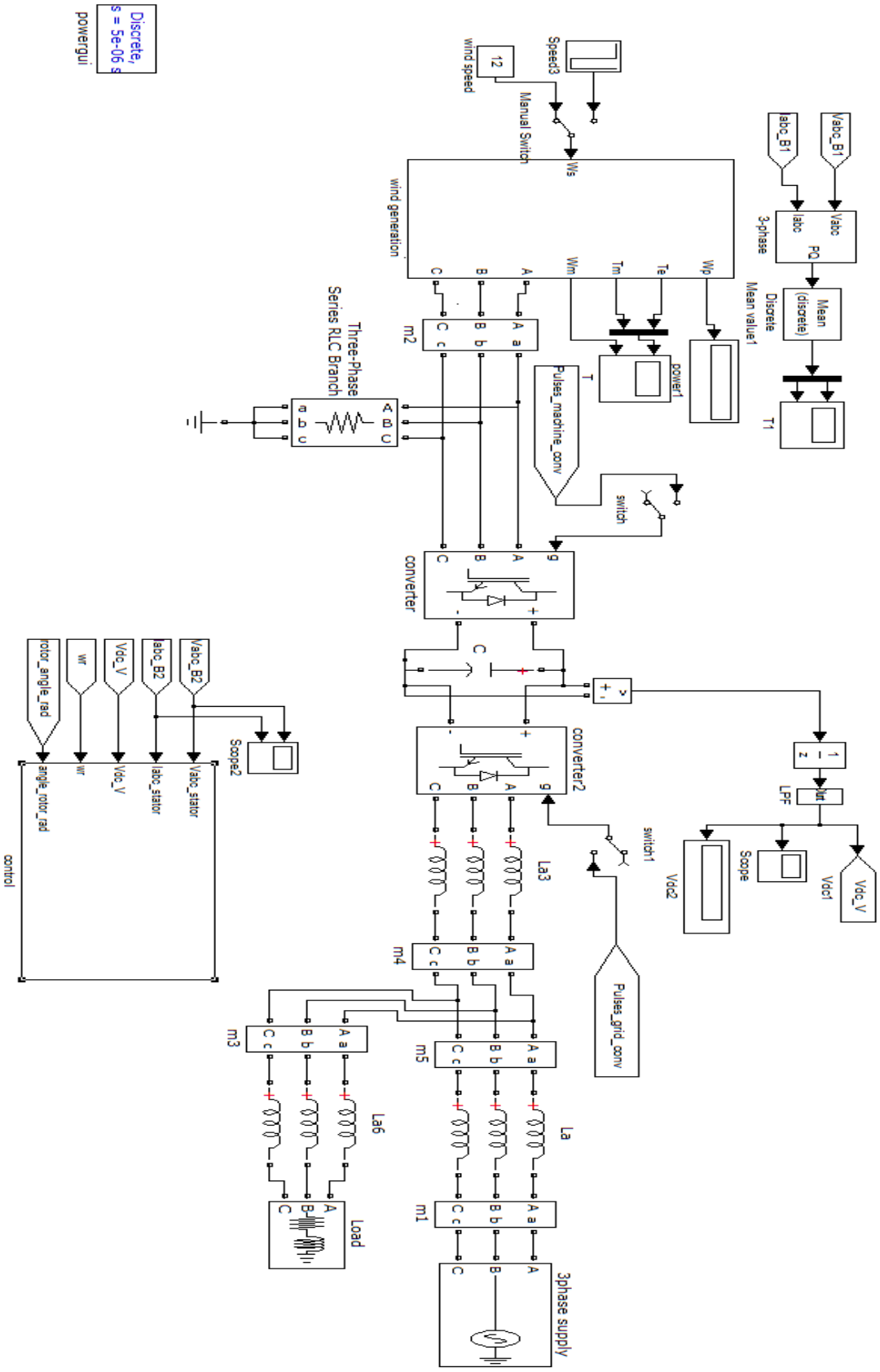

Fig.5.4 Matlab/Simulink model for PMSG system

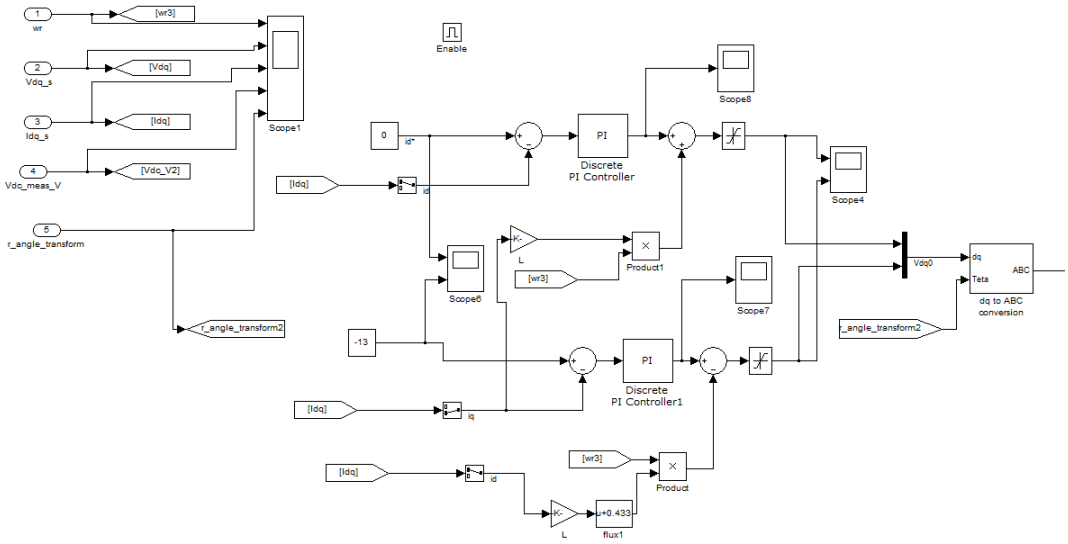

Fig.5.5 Matlab/Simulink model of PMS side converter control

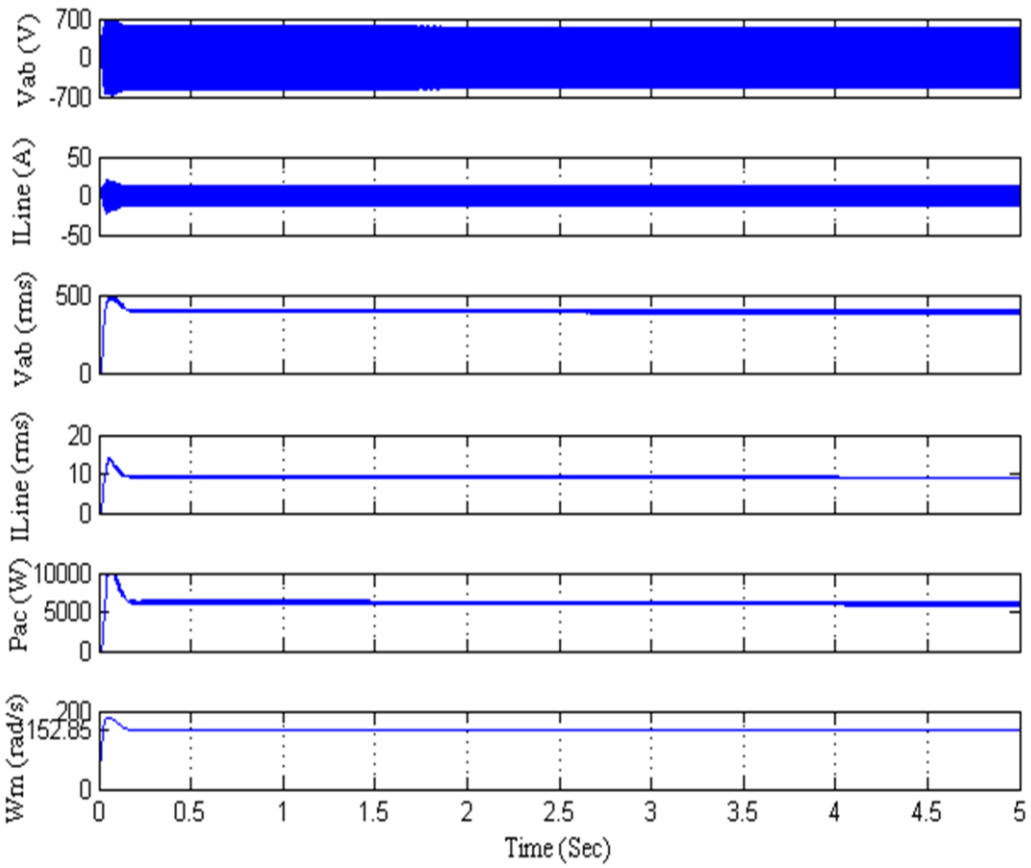

Fig.5.6 PMSG output signals

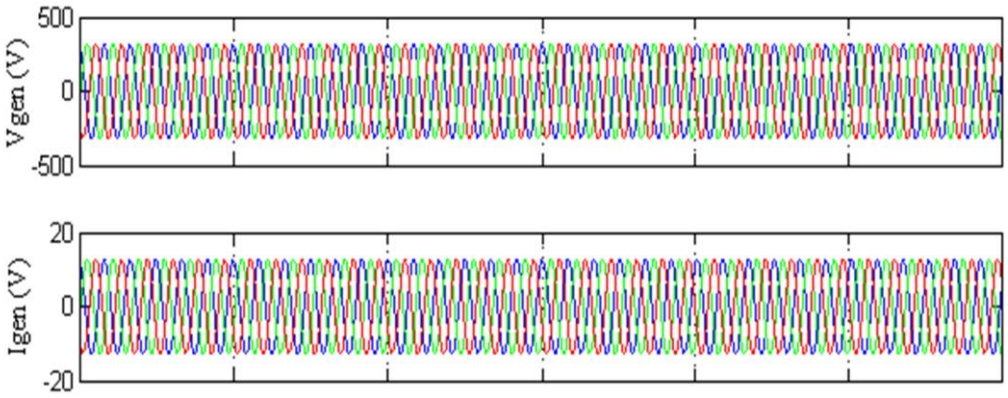

Fig.5.7 PMSG voltages and currents

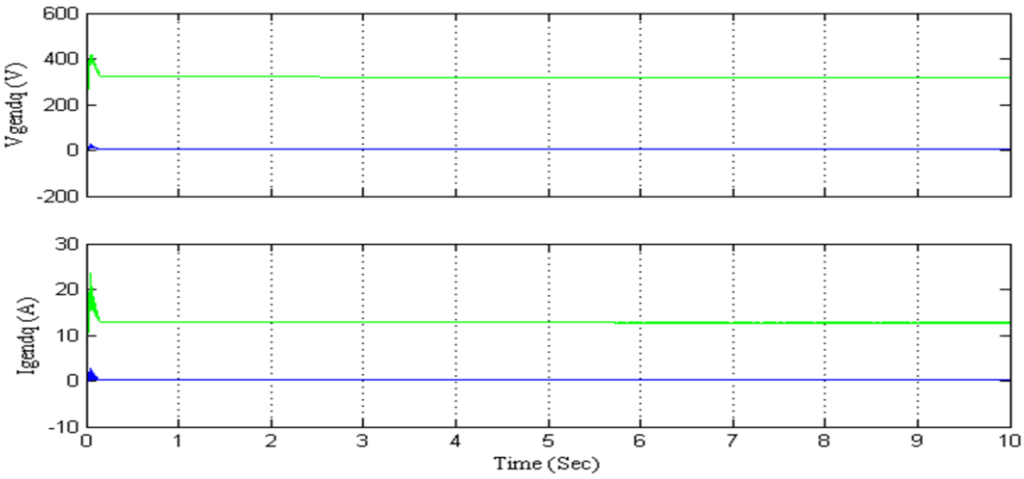

Fig.5.8 Voltage and currents converted to dq form for PMSG

5.5Conclusion

The Simulink model of PMSG has been developed and results are taken for open loop operation of PMSG. The reference current i_{qs}^{*} is calculated using PMSG parameters. The control is depicted in Fig.5.3. The grid side control scheme and integration of PMSG with grid will be a part of future scope of work although the results for intermediate signals are taken for PMSG side.

Future Scope of Work

This thesis presents a vast investigation on control of DSTATCOM and many control algorithms have been worked upon both conventional and non-conventional. In recent times there is rising interest in the integration of Renewable resources to the Grid and use of solar energy and wind energy has become more popular. In chapter 5 study on integration of wind connected permanent magnet synchronous generator to AC grid is presented and its implementation requires control of two VSC having a common Dc link simultaneously. However this thesis does not presents complete implementation of PMSG based system to the grid and is considered to be part of future scope of work

References

[1] R. C. Dugan, M. F. McGranaghan and H. W. Beaty, "Electric Power Systems Quality", 2nd Edition, McGraw Hill, New York, 2006.

[2] K. R. Padiyar, "FACTS Controllers in Power Transmission and Distribution," New Age International (P) Limited, Publishers, New Delhi, 2007.

[3] H. Akagi, E.H. Watanable and M. Aredes, "Instantaneous power theory and application to power conditioning," Jhon Wiley & sons, New Jersey, USA, 2007.

[4] Antonio Moreno-Munoz, Power Quality: "Mitigation Technologies in a Distributed Environment", Springer-Verlag, London limited, London, 2007.

[5] Angelo Baggini, "Handbook on power quality," John Wiley & Sons, New Jersey, USA,2008.

[6] P. Jayaprakash, B. Singh, and D.P. Kothari, "Three-Phase 4-Wire DSTATCOM Based on H Bridge VSC with a Star/Hexagon Transformer for Power Quality Improvement," ICIIS 2008, pp.1-6, Dec.2008.

[7] B. Singh, P. Jayaprakash, and D.P. Kothari, "Three-phase four-wire Dstatcom with H-bridge VSC and star/delta transformer for power quality improvement," in Proc. of INDICON 2008, Vol. 2, pp.412 – 417, Dec. 2008.

[8] Hurng- Liahng Jou, Jinn- Chang Wu, Kuen- Der Wu, Wen- Jung Chiang and Yi-Hsun Chen, "Analysis of zig-zag Transformer applying in the three-phase Four-Wire Distribution Power System," IEEE Trans. On Power Delivery, vol. 20, no. 2, pp.1168- 1173, April 2005.

[9] F.N. Belchior, J.F.V. Ferreira, J.C. Oliveira, R. Apolonio and A.B. Vasconcellos, "Three-phase electromagnetic filter for zero-sequence harmonics," IEEE Trans. on Magnetics, Vol. 42, pp.2201 –2207, Sept.2006.

[10] Sewan Choi and Minsoo Jang, "Analysis and Control of a Single-Phase- Inverter–Zigzag-Transformer Hybrid Neutral-Current Suppressor in Three-Phase Four-Wire Systems," IEEE Trans. on Industrial Electronics,Vol. 54, pp.2201-2208, Aug 2007.

[11] Hurng-Liahng, Kuen- Der Wu, Jinn- Chang Wu and Wen- Jung Chiang, "A three phase four- wire power filter comprising a three phase threewire active filter and a zig-zag transformer," IEEE Trans. on Power Electronics, vol. 23, no. 1, pp. 252-259, January 2008.

[12] B. Singh, P. Jayaprakash, T.R. Somayajulu, D.P. Kothari, A. Chandra, and K. Al-Haddad, "Integrated three-leg VSC with a zig-zag transformer based three-phase four-wire DSTATCOM for power quality improvement," in Proc. of IECON 2008, pp. 796-80. Nov. 2008.

[13] B. Singh, K. Al-Haddad, and A. Chandra, "A new control approach to three-phase active filter for harmonics and reactive power compensation," IEEE Trans. on Power Systems, vol. 13, no. 1, pp. 133– 138, Feb. 1998.

[14] B.N. Singh, B. Singh, A. Chandra and K. Al-Haddad, "Design and digital implementation of active filter with power balance theory," IEE Proc.-Electr. Power Applications, vol. 152, no. 5, pp. 1149-1160, September 2005.

[15] B.N. Singh, B. Singh, A. Chandra, P. Rastgoufard and K. Al-Haddad, "An Improved Control Algorithm for Active Filters," IEEE Trans. On Power Delivery, vol. 22, pp. 1009-1020, April 2007.

[16] Norouzi, A.H., Sharaf, A.M.: 'Two control schemes to enhance the dynamic performance of the STATCOM and SSSC', IEEE Trans. Power Deliv., 2005.

[17] Chatterjee, K., Ghodke, D.V., Chandra, A., Al-Haddad, K.: 'Simple controller for STATCOM-based var generators', IET Power Electron., pp. 192–202, 2009.

[18] Garica-Gonzalez, P., Garcia-Cerrada, A.: 'Control system for aPWM-based

STATCOM', IEEE Trans. Power Deliv., pp. 1252–1257, 2000.
[19] Mohod, S.W., Aware, M.V.: 'A STATCOM-control scheme for grid connected wind energy system for power quality improvement', IEEE Syst. J., pp. 346–352, 2010.
[20] Ghosh, A., Ledwich, G.: 'Power quality enhancement using custom power devices', Power Electronics and Power Systems Series, Kluwer, 2002.
[21] Rao, P., Crow, M.L., Yang, Z.: 'STATCOM control for power system voltage control applications', IEEE Trans. Power Deliv., pp. 1311–1317, 2000.
[22] M. Qasim, V. Khadkikar, "Application of Artificial Neural Networks for Shunt Active Power Filter Control," IEEE Trans. Industrial Informatics, Vol.10, Issue 3, pp.1765-1774, 2014.
[23] A. Bhatacharya, C. Chakraborty, "A shunt active power filter with enhanced performance using ANN based Predictive and adaptive controllers,"IEEE Trans. Industrial Electronics, Vol.58, Issue 2, pp.421-428, 2011.
[24] S. R. Arya, B. Singh, "Neural Network based conductance estimation control algorithm for shunt compensation," IEEE Trans. Industrial Electronics, Vol.10, Issue 1, pp.569-577, 2014.
[25] M. Qasim, P. Kanjiya,V. Khadkikar, "Optimal current harmonic extractor based on unified adalines for shunt active power filters," IEEE Trans. PowerElectronics, Vol.29, Issue 9, pp.6383-6393, 2014.
[26] M. Badoni, A. Singh and B.Singh, "Design and Implementation of adaptive neuro fuzzy inference system based control algorithm for Distribution Static Compensator," Electrical Power Components and Systems, pp.1741-1751, 2015.
[27] S. R. Arya, B. Singh, A. Chandra, K. Al-Haddad, "Learning based Anti-Hebbian Algorithm for control of Distribution Static Compensator," IEEE Trans. Industrial Electronics, Vol.61, Issue 11, pp.6004-6012, 2014.
[28] N. D. Dinh, N. D. Tuyen, G. Fujita, F. Funabashi, "Adaptive notch filter solution under unbalanced and/or distorted point of common coupling voltage for three phase four wire shunt active power filter with sinusoidal utility current strategy", IET Generation, Transmission and Distribution, Issue13, Vol. 9,pp.1580-1596, 2015.
[29] M. Badoni, A. Singh and B.Singh, "Variable forgetting factor recursive least square control agorithm for DSTATCOM," IEEE Trans. Power Deliv., Vol.30, No.5,pp.2353-2361, 2015.
[30] Hua, C.C., Li, C.H., Lee, C.S.: 'Control analysis of an active power filter using Lyapunov candidate', IET Power Electron., pp. 325–334, 2009.
[31] Odavic, M., Biagini, V., Zanchetta, P., Sumner, M., Degano, M.: 'One-sample-period-ahead predictive current control for high-performance active shunt power filters', IET Power Electron., pp. 414–423, 2011.
[32] Loh, P.C., Tang, Y., Blaabjerg, F., Wang, P.: 'Mixed-frame and stationary-frame repetitive control schemes for compensating typical load and grid harmonics', IET Power Electron., pp. 218–226, 2011.
[33] Benhabib, M.C., Saadate, S.: 'New control approach for four-wire active power filter based on the use of synchronous reference frame', J. Electr. Power Syst. Res., pp. 353–362, 2005.
[34] Flota, M., Alvarez, R., Nunez, C.: 'Sliding mode observer-based control for a Series active filter'. Proc. Second IEEE Int. Conf. Electrical and Electronics Engineering, pp. 254–257, 2005.
[35] Tilli, A., Ronchi, F., Tonielli, A.: 'Shunt active filters: selective compensation of current harmonics via state observer'. Proc. 28th IEEE Annual Conf. the Industrial

Electronics Society, vol. 2, pp. 874–879, 2002.
[36] Selvajyothi, K., Janakiraman, P.A.: 'Analysis and simulation of single phase composite observer for harmonics extraction'. Proc. IEEE Int. Conf. Power Electronics, Drives and Energy Systems, pp. 1–6, 2006.
[37] Selvajyothi, K., Janakiraman, P.A.: 'Extraction of harmonics using composite observers', IEEE Trans. Power Deliv., pp. 31–40, 2008.
[38] Changyong, W., Liqiao, W., Taotao, J., Zhongchao, Z.: 'Analysis of control system of current source active power filter based on multi-modular phase-shifting SPWM technique'. Proc. Third IEEE Int. Power Electronics and Motion Control Conf., vol. 3, pp. 1431–1435, 2000.
[39] Vodyakho, O., Kim, T., Kwak, S., Edrington, C.S.: 'Comparison of the space vector current controls for shunt active power filters', IET Power Electron., pp. 653–664, 2009.
[40] G.Shen, X.Zhu, J.Zhang and D.Xu, "A new feedback method for PR current control of LCL filter based grid connected inverter,"IEEE Trans. Industrial Electronics, Vol. 57, No.6,pp.2033-2041, 2010.
[41] R. Teodorescu, F. Blaabjerg, M. Liserre and P.C. Loh,"Proportional resonant controller and filters for grid connected voltage source converters," IEE Electric power Appl, Vol.153,No.5, pp.750-762, 2006.
[42] A. Hasanzadeh, O.C. Onar, H. Mokhtari and A. Khaligh, "A proportional resonant controllerbased wireless control strategy with a reduced number of sensors for parallel operated UPSs," IEEE Trans. Power Deliv., Vol.25, No.1,pp.468-478, 2010.
[43] L.Herman, I. Papic and B. Blazic, "A proportional resonant current controller for selective harmonic compensationin a hybrid active power filter," IEEE Trans. Power Deliv., Vol.29, No.5,pp.2055-2065, 2014.
[44] W.L.Chen and B.Y.Jiang, "Harmonic Suppression and Performance Improvement for a small scale grid tied wind turbine using proportional resonant controllers," Electric Power Components and Systems, pp.970-981,2015.
[45] W. Chen and Zhe Lin,"One dimensional optimization for PR controller design against the change in source impedance and solar irradiance in PV systems," IEEE Trans. Industrial Electronics, Vol. 61, No.4,pp.1845-1854, 2014.
[46] J.Hu and Y.He, "Modeling and control of grid connected voltage source converterunder generalised unbalanced operating conditions", IEEE Trans. Energy Conversion, Vol.23, No.3,pp.903-913, 2008.
[47] A. G. Yepes, F.D. Freijedo, O. Lopez, and J.D. Gandoy, "High performance Digital Resonant controllers implemented with two integrators," IEEE Trans. Power Electronics, No.2,pp.563-573, 2011.
[48] A. G. Yepes, F.D. Freijedo,O. Lopez and J. D. Gandoy, "Effect of Discretization methods on the performance of resonant controllers," IEEE Trans. Power Electronics, No.7,Vol.25,pp.1692-1712, 2010.
[49] R. Zavadil, N. Miller, A. Ellis, and E. Muljadi, "Making connections: Wind generation challenges and progress," IEEE Power Energy Mag., vol. 3, no. 6, pp. 26–37, Nov, 2005.
[50] Z. Chen, J. M. Guerrero, and F. Blaabjerg, "A review of the state of the art of power electronics for wind turbines," IEEE Trans. Power Electron., vol. 24, no. 8, pp. 1859–1875, Aug. 2009.
[51] S. J¨ockel, "High energy production plus built in reliability—The new Vensys 70/77 Gearless wind turbines in the 1.5 MW class," presented at the 2006 Eur.Wind Energy Conf., Athens, Greece, Feb. 27–Mar. 2, 2006.

[52] Y. Chen, P. Pillary, and A. Khan, "PM wind generator topologies," IEEE Trans. Ind. Appl., vol. 41, no. 6, pp. 1619–1626, Nov./Dec. 2005.
[53] H. Polinder, S.W. H. de Haan,M. R. Dubois, and J. Slootweg, "Basic operation principles and electrical conversion systems of wind turbines," presented at the Nordic Workshop Power Ind. Electron., Trondheim, Norway, Jun. 14–16, 2004.
[54] G. Michalke, A. D. Hansen, and T. Hartkopf, "Control strategy of a variable speed wind turbine with multipole permanent magnet synchronous generator," presented at the 2007 Eur.Wind Energy Conf. Exhib., Milan, Italy, May 7–10, 2007.
[55] A. Grauers, "Efficiency of three wind energy generator systems," IEEE Trans. Energy Convers., vol. 11, no. 3, pp. 650–657, Sep. 1996.
[56] K. Tan and S. Islam, "Optimum control strategies in energy conversion of PMSG wind turbine system without mechanical sensors," IEEE Trans. Energy Convers., vol. 19, no. 2, pp. 392–399, Jun. 2004.
[57] F. Velenciaga and P. F. Puleston, "High-order sliding control for a wind energy conversion system based on a permanent magnet synchronous generator," IEEE Trans. Energy Convers., vol. 23, no. 3, pp. 860–867, Sep. 2008.
[58] North American Electric Reliability Corporation. (2009 Apr.) Accommodating High Levels of Variable Generation [Online]. Available: http://www.nerc.com/files/IVGTF_Report_041609.pdf
[59] Clipper Windpower, The Liberty 2.5 MW Wind Turbine: Clipper Design. (Dec. 2011).
[60] J. Belhadj and X. Roboam, "Investigation of different methods to control a small variable-speed wind turbine with PMSM drives," J. Energy Resources Technol., vol. 129, pp. 200–213, Sep. 2007.
[61] M. Chinchilla, S. Arnaltes, and J. C. Burgos, "Control of permanentmagnet generators applied to variable-speed wind-energy systems connected to the grid," IEEE Trans. Energy Convers., vol. 21, no. 1, pp. 130– 135, Mar. 2006.
[62] W. Qiao, L. Qu, and R. G. Harley, "Control of IPM synchronous generator for maximum wind power generation considering magnetic saturation," IEEE Trans. Ind. Appl., vol. 45, no. 3, pp. 1095–1105, Jun. 2009.
[63] S. Li, T. A. Haskew, and L. Xu, "Conventional and novel control designs for direct driven PMSG wind turbines," Electr. Power Syst. Res., vol. 80, no. 3, pp. 328–338, Mar. 2010.
[64] S. Li, T. A. Haskew, and Y. Hong, "PMSG maximum wind power extraction c control using adaptive virtual lookup table approach in direct-current vector control structure," Int. J. Energy Res., vol. 35, no. 11, pp. 929–1022, Sep. 2011.
[65] S. Li, T. A. Haskew, and L. Xu, "Control of HVDC light systems using conventional and direct-current vector control approaches," IEEE Trans. Power Electron., vol. 25, no. 12, pp. 3106–3118, Dec. 2010.
[66] B. Wu, Y. Lang, N. Zargari, and S. Kouro, Power Conversion and Control of Wind Energy Systems. Hoboken, NJ: Wiley, 2011.
[67] Chinchilia M, Arnaltes S, Burgos J. Control of permanent-magnet generator applied to variable-speed wind-energy systems connected to the grid. IEEE Trans Energy Convers 2006;21(1).
[68] Heier S. Grid integration of wind energy conversion systems. John Wiley and Sons Ltd.; 1998, ISBN 0-471-97143-X.
[69] Kasem AH, El-Saadany EF, El-Tamaly HH, Wahab MAA. An improved fault ride-through strategy for doubly fed induction generator-based wind turbines. IET Renew Power Gener 2008;2(4):201–14.
[70] Muyeen SM, Takahashi R, Murata T, Tamura J. A variable speed wind turbine

control strategy to meet wind farm grid code requirements. IEEE Trans Power Syst 2010;25(1).
[71] Mehrzad D, Luque J, Quenca MC. Vector control of PMSG fo grid connected wind turbine application, Project for Master Thesis, Institute of Energy Technology, Alborg University, Spring; 2009.
[72] Shuhui Li, Timothy A Haskew, Richard P swatloski and William Gathings, "Optimal and Direct-current vector control of direct driven PMSG wind turbines", IEEE Trans. On Power Electronics, Vol. 27 no.5, May 2012.
[73] Ali H Kasem Alaboudy, Ahmad A Daodu, Sobhi S Desouky, Ahmed A Salem, " Converter controls and flicker study of PMSG-based grid connected wind turbine". Ain Shams Engineering Journal, july 2012
[74] S. Mohammad-Reza Rafiei, Hamid A Toliyat, Reza Ghazi, Tilak Gopalarathnam, "An Optimal and flexible control strategy for active filtering and power factor correction under non sinusoidal line voltages". IEEE Trans. On Power Delivery, Vol 16, no. 2, April 2001
[75] IEEE 100 The Authoritative Dictionary of IEEE Standard Terms, Standards Information Network, IEEE Press, pp855.

LIST OF PUBLICATIONS

Conference paper

1. Kuldeep Singh, Alka Singh, "Design and Analysis of LQR based controller for Reactive Power Compensation". IEEE 6th International Conference on Power Systems (ICPS). March 2016.